Removal of the host rock response from time domain electromagnetic data by transforming to, and filtering in the frequency domain.

JAN CHRISTIAAN SLEE

Submitted in partial fulfilment of the requirements
for the degree of

MAGISTER SCIENTIAE

in the Faculty of Science of the
University of Pretoria.

PRETORIA

1988

Removal of the host rock response from time domain electromagnetic data by transforming to, and filtering in the frequency domain

By

JAN CHRISTIAAN SLEE

Supervisor: Prof W J Botha
Department: Geology
Degree : Magister Scientiae in Applied Geophysics

ABSTRACT

The time domain electromagnetic method is mostly used for the mapping of confined conductors. When interpreting the data obtained from such a survey it is necessary to determine and subtract the response due to the host rock or overburden from the survey data. This is done in order to make a correct interpretation of the anomaly responses in the residual signal. In this thesis an overview of the existing host rock removal methods is given whereafter an alternative frequency domain filtering method is discussed and advocated. At first the filtering method is applied on theoretical combinations of host rock and plate responses in order to determine the applicability limits. Thereafter two case histories are studied with special emphasis on the comparison between the traditional and the filtering host rock removal methods. It was found that the speed of data reduction was greatly increased by use of the filter method. Furthermore, the decay constants calculated from results obtained by the filtering method correlates well with the corresponding decay constants calculated from traditional method results. It was also found that the isolated anomalies tend to be of a higher frequency than the corresponding anomalies obtained by means of the traditional host rock response removal methods. However the shape with regard to the side lobes, and the position of the anomalies are correct.

Removal of the host rock response from time domain electromagnetic data by transforming to, and filtering in the frequency domain

Deur

JAN CHRISTIAAN SLEE

Leier : Prof W J Botha
Departement: Geologie
Graad : Magister Scientiae in Toegepaste Geofisika

SAMEVATTING

Die tyd domein elektromagnetiese metode word meestal gebruik om eindige geleiers te karteer. Tydens die interpretasie van sodanige data is dit nodig om die gasheergesteente-responsie te identifiseer en te verwyder om sodoende 'n korrekte interpretasie te verkry van die residuele data. 'n Kort oorsig oor die bestaande metodes vir die verwydering van die gasheergesteente-responsie word gegee. 'n Alternatiewe frekwensie domein filtreringsmetode word dan gepostuleer en bespreek. Die filtreringsmetode is ten eerste op teoretiese kombinasies van gasheergesteente- en plaatgeleier-responsies toegepas om sodoende die toepassingslimiete te bepaal. Daarna is die resultate van twee gevalle studies wat ten eerste verkry is m.b.v. die bestaande- en daarna met die nuwe filtreringsmetode vir die verwydering van die gasheergesteente-responsie, met mekaar vergelyk. Daar is bevind dat data redusering baie vinniger kan geskied indien daar van die filtreringsmetode gebruik gemaak word. Verder stem die vervalkonstantes van ooreenstemmende anomalieë wat met beide die metodes geïsoleer is baie goed ooreen. Daar is ook bevind dat, alhoewel die resultate van die filtreringsmetode hoër frekwensie anomalieë lewer as wat verkry word met die bestaande metodes, die posisie en vorm ten opsigte van die kant lobbe van die anomalieë egter korrek is.

ACKNOWLEDGEMENTS

I would like to extend my gratitude and appreciation towards the following persons and institutions:

1. My supervisor Prof W J Botha for his guidance and support throughout this project and Dr J H de Beer* for his advice and interest.

2. Dr E H Stettler** for his valuable help, discussions and critical proofreading of each chapter.

3. The Foundation for Research Development of the CSIR for the bursary awarded to me.

4. The companies Rio Tinto Exploration (Pty) Ltd and Sasol for the permission to use their data for the case histories.

Lastly I would like to thank all my family, friends and colleagues for their support and help.

* National Physical Research Laboratory, CSIR
** Geological Survey of South Africa

CONTENTS

APPENDIXES

LIST OF FIGURES AND TABLES

LIST OF ABBREVIATIONS AND SYMBOLS

t	Denotes time
a_o, a_n, b_n	Fourier coefficients
$f(t)$	Periodic continuous time function
f	Cut-off frequency for filter
λ	Dummy integration variable
ω	Angular frequency
T	Period
F	Fourier transformation of f(t)
a	Sharpness of filter or smallest plate dimension
θ	Dimensionless number
μ_0	Magnetic permeability of free space
S	Conductivity-thickness product
TEM	Time domain electromagnetic
$\dot{B}z$	Time derivative of the vertical component of the secondary magnetic field, sometimes abbreviated Z component
$\dot{B}x$	Time derivative of the horizontal component of the secondary magnetic field, sometimes abbreviated X component

CHAPTER 1

INTRODUCTION

Time domain electromagnetic (TEM) prospecting has seen widespread use in mineral exploration for over a decade, for example the Hellyer ore deposit in Australia (Silic *et al.*, 1985).

When mapping a confined conductor, the TEM field method most commonly used is that of the Turam type survey. A large fixed rectangular or square loop is placed in such a way that maximum coupling is obtained with the suspected conductor, as depicted in Figure 1.1. A portable receiver loop is used to measure three components of the time derivative of the secondary magnetic field, at regular intervals along a profile perpendicular to the strike of the suspected conductor (Mc Cracken, 1983).

In general the response due to a large transmitter loop TEM system is a combination of the host rock response, conductor response and a possible galvanic response induced by the interaction between the host rock and the conductor (McNeill, 1980, 1982). However in a highly resistive environment, the measured response can with some degree of success be treated as a linear combination of only the host rock and the conductor response (McNeill *et al.*, 1984). Fortunately for a conductive environment there is a time window, where the same linear combination can be assumed, (Kaufman, 1981; Spies, 1980; Nabighian, 1982; Eaton and Hohmann, 1984; San Filipo *et al.*, 1985; McNeill, 1980).

It is well known that the TEM method was primarily developed for the search for conductive minerals in a resistive host rock (Hoekstra and Pesowski, 1982; Spies, 1980). In most cases the target is a finite conductor with a high conductivity-thickness product, surrounded by a more resistive host rock. The characteristic transient response from such a target can normally be obtained by considering the measured response after 2 milliseconds for the GEONICS EM37 system . At these times, the host rock response normally has decayed to a value having an insignificant contribution to the measured response due to the conductive target.

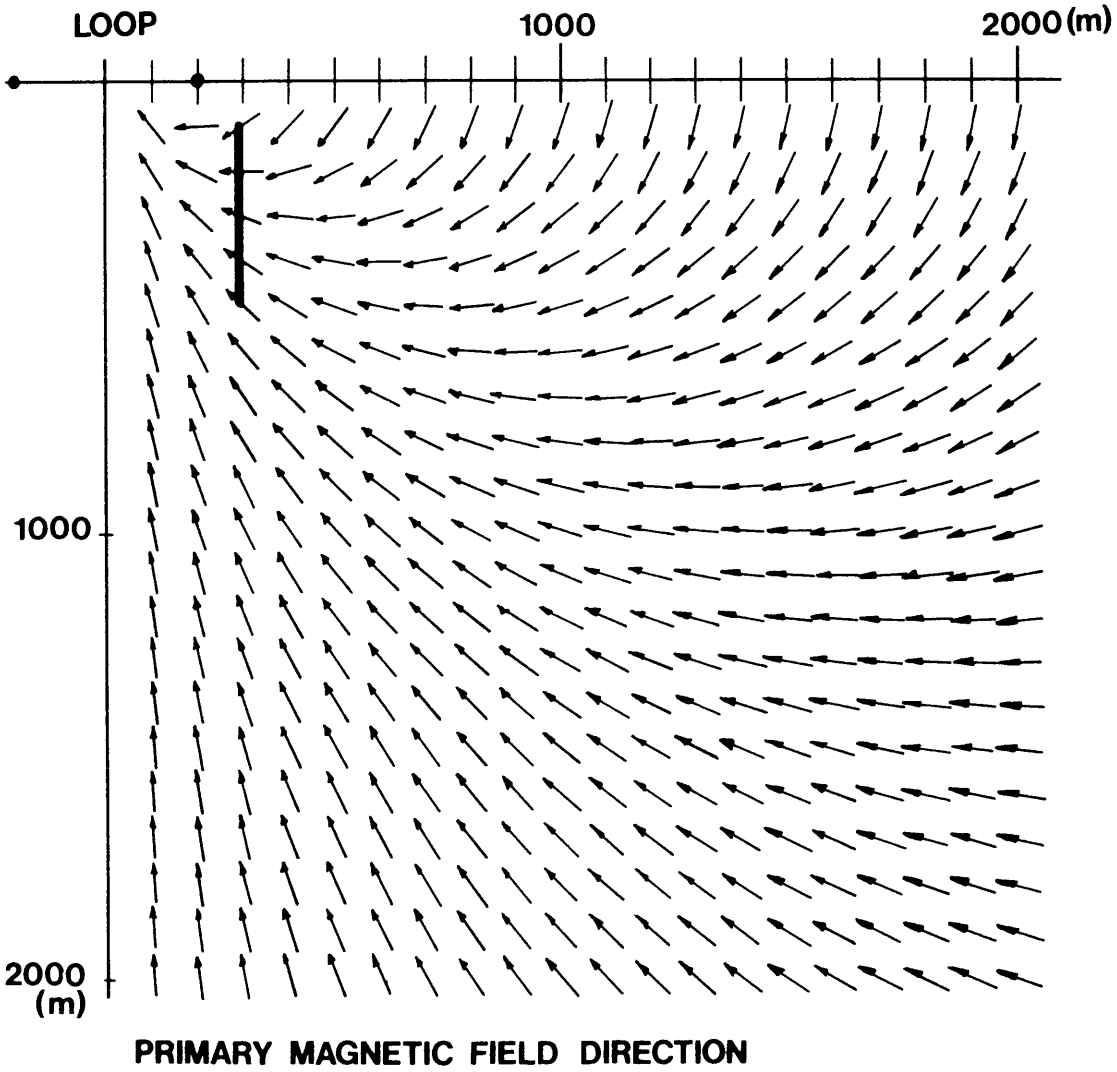

Figure 1.1 Primary magnetic field direction.

It should however also be possible to use the TEM method to map weaker conductors such as weathered faults and fractured zones. Two fields of immediate application would be in groundwater exploration and coal mine planning. Faults and fractures constitute important secondary aquifers in sedimentary, metamorphic and igneous environments (Davis and De Wiest, 1966). In coal mines, unexpected faults can lead to serious loss of revenue when using the long wall mining technique.

In this thesis, all reference to time channels and responses are given with respect to the GEONICS EM37* transient system. For this system the amplitude of a signal from a poor conductor such as a weathered fault would decay to below noise level by probably channel 10 (0,673 ms). Unfortunately the host rock response, even for a relative resistive environment, will constitute a very large percentage of the measured signal in the early time channels. Recognising and isolating confined conductor responses from the early channels poses a difficult problem.

Assuming a linear combination of host rock and conductor responses only, various techniques for stripping the host rock response from the field data have been advocated to at least obtain a first order interpretation. A brief overview of these methods will follow, after which an alternative spatial filter technique will be discussed and advocated.

1.1 STANDARD PROCEDURES FOR THE ROMOVAL OF THE HOST ROCK RESPONSE

1.1.1 Calculating and subtracting of a host rock response

The survey procedure depicted in Figure 1.2 can be applied successfully and cost-effectively to map a good conductor in a resistive environment. By choosing the field lay-out as depicted in Figure 1.2 it is usually found that the anomaly is only apparent on one side of the transmitter loop. The opposite side represents only

*GEONICS Ltd, 1745 Meyerside Dr. Unit 8, ONTARIO, Canada.

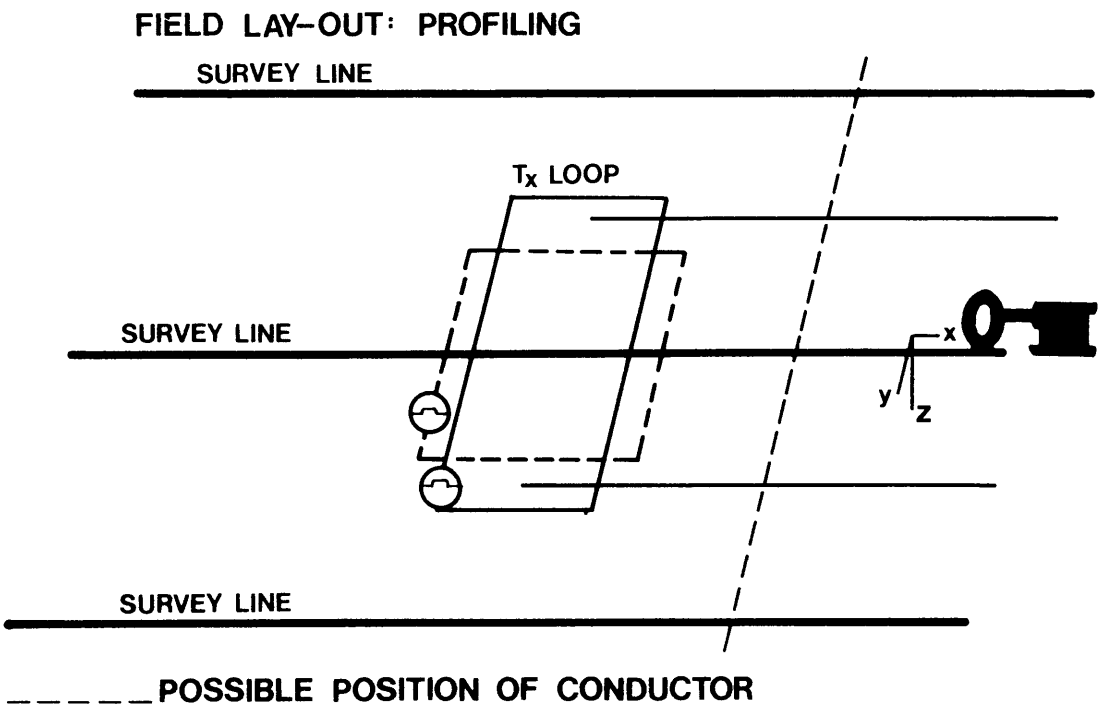

Figure 1.2 Symmetrical field lay-out for profiling.

the contribution from the host rock. Using the formulae and method discussed in Chapter 2 it is possible to calculate the theoretical host rock response. By varying the host rock resistivity a best fit between the calculated response and the non-anomalous side of the profile is obtained and subtracting the host rock response from the anomalous part of the profile isolates the anomaly. This in itself represents two major disadvantages of this approach, namely:

i. Where a conductor is being mapped this procedure is very tedious unless a good estimate of the host rock resistivity is available.

ii. When mapping a deep conductor one usually finds that the anomaly tends to spread out along the profile thus making it difficult to determine whether one is fitting a theoretical response to a low frequency anomaly or to a host rock response.

Figure 1.3 depicts a typical field profile together with the best fitting host rock response and the isolated anomaly.

The problems mentioned in (i) and (ii) can be partially overcome by using one of the following field procedures.

1.1.2 Combined Mode TEM Survey

In the combined mode survey technique, (Rozenberg *et al.*, 1985) a traverse is surveyed using a constant separation between the transmitter and receiver loops, as depicted in Figure 1.4. The advantage of this survey mode is that the host rock response, which is assumed to be that of a layered earth, will remain constant. Any confined conductor anomaly would thus be clearly identifiable.

The disadvantage of a fixed transmitter-receiver geometry is its low survey productivity. The constantly changing transmitter loop location relative to the target also leads to variations in the transmitter-target coupling which complicates the anomaly interpretation.

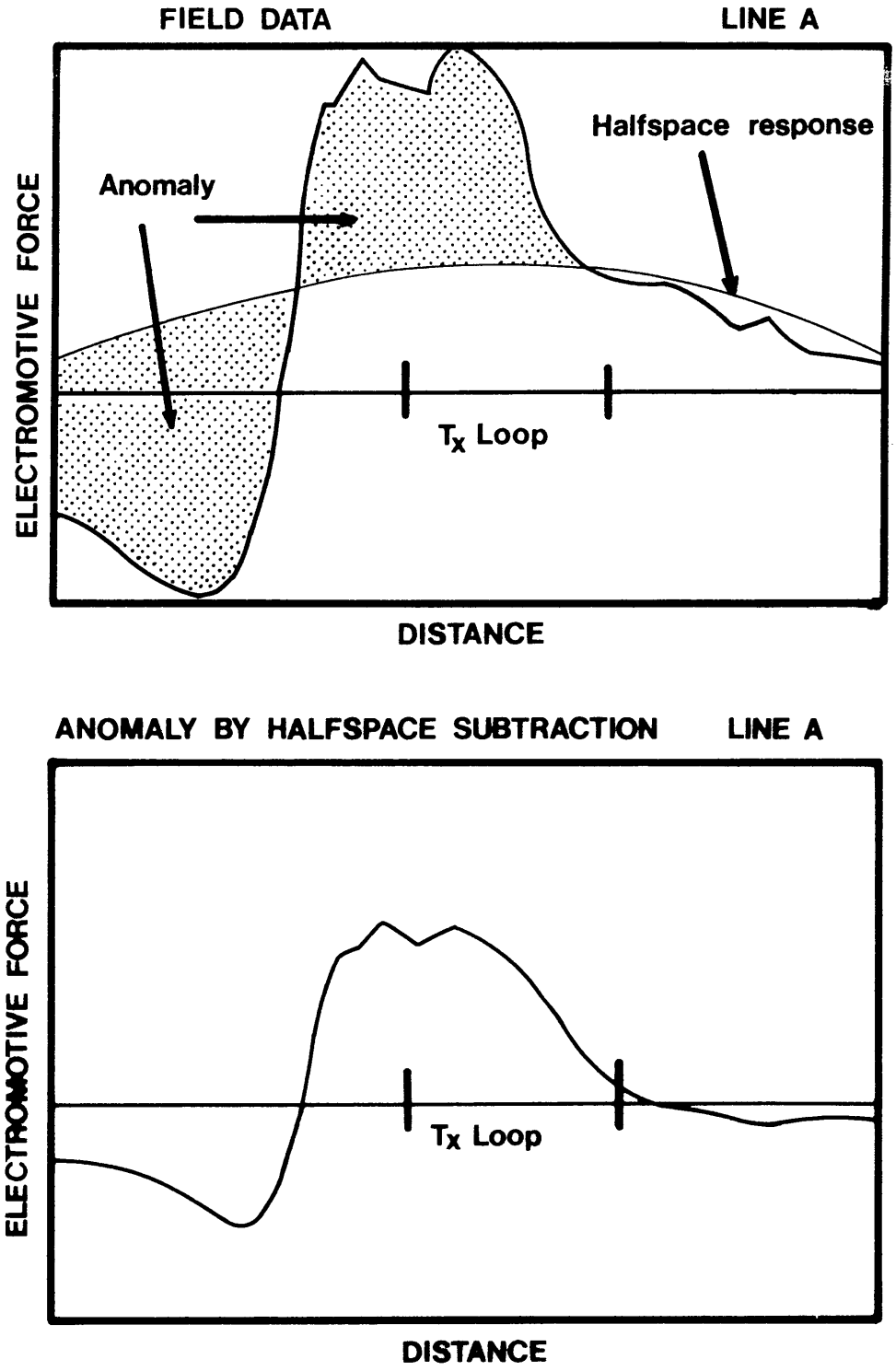

Figure 1.3 Typical observed field profile, best fitting calculated host rock response and isolated anomaly.

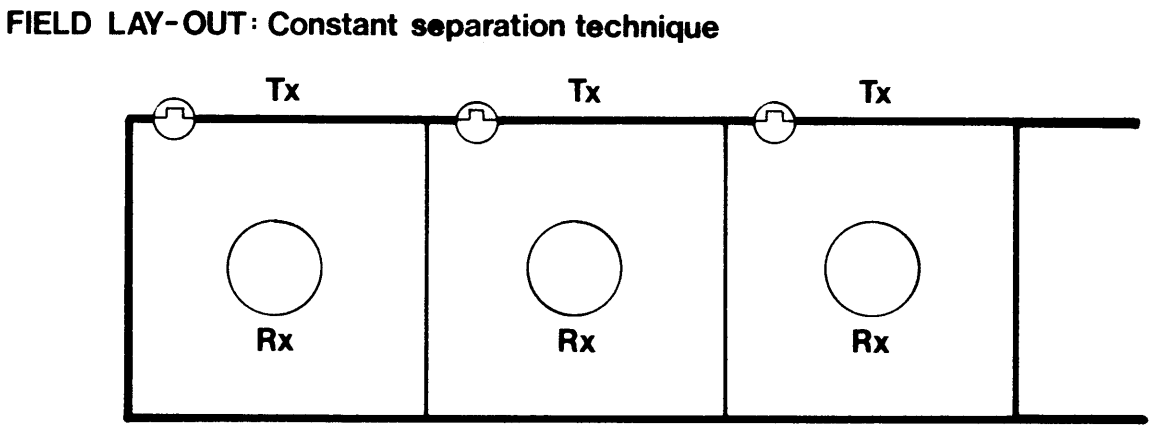

Figure 1.4 Constant separation survey technique - field lay-out. (Combined mode).

1.1.3 Symmetrical Field Procedure

Where the anomaly associated with the target lies entirely to one side of the centre of the transmitter loop, the survey data obtained symmetrical on the opposite side of the loop and target can be subtracted from the target side, thus isolating the anomaly. Figure 1.5 illustrates the use of this technique.

The disadvantage of this technique is the fact that a target has to be relatively shallow to have an anomaly confined to one side of the transmitter loop.

1.2 HOST ROCK REMOVAL BY FILTERING IN THE FREQUENCY DOMAIN

A spatial frequency domain filtering technique was suggested by the following observation; for practical exploration conditions, where a large transmitter loop is used, and targets are usually between 100m and 400m deep, the host rock response is of larger wavelength than any target response.

This led to the idea that if a TEM field profile was transformed to the frequency domain, the host rock response would be contained in the low frequency part of the resulting amplitude spectrum. The anomalies, if any, would thus be represented by the high frequencies. By using an appropriate filter, the low frequency part of the amplitude spectrum could be eliminated and the remainder, if transformed back to the time domain, would represent the isolated anomalies.

Before commencing on the investigation of the proposed filtering method, a literature search to obtain a list of all relevant work done, was conducted through the library of the University of Pretoria. This world wide search revealed no articles of relevance.

From preliminary investigations it became evident that the filtering method would be a very fast method of removing the host rock response from a measured TEM field profile. Although certain problems would certainly arise from the filtering of the data it was still felt that

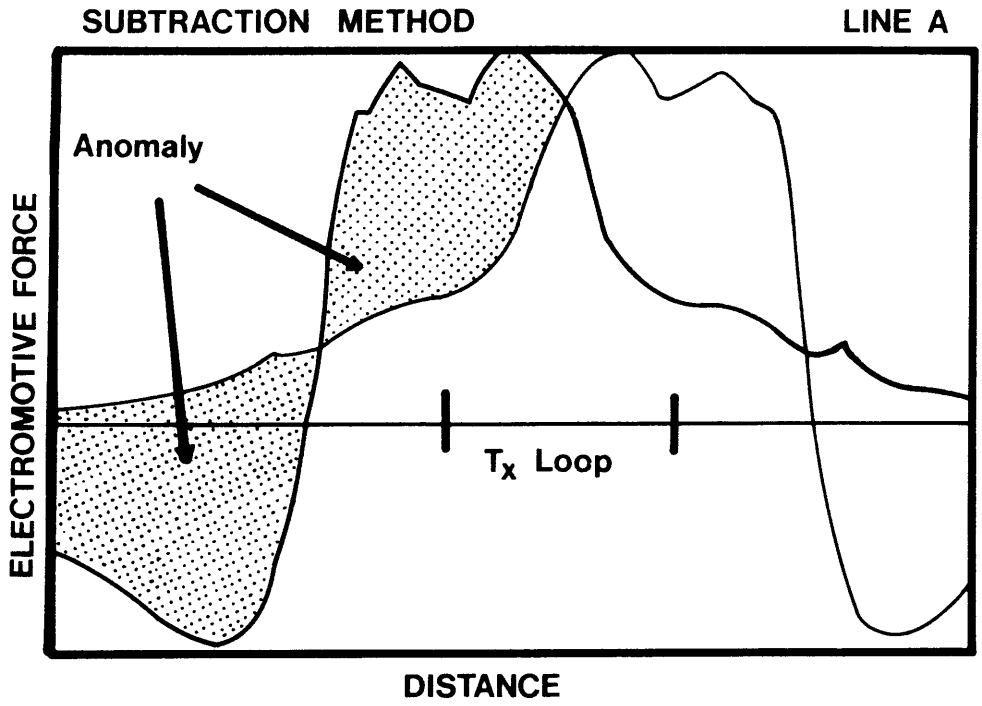

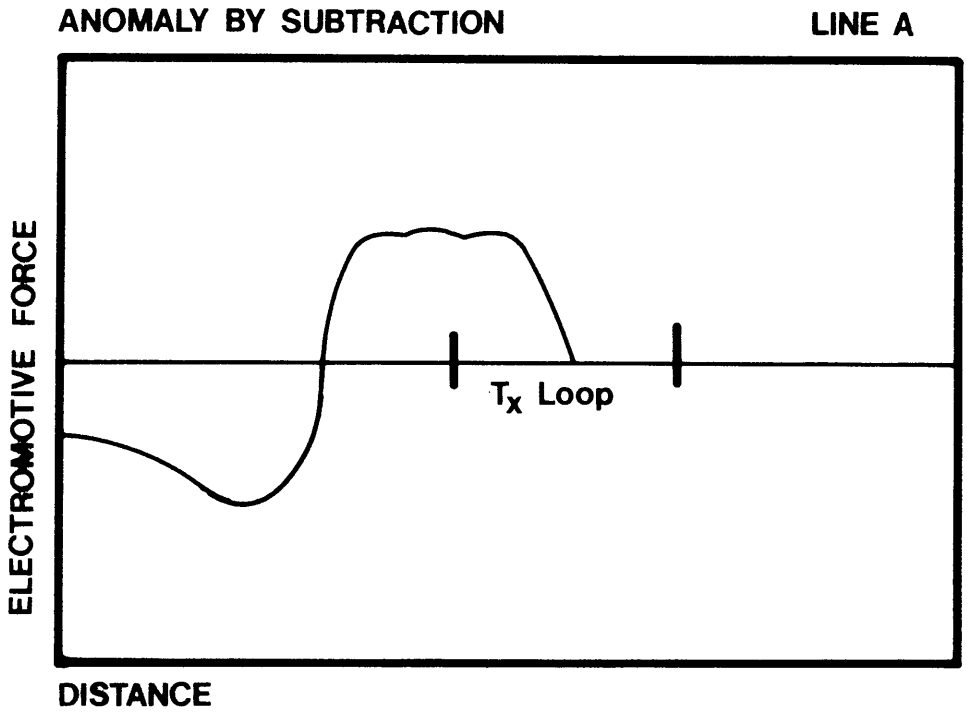

Figure 1.5 Mirrored field profile for subtraction method and isolated anomaly.

the technique could be developed as a fast preliminary interpretation tool for the isolation of anomalies on TEM field profiles. The distortion of the resulting anomalies will have to be weighed against the considerable time saving that results from the use of the filter technique as opposed to the mathematically complex and time consuming processes of calculating the host rock response and then subtracting it from the TEM field profile.

The basic principles and applications of this technique as well as its limitations, advantages and disadvantages will now be discussed in the remainder of this thesis.

CHAPTER 2

THE TIME DOMAIN ELECTROMAGNETIC PROSPECTING (TEM) METHOD

2.1 BASIC PRINCIPLES OF THE TEM METHOD

In the GEONICS EM37 system, an alternating current is generated in the transmitter loop, with a waveform as shown in Figure 2.1. The current waveform consists of an alternating bipolar stepfunction with a slow turn-on and a rapid controlled ramp turn-off.

When the primary field created by a current carrying transmitter loop over a homogeneous earth is suddenly terminated, the transient secondary magnetic field can be represented by a simple current filament of the same shape as the transmitter loop. These filaments move downward and outward with a decreasing amplitude and velocity resembling a system of smoke rings "blown" by the transmitter loop (Nabighian, 1979).

Immediately after turn-off the current is distributed in such a manner as to maintain the magnetic field everywhere at the value that existed before turn-off. The surface currents near the transmitter will start to diffuse into the half-space whereas the current at great distance from the transmitter loop maintains its distribution as it was before turn-off.

The magnitude of the surface current just after turn-off is not a function of the conductivity. However from the relationship of the location of the current density maximum (d) from the centre of the source and the conductivity (σ) namely:

$$d = 2\pi \left(\frac{2t}{\mu\sigma} \right)^{\frac{1}{2}} \qquad \text{(McNeill, 1980)}$$

with (t) the time elapsed after turn-off it is evident that, for increase in conductivity, the distance with which the current density maximum diffuses outwards and downwards, decreases. This illustrates the fact that diffusion in conductive media is a slow process.

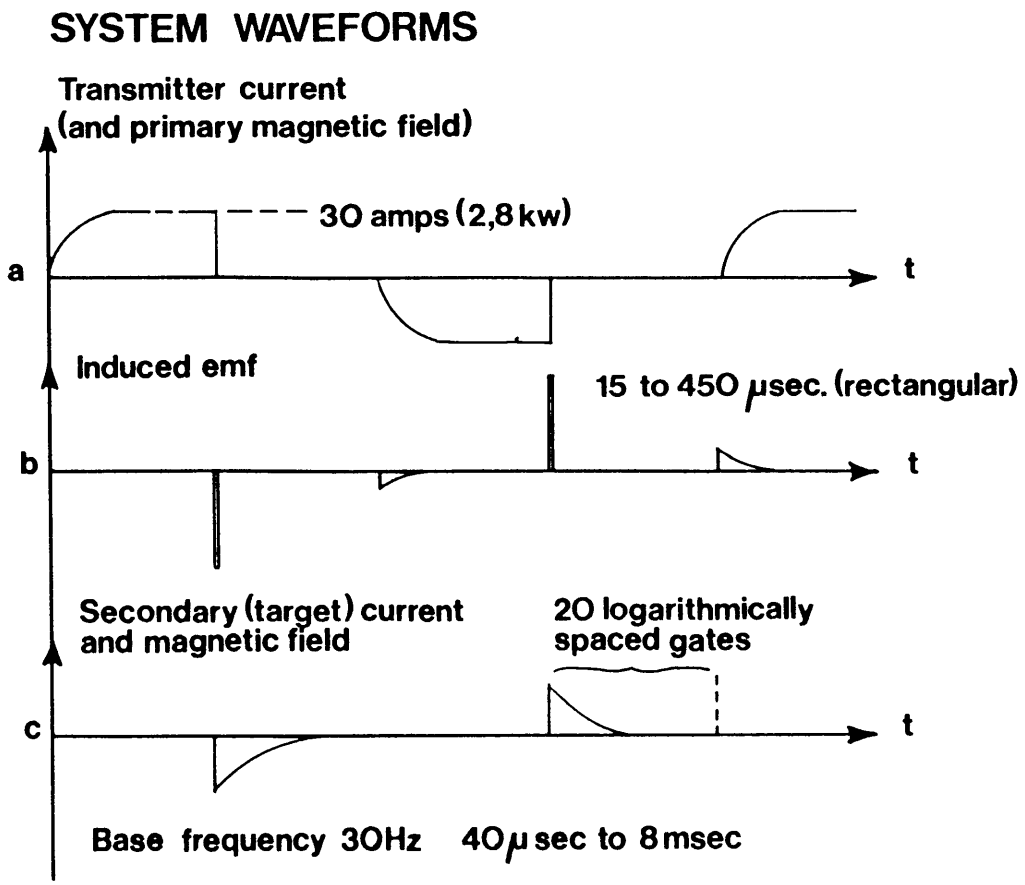

Figure 2.1 System waveforms for the GEONICS EM37 transient electromagnetic system.

If a horizontal thin finite conductive sheet in free space is excited, the behaviour of the surface current flow is similar to that of a homogeneous half-space (McNeill, 1980). Again the initially induced surface current is not a function of the conductivity of the thin sheet. However, here the maximum current density position moves linearly with time as opposed to an outward movement proportional to the square-root of time as in the case of the homogeneous half-space.

In the situation where a target is imbedded below the transmitter loop in a conductive host rock, the secondary field measured at early times, before the diffusing current arrives at the target, will be entirely due to the conductive host rock. As the diffusing current approaches the target the changing magnetic field of the current ring generates the eddy current flow in the target. During this time there is a good deal of electromagnetic coupling between the ring and the target. As time progresses the current ring diffuses onward and the currents in the conductive target commence to decay and later to diffuse outwards into the conductive half-space. At still later times the currents from the target will have dissipated to zero and once again the measured response is that of the homogeneous half-space.

However, McNeill (1980) states that for targets of such size, location and geometry as to give a large response compared to the homogeneous half-space, a time interval exists during which the response of the target and that of the half-space are relatively uncoupled. It is for this case that the filtering method for the removal of the host rock response was investigated.

The base frequencies of the Geonics EM37 can be set at 3, 7.5 and 30 Hz. A base frequency of 30 Hz was used for all the calculations in this thesis. With the Geonics EM37 the transient decay is measured using a portable receiver loop. The measurements are taken at 20 logarithmically spaced time gates or channels. The time windows used for a base frequency of 30 Hz are given in Table 2.1.

CHANNEL NUMBER	GATE CENTRE (Microseconds)	GATE WIDTH (Microseconds)
1	89	18
2	110	24
3	140	27
4	177	36
5	220	40
6	280	72
7	355	76
8	443	100
9	564	142
10	713	156
11	881	180
12	1096	250
13	1411	380
14	1795	390
15	2224	500
16	2850	720
17	3600	780
18	4490	1080
19	5700	1420
20	7190	1560

Table 2.1 Table of gate centres and width for the time channels of the GEONICS EM37 transient system.

Three components of the time-rate of change of the secondary magnetic field can be measured. These are: the component perpendicular to the surface dBz/dt or $\dot{B}z$, the components parallel to the survey line, dBx/dt or $\dot{B}x$ and the component perpendicular to the survey line, dBy/dt or $\dot{B}y$. The observed data are presented as profiles of emf (mV) against distance for a constant time. An example of a field data plot is shown in Figure 2.2.

In the absence of a conductor or if the strike of the conductor is perpendicular to the survey line, $\dot{B}y$ is zero along a survey line that runs through the centre of the transmitter loop. Since only survey lines running through the centre of the transmitter loop are concidered in this thesis, the need to strip the host rock response from $\dot{B}y$ thus does not exist. Therefore only $\dot{B}z$ and $\dot{B}x$ are considered in this thesis. There is no reason to believe that this technique can not be applied to all components or survey lines not running through the centre of the transmitter loop.

2.2 THE TEM HOST ROCK RESPONSE

In order to determine the applicability of the filter technique on field data, the limitations of the technique has to be ascertained on theoretical data where the parameters of the theoretical models can be varied in a controlled manner.

It was decided to:

i. Determine the effect of the filter on host rock (homogeneous isotropic halfspace) responses without a conductor anomaly in order to find the filter parameters needed to completely remove host rock responses. This was done empirically to simulate field interpretation conditions.

ii. Apply the above filter on linear combinations of host rock and plate responses of different parameters in order to determine whether the linear added response can be isolated and to define the range of model parameters for which this can be done.

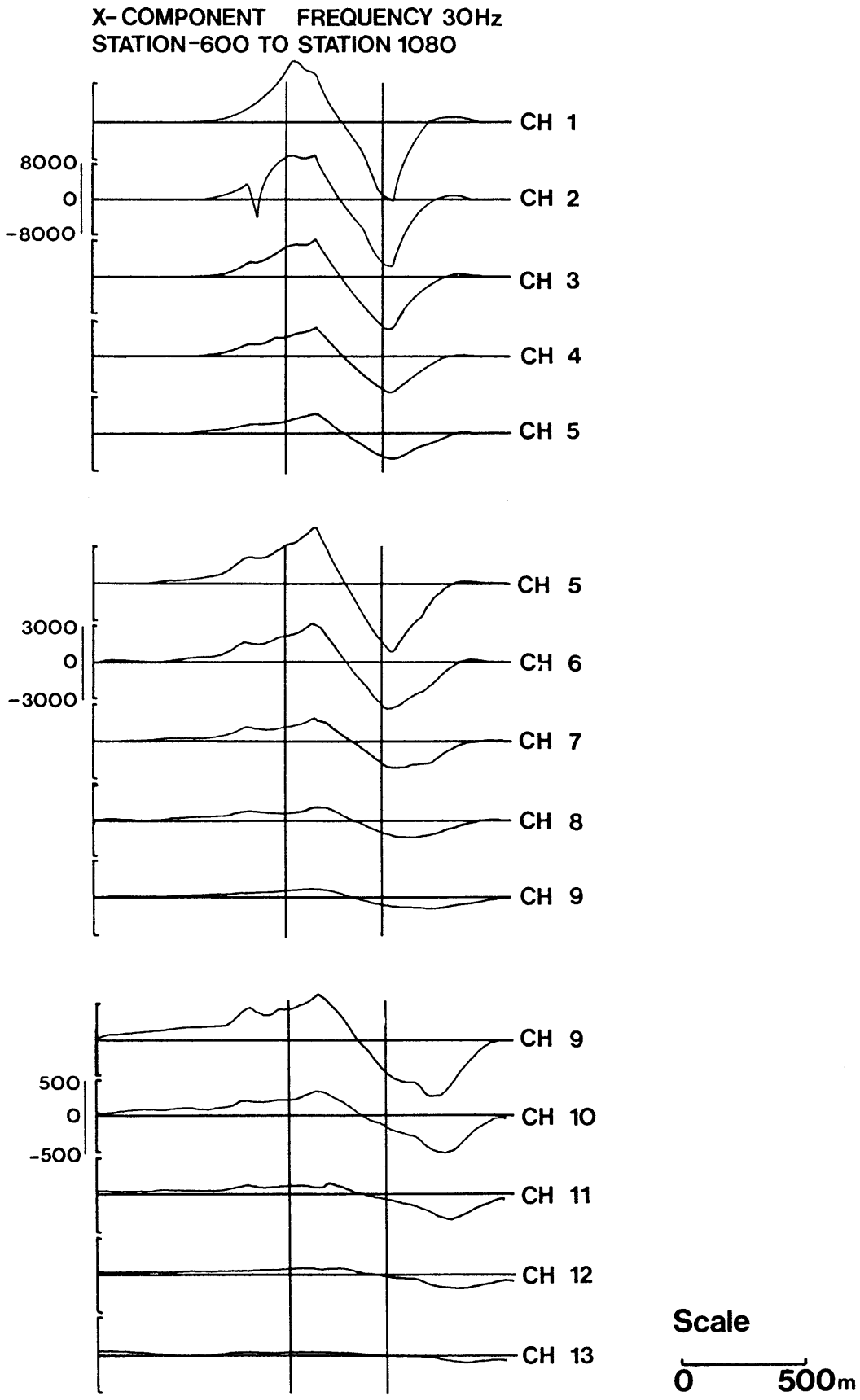

Figure 2.2 Example of a transient electromagnetic field profile plot.

To perform the abovementioned modus operandi theoretical host rock responses were calculated for a host rock varying in conductivity for an arbitrary transmitter loop at any location and at any time, according to the halfspace expression obtained from M. Goldman (pers. comm.) which was adapted for a rectangular loop.

Calculated host rock responses are depicted in Figures 2.3 and 2.4.

2.3 PLATE RESPONSE

To obtain theoretical plate responses the microcomputer based Geonics Plate Program was adapted to run on the Hewlett Packard 9816 microcomputer.

This program is an adaptation of the University of Toronto Plate program (Dyck, *et al.*, 1980). Using this program and free space modelling McNeill (1982) derived a simple late stage behaviour of a rectangular plate. It was found that the plate can be reasonably approximated by a single rectangular loop, 70 percent of the full plate size, and carrying a current $I_0 e^{-t/\tau}$.

Where $I_0 = 0{,}64\, b\, H_0 f_2 \left(\frac{a}{b}\right)$

and $\tau = \mu_0 S a f_1 \left(\frac{a}{b}\right)/10$

with S the conductivity-thickness of the plate, a and b the minor and major plate dimensions, and H_0 the average primary field over the full plate. f_1 and f_2 very slowly with (a/b), both being 1 for a/b=1, and increasing to 1,3 for f_1 and 1,9 for f_2, as a/b goes to zero.

This formed the basis of the Geonics Plate program that was used for plate response calculations in this thesis.

Typical plate responses for $\dot{B}z$ and $\dot{B}x$ are depicted in Figure 2.5.

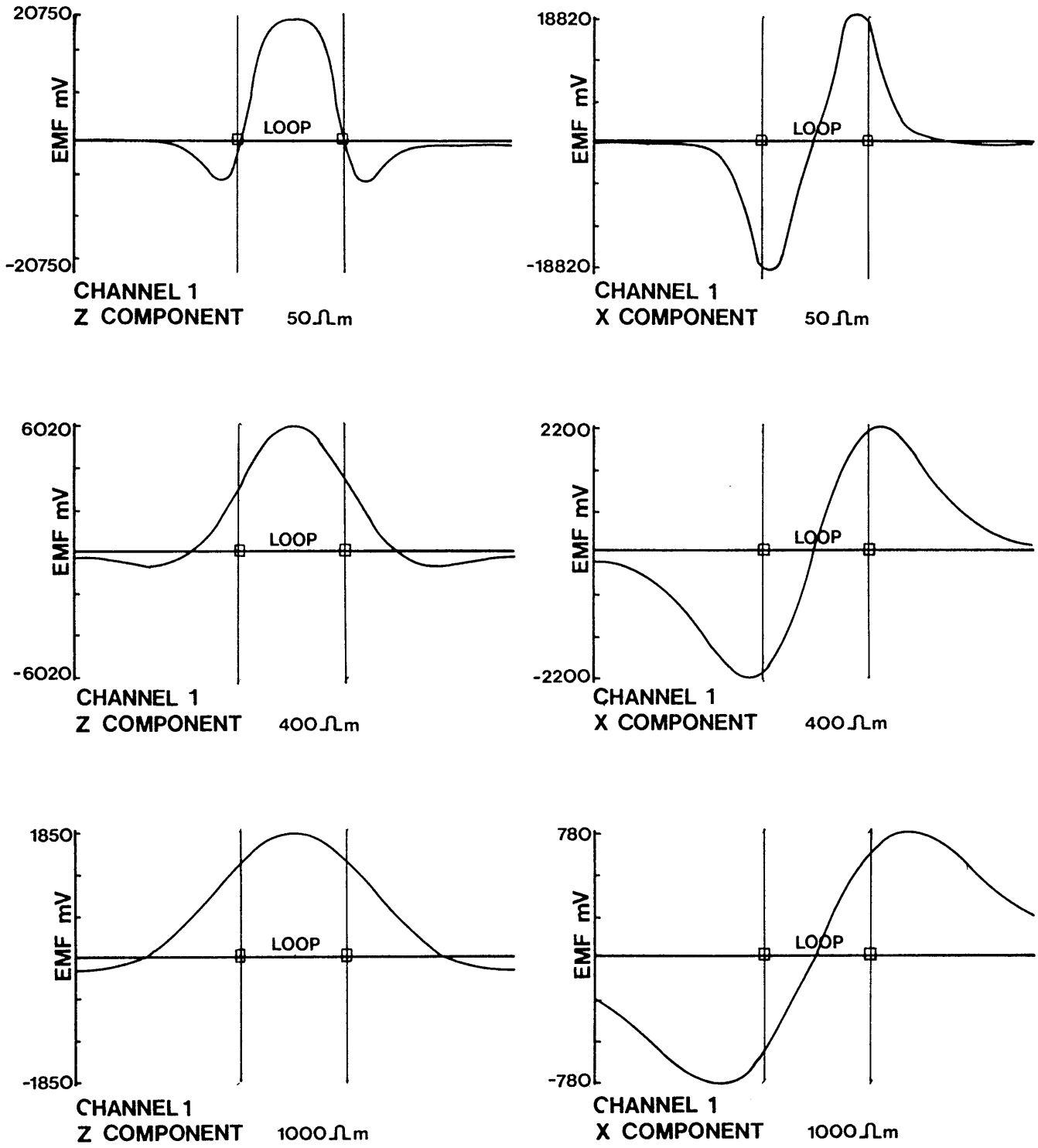

Figure 2.3 Calculated host rock responses for 50, 400 and 1000 ohm.m for channel 1. Bz and Bx components.

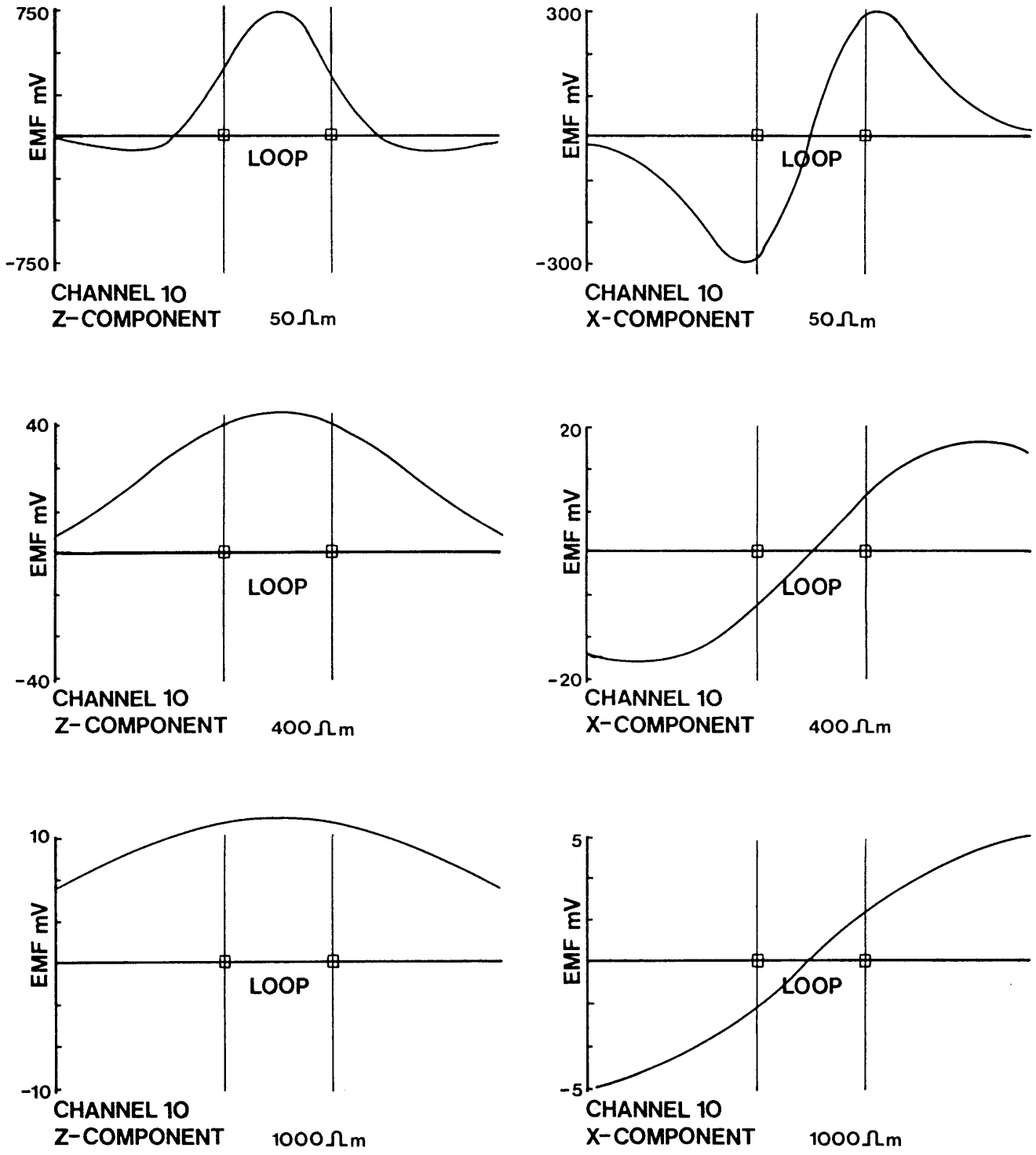

Figure 2.4 Calculated host rock responses for 50, 400 and 1000 ohm.m for channel 10. $\dot{B}z$ and $\dot{B}x$ components.

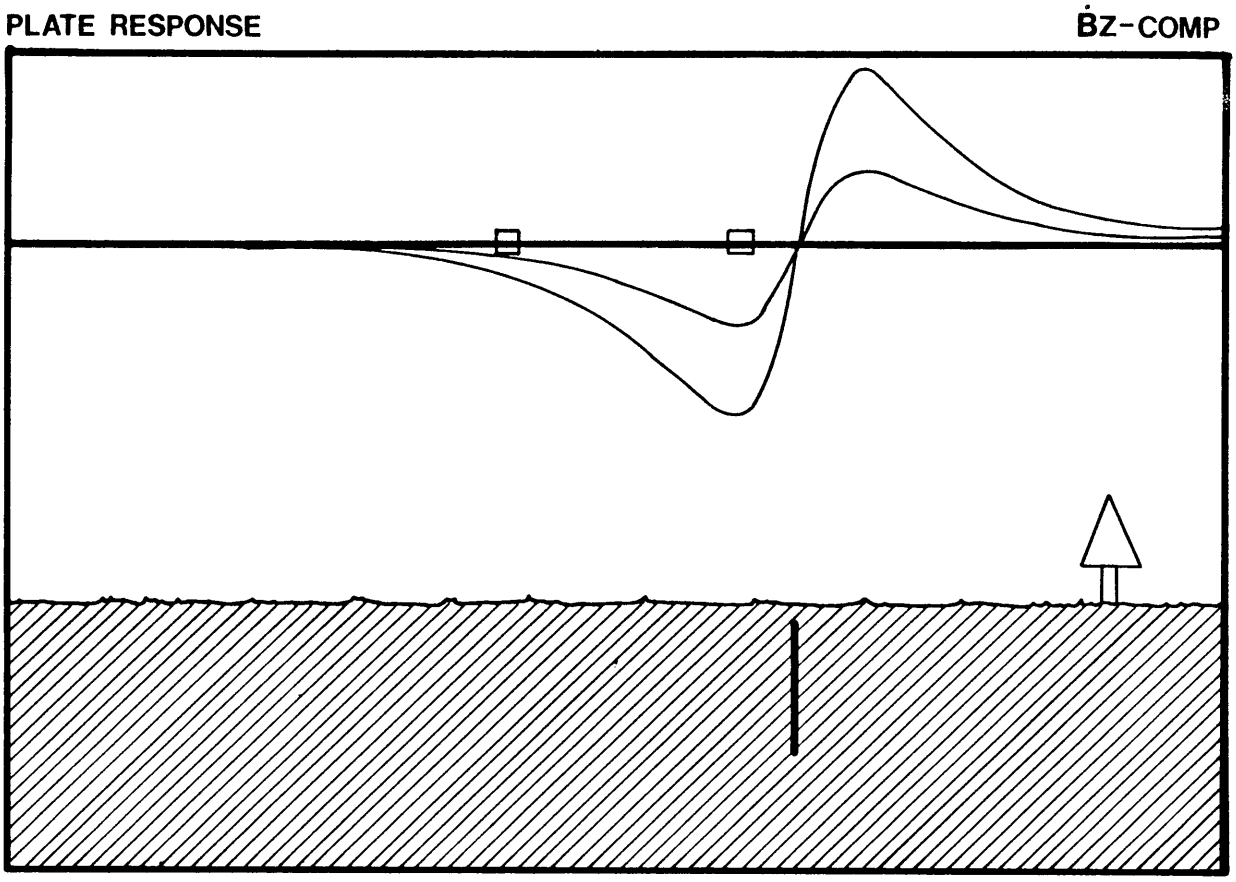

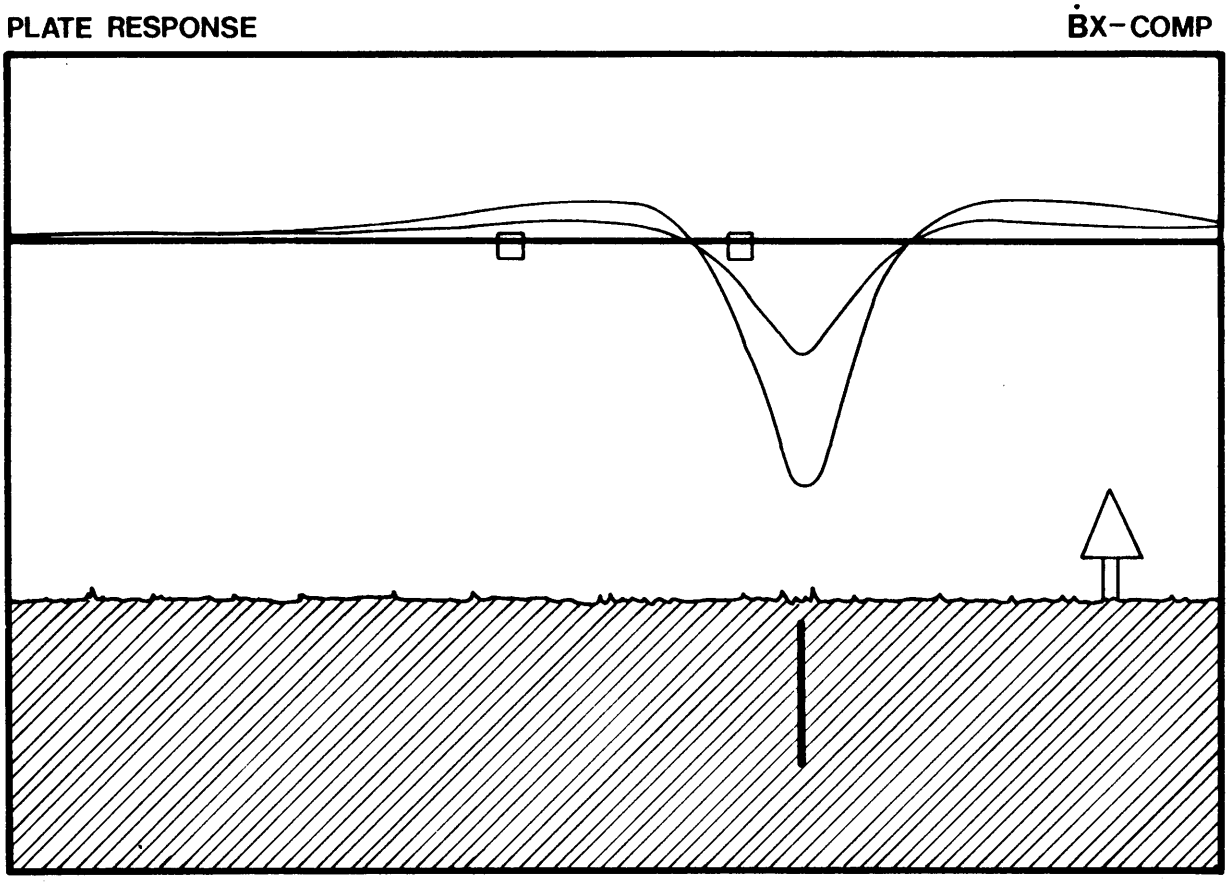

Figure 2.5 Typical plate responses for $\dot{B}z$ and $\dot{B}x$ components.

CHAPTER 3

TIME TO FREQUENCY DOMAIN TRANSFORMATION

3.1 FOURIER TRANSFORMATIONS

In order to examine the frequency content of the time domain electromagnetic data it is necessary to have a complete understanding of the Fourier theorem and transforms.

The Fourier Transform was initially developed for continuous, periodic functions. Since most cases in geophysics represents discrete non-periodic functions, it is necessary to expand the initial Fourier Transform to accommodate discrete non-periodic functions.

By replacing integrals with summations and summing over small enough intervals, the Fourier Transform of discrete functions are performed. Periodicity is achieved by assuming that any data beyond the last data points will produce an exact repetition of the data set.

The mathematical principles outlining the above-mentioned are highlighted in Appendix A. A fast algorithm to perform Fourier Transforms digitally, making use of 2 data points, n=3,4,5---, and the binary pairing of Fourier coefficients, was made popular by Cooley and Tukey (1965).

A suitable computer program, that calculates the Fast Fourier Transform (Clearbout, 1976) was obtained in basic (Higgins, 1976) and was adapted to run on the Hewlett Packard 9816 microcomputer. The FFT program in HP Basic 3.0 is given in Appendix B.

3.2 WINDOWING AND PADDING OF THE DATA SET

Since the discreet Fourier transform cannot approximate discontinuities in the data set the ends of the data set must be tapered down to the mean value which is mostly zero. This also implies the removal of a trend.

As described by Kaufman and Keller (1981):

"The effect of truncation of the time function during sampling is a smearing of the spectral curve. The smeared curve is a damped oscillatory function in which numerous subsidiary peaks appear where no actual energy was present in the correct spectrum. This is termed "leakage" of energy from the existing frequency to other frequencies which do not exist. If in the true spectrum, very small amounts of energy are present at these frequencies where side lobes occur, the spectrum will produce erroneous values for impedance terms. It is important to minimise this leakage effect; it can be done in two ways."

Because the second method refers to analogue filters it is not applicable to this thesis and the first method is quoted.

"(1) Leakage can be reduced by using windows which are not abrupt at ends. Two popular windows are the Hamming and the Hanning windows. The equation for these two windows in the time domain are:

Hanning: $d_2(\tau) = \frac{1}{2}\left(1+\cos\pi(n/N)\Delta t\right)$, $\tau \leq N\Delta t$ (15.11)

$= 0$, otherwise

Hamming: $d_3(\tau) = 0{,}54\left(1+0{,}85\cos\pi(n/N)\Delta t\right)$, $\tau \leq N\Delta t$ (15.12)

$= 0$, otherwise

The Fourier transforms of the two windows are:

$$D_2(\omega) = \frac{\sin\omega N\Delta t}{\omega} = \frac{\pi(n/N)\Delta t}{\omega^2-\left(\pi(n/N)\Delta t\right)^2}\sin\omega\pi\frac{n}{N}\Delta t \qquad (15.13)$$

$$D_3(\omega) = \frac{0{,}54\sin\omega N\omega t}{\omega} + \frac{0{,}46\pi(n/N)\Delta t}{\omega^2-\left(\pi-(n/N)\Delta t\right)^2}\sin\omega\pi\frac{n}{N}\Delta t \qquad (15.14)$$

Thus by making the digitized record sufficiently long, and by applying the appropriate tapering function such as a Hamming or Hanning window, the leakage from the strong frequency component to the adjacent frequencies can be made quite small." (Kaufman and Keller, 1981, p.461).

It was decided to use a Hamming filter on the data. However, a Hanning filter could just as easily been used before transformation.

However, the FFT routine as described required the amount of data set values to be of the form 2^{γ} with γ an integer. It was thus necessary to pad the field data sets to the desired length. Since the average TEM field profile considered in this study, contains between 50 and 60 data points, a padded data set of 64 was considered nearest to the ideal case.

In order to counter the loss of real data when the windowing function is applied to the data, it is necessary to pad the data set symmetrically.

Two approaches for padding the data set normally exists.

i. A low order polynomial background field is removed whereafter the data set can be padded with zero's.

ii. Extending the dataset symmetrically by padding it to the left and right of the first and the last value respectively. Thereafter a Hamming window is used to smooth down the dataset to zero at the edges.

Figure 3.1 depicts a dataset that was padded with 10 values to the left and right hand side with respectively decreasing values as shown. After removal of the low frequency content of the spectrum by filtering, the effect of the sharp angle cut off, can be clearly seen on the reverse transformed dataset. This clearly illustrates the problems that may occur if an incorrect padding/windowing is used.

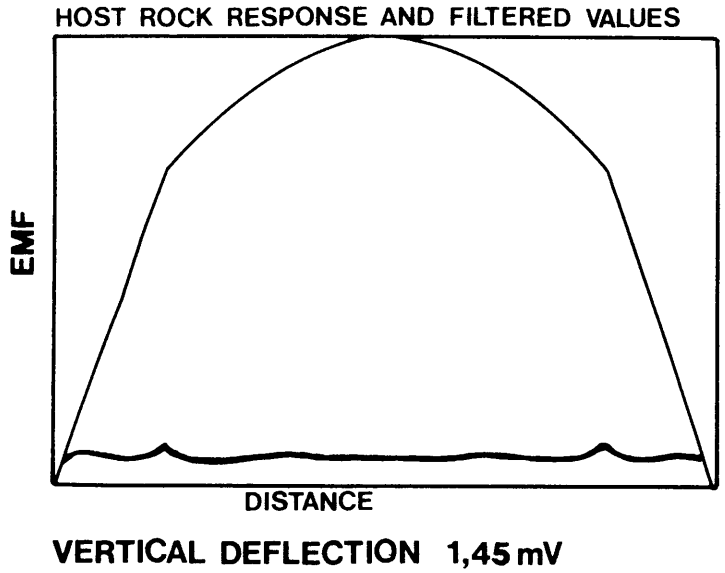

Figure 3.1 Typical host rock response padded with 10 per cent decreasing end values including the reverse transformed graph.

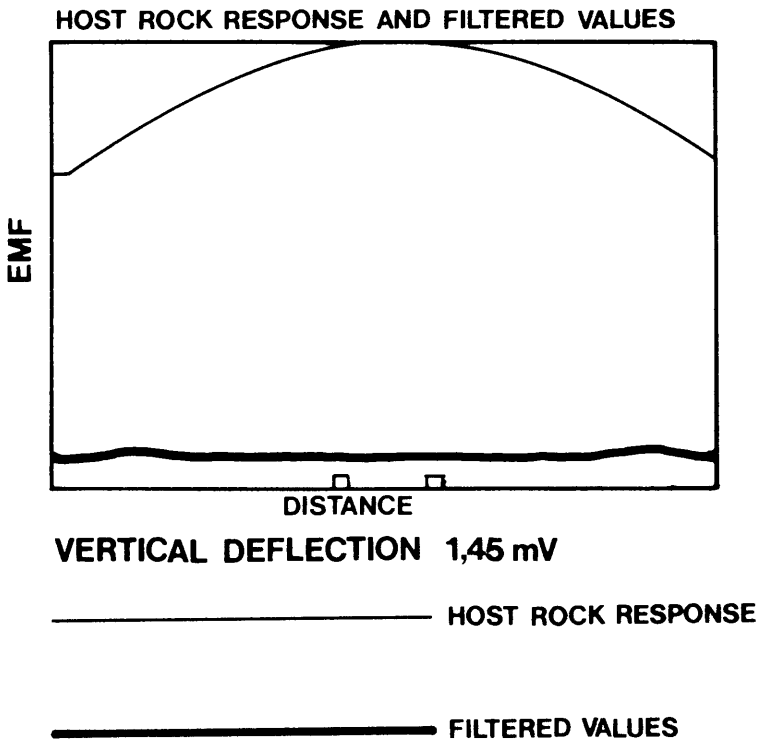

Figure 3.2 Typical host rock response padded with first and last values including the reverse transformed graph.

With the abovementioned facts in mind it was decided to expand the data set by repeating the first and the last observed value to obtain the desired amount of data points. Figure 3.2 depicts the same data set as in Figure 3.1 but on this profile it was padded using the abovementioned padding technique. The data was also subjected to a Hamming windowing function before transformation. Comparing this graph with Figure 3.1 it can be seen that, after removal of the low frequency content of the spectrum, the effect of the change over between the data set and the padding is drastically reduced in the reverse transformed plot.

The abovementioned type of data set was specifically chosen because in EM37 profiling it represents the worst case data set as far as edge effects for host rock responses are concerned, i.e.

i. The start and end values lie far off from the zero level.

ii. The gradient of the start and end point is not close to zero as is the case in most of the host rock responses.

iii. The data set considered, is for a late time channel where the maximum amplitude is quite small. Furthermore an anomaly in a late time channels is of very small amplitude and consequently any effects added to the data as a result of filtering would distort the anomaly completely.

The host rock removal filtering method was then tried on a variety of theoretical host rock response profiles to determine its effectiveness. In each case the profile was transformed, filtered and transformed back to the time domain to yield a filtered profile. Figures 3.3 depicts a flow diagram that explains the modus operandi for the removal of the host rock response by filtering in the frequency domain.

Figure 3.4 depicts examples of early and late channel host rock responses for both $\dot{B}z$ and $\dot{B}x$ components. It can clearly be seen that the reverse transformed profiles contain minimum edge effects.

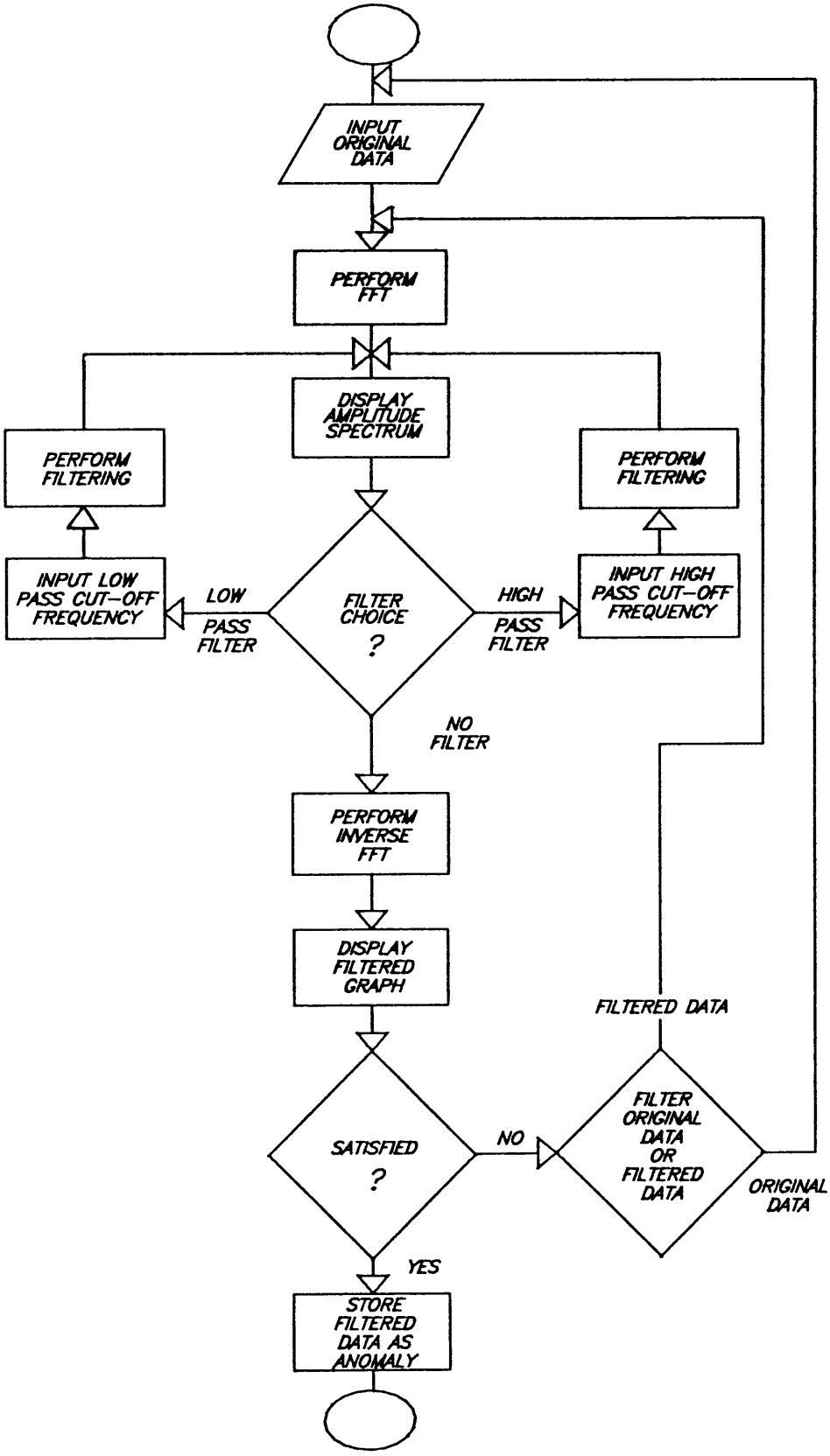

Figure 3.3 Flow diagram to illustrate the removal of a host rock response from time domain electromagnetic data using the filtering method.

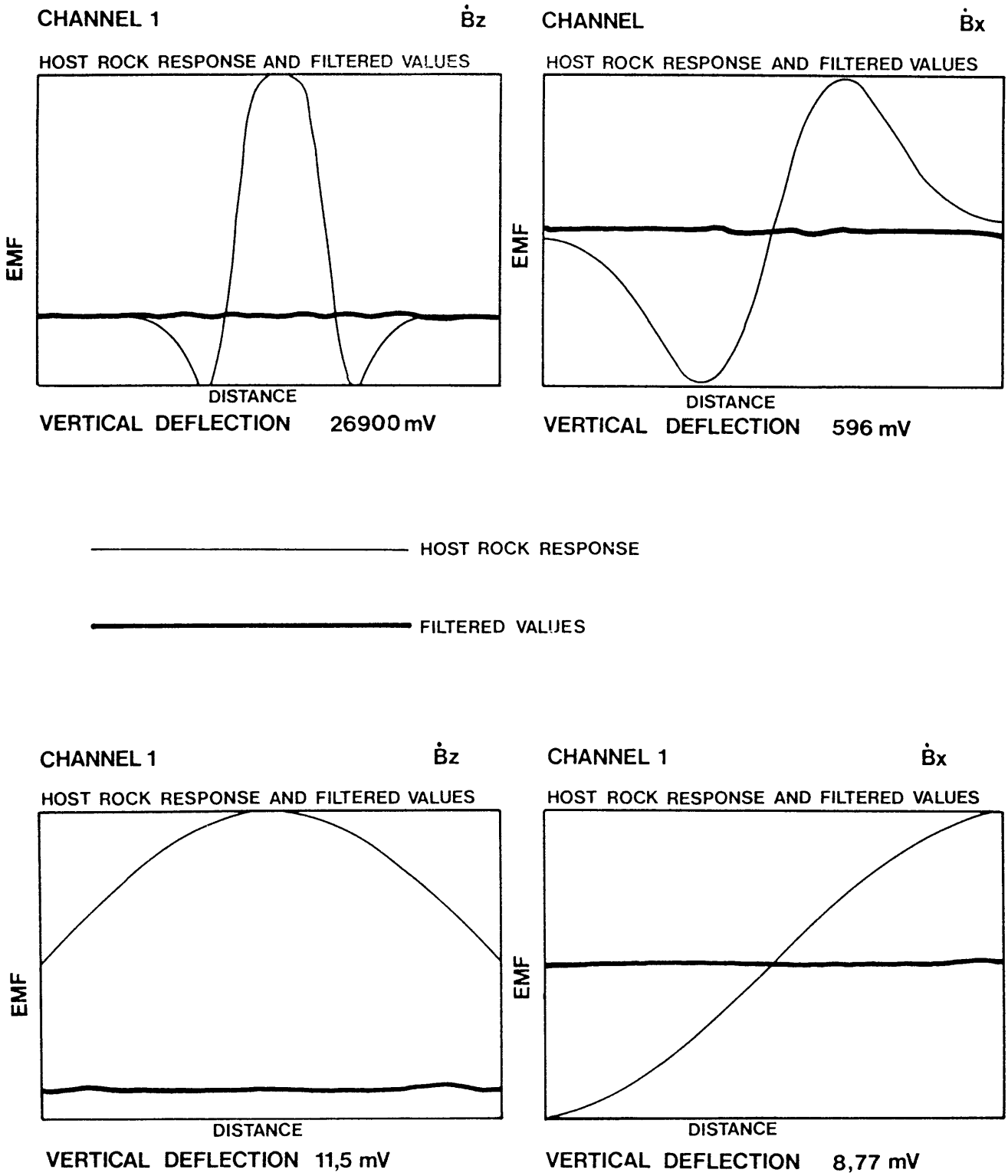

Figure 3.4 Examples of host rock responses. Pre- and filtered values.

Finally the filtering method was applied to combined profiles consisting of host rock and plate responses. Figure 3.5 depicts various combinations of host rock and plate responses for different time channels but only the reverse transformed graphs are shown. In each case it can be seen that the edge effects are reduced to an extent where it would not pose any problem as far as anomaly recognition is concerned.

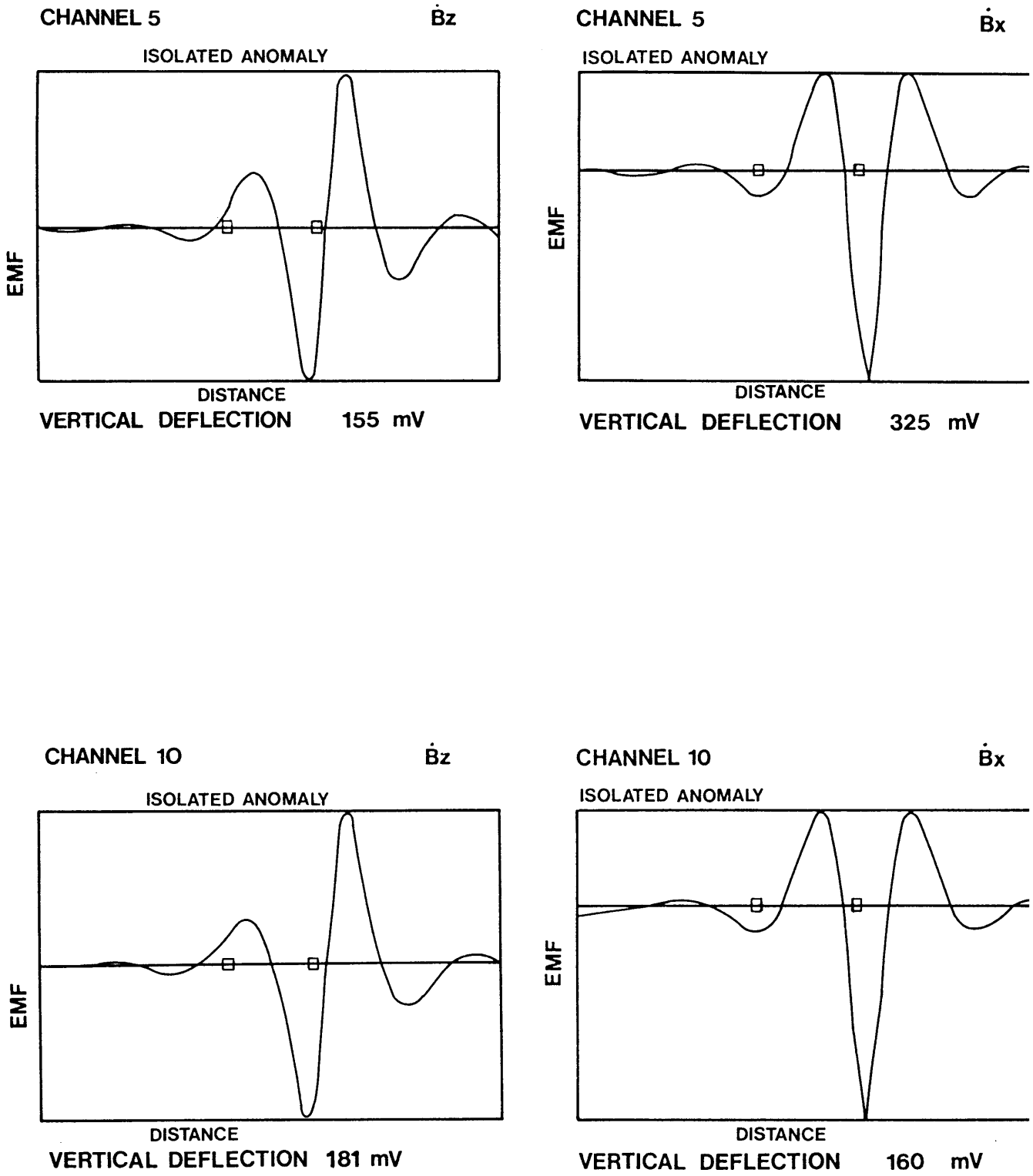

Figure 3.5 Examples of combined host rock responses after filtering of the data.

CHAPTER 4

CHOICE OF FIELD SURVEY PARAMETERS

4. RESEARCH AREA

In order to make a successful appraisal of the filter technique it is necessary to limit the area of interest to coincide with real survey situations. Without this one could fall into the trap of employing model parameters which are of no use to the interpreter.

4.1 PRACTICAL CONSIDERATIONS

From field experience it has been learned that the host rock resistivities most often encountered in mineral exploration in South Africa, varied between 50 and 1000 ohm.m. Although terrains with resistivities of more than 1000 ohm.m do exist in South Africa it was found that the host rock responses of host rocks with resistivities higher than 1000 ohm.m is relatively flat and does not interfere with anomaly recognition. Host rock response calculations were made for host rock resistivities ranging from 50 to 1000 ohm.m with a non-linear incrementation, and the smallest increments at the lower resistivities.

References to late and early times, except where specifically otherwise mentioned, is given with respect to the Geonics EM37 time gates (Table 2.1). For the considered resistivity range, channels 1 to 10 are referred to as early time/channels and channels 10 to 20 as late time/channels.

Since a change in the field lay-out and survey parameters, listed below, are fairly constant in any profiling survey situation, default values, obtained from field experience, were assigned to them. The values were kept constant for all the calculated responses.

Transmitter loop current	:	16A
Transmitter turn-off time	:	220µs
Transmitter loop dimension	:	400m x 400m
Base frequency	:	30Hz
Station spacing	:	50m

The standard survey line used extended 1000m on both sides from the centre of the transmitter loop.

The results obtained from the host rock response program are millivolts and are normalised to a gain of 64.

The examination of host rock responses for which the parameters fall within the specified range and experience gained from the use of the traditional host rock removal techniques mentioned in Chapter 1 revealed the following:

I. For TEM field profiles where the host rock resistivity, time (ρt) relationship is large, the removal of the host rock response is not a problem. This is due to the fact that the host rock response has either decayed to an insignificant contribution of the total response (low resistivity, late time) or is relatively flat representing a D.C. off-set (high resistivity, early time).

II. On late time profiles where the host rock resistivity is high (ρt very high) the anomaly can easily be recognised and with some degree of success be interpreted without the removal of the host rock response.

Based on these observations it was felt that the filter technique could make its biggest contribution to anomaly recognition and isolation in the early channels and for low resistivities (ρt low values). It was thus decided to, with the specified host rock resistivity range, confine the times for investigation to channels 1 to 10.

4.2 PARAMETER DESCRIPTION OF THE PLATE RESPONSE

The plate model and survey configuration used are depicted in Figure 4.1.

The plate reference is defined at the midpoint of the top edge of the length of the plate. The two plate dimensions are the strike length and the depth extent. The depth referred to throughout this thesis, is to the top of the plate.

i. Strike

The strike direction is parallel to the edge of the transmitter loop. The plunge is 0 degrees for all the models calculated.

ii. Dip

The dip direction measured clockwise from the positive x-axis. It was decided that only plates of 90 degrees would be examined.

iii. Depth extent

The depth extent of the plate was chosen to be 300m although a change in depth extent does change the anomaly it was decided to keep it constant because varying the depth extent would increase the amount of combinations to such an extent that it would be virtually impossible to examine all the responses. Since the depth to the top of the conductor has a much stronger influence on the anomaly, this parameter was varied.

iv. Strike length

In order to have a plate with a strike length larger than the depth extent, the strike length was set on 600m. (This is an adjustable parameter in the program.)

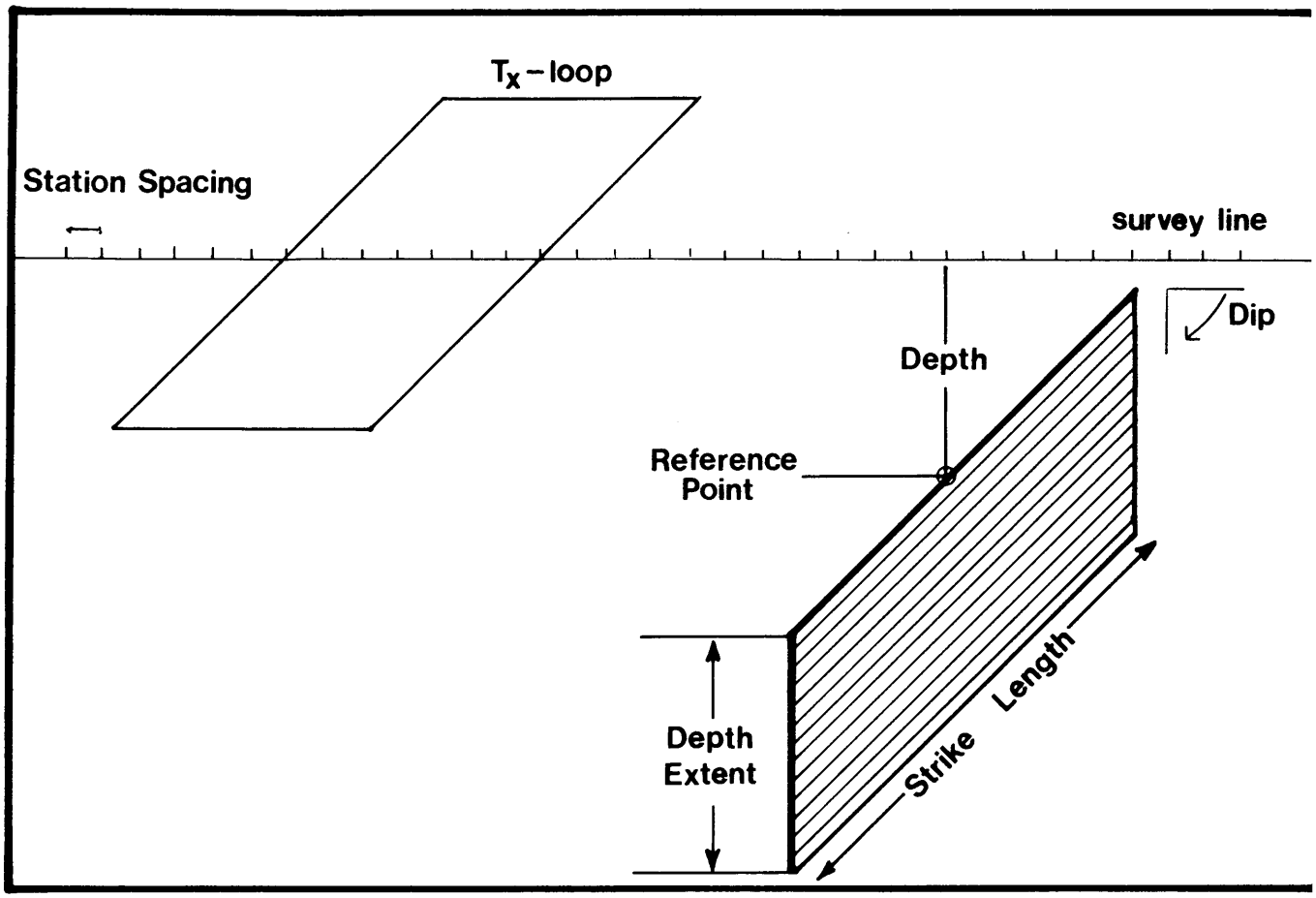

Figure 4.1 Plate model and survey configuration.

v. Depth to top of plate

The depth to the top of the plate was chosen to be within the range of 20 m to 140 m. An upper limit of 20m was chosen, since a plate with a depth of less than 20m would have an easily recognizable anomaly. At a depth greater than 140m the spatial extent of the anomaly becomes large with a corresponding spectral shift into the low frequency spectrum and thus merging with the low frequency content of the host rock response. It was thus decided not to examine plates with depths larger than 140m.

vi. The conductivity-thickness product (S)

Because the plate programs results are only valid for the late time plate responses, three conductivity-thickness products were calculated. The first represents the late time plate response for channel 1, the second for channel 5 and the third for channel 10. These were determined using the following formula: $\theta=\mu_0 Sa/4t$ (Gallagher *et al.*, 1985). Here μ_0 is the magnetic permeability of free space, t is the time measurement and a is the shortest dimension of the plate.

For the late time range θ=2,0 to 2,3 (Gallagher *et al.*, 1985) and with the shortest length dimension 300 m (downward extension) the following conductivity thickness products were calculated and used:

Channel 1 (t=0,089ms)	S=2 siemens
Channel 5 (t=0,11ms)	S=5 siemens
Channel 10 (t=0,14ms)	S=20 siemens

With all the above parameters decided upon it was now necessary to calculate host rock and plate responses for various combinations.

4.3 HOST ROCK AND PLATE RESPONSES CALCULATED

Table 4.1 contains a list of the host rock responses calculated. Table 4.2 contains a list of all the plate responses that were calculated.

HOST ROCK RESISTIVITY (ohm.m)	CHANNELS	COMPONENTS
50	1,5,10	$\dot{B}z$ and $\dot{B}x$
100	1,5,10	$\dot{B}z$ and $\dot{B}x$
200	1,5,10	$\dot{B}z$ and $\dot{B}x$
300	1,5,10	$\dot{B}z$ and $\dot{B}x$
400	1,5,10	$\dot{B}z$ and $\dot{B}x$
600	1,5,10	$\dot{B}z$ and $\dot{B}x$
800	1,5,10	$\dot{B}z$ and $\dot{B}x$
1000	1,5,10	$\dot{B}z$ and $\dot{B}x$

Table 4.1 Host rock parameters of all the responses calculated.

DEPTHS (m)	CHANNELS	CONDUCTIVITY THICKNESS PRODUCT (Siemens)	COMPONENTS
20	1,5,10	2,5,20	$\dot{B}z$ and $\dot{B}x$
40	1,5,10	2,5,20	$\dot{B}z$ and $\dot{B}x$
60	1,5,10	2,5,20	$\dot{B}z$ and $\dot{B}x$
80	1,5,10	2,5,20	$\dot{B}z$ and $\dot{B}x$
100	1,5,10	2,5,20	$\dot{B}z$ and $\dot{B}x$
120	1,5,10	2,5,20	$\dot{B}z$ and $\dot{B}x$
140	1,5,10	2,5,20	$\dot{B}z$ and $\dot{B}x$

Table 4.2 Plate parameters of all the responses calculated.

CHAPTER 5

AMPLITUDE SPECTRA AND FILTERING IN THE FREQUENCY DOMAIN

In order to make an assessment of the use of the technique, all the host rock and plate responses calculated, were, in order to obtain amplitude spectra, transformed to the frequency domain via the FFT algorithm as previously discussed. These amplitude spectra were then examined visually.

5.1 AMPLITUDE SPECTRA OF HOST ROCK RESPONSES

Figure 5.1 to 5.3 depicts the amplitude spectra of the following host rock responses. Resistivities of 50, 400 and 1000 ohm.m for channel 1 and both components $\dot{B}z$ and $\dot{B}x$.

From this one can clearly see that:

i. the frequency content of low resistivity host rock responses differs from that of higher resistivities;

ii. low resistivity host rock responses have amplitude spectra with relative high frequency content.

The above can be explained if one investigates the diffusion velocities and eddy current behaviour (Nabighian, 1979) for conductive and a resistive host rock. As explained in Chapter 2, the more conductive the host rock media the lower the diffusion velocity of the "smoke rings". However, the eddy current for a conductive media is a combination of a set of small intricate eddy currents each with its own secondary magnetic field. The total response is the sum of all the responses of small eddy current systems. The frequency content of such a response thus contains a higher frequency content contributed by the individual high frequency eddy current systems.

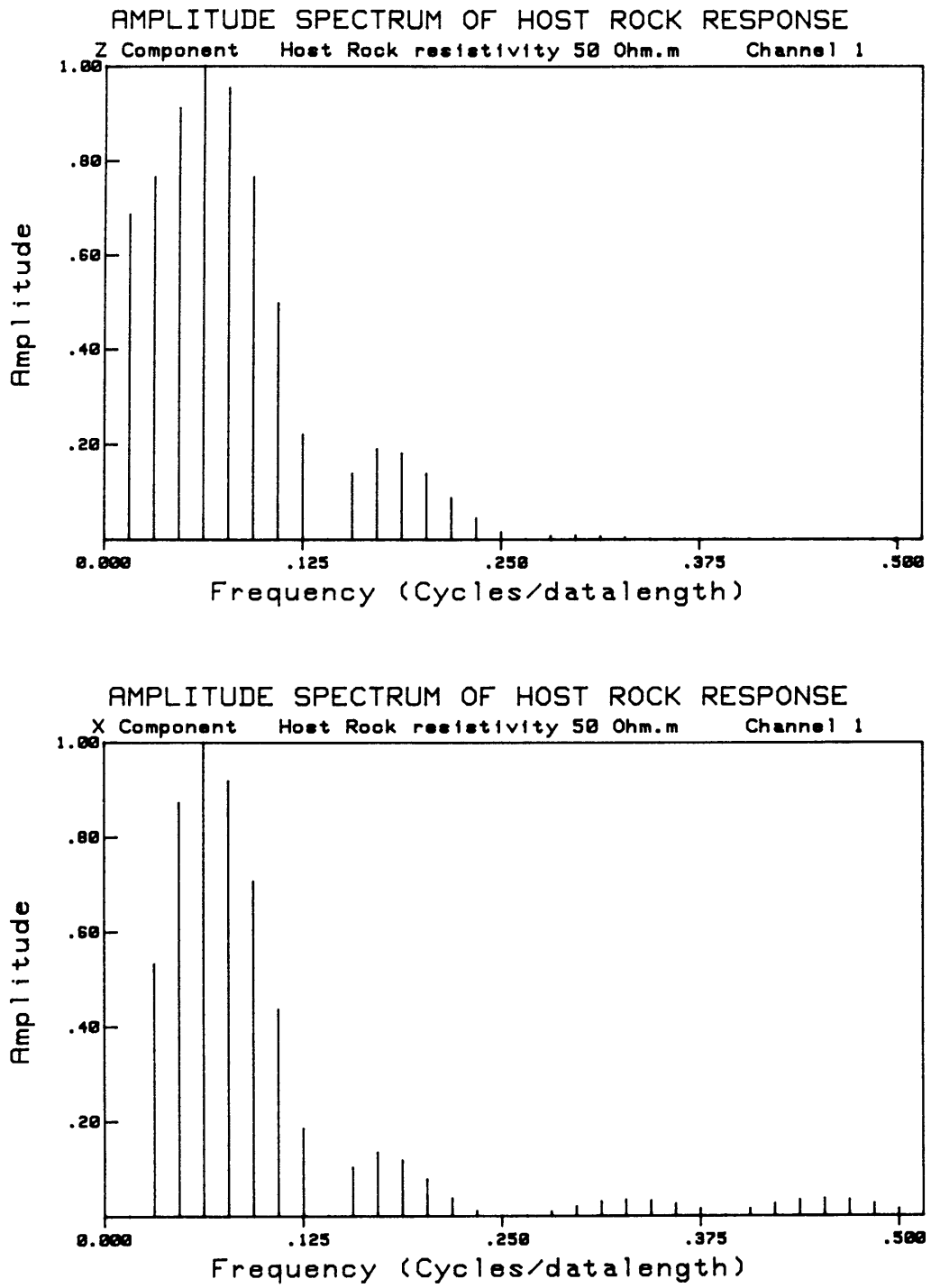

Figure 5.1 Channel 1 amplitude spectra of 50 ohm.m host rock response for both $\dot{B}z$ and $\dot{B}x$ components.

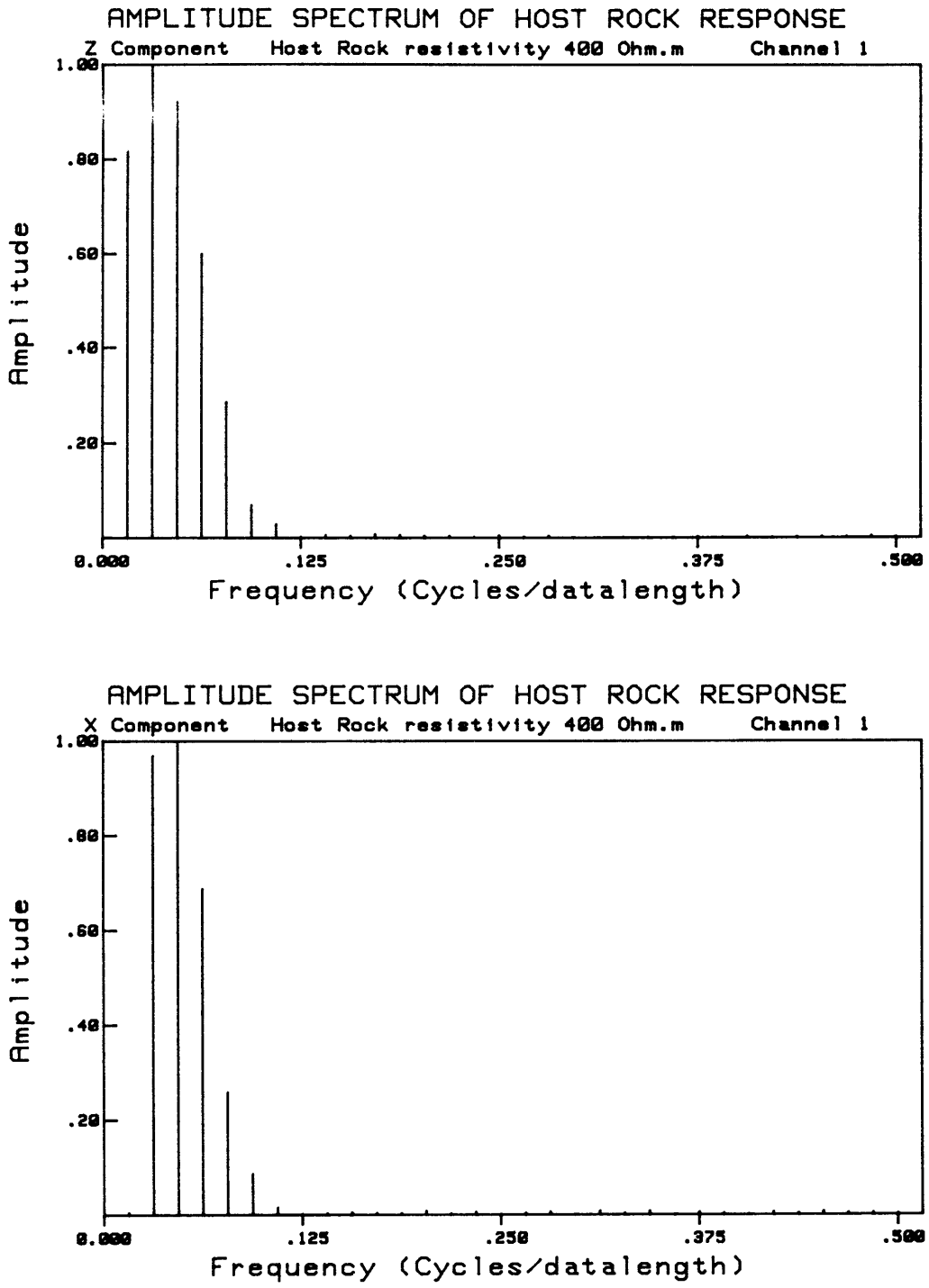

Figure 5.2 Channel 1 amplitude spectra of 400 ohm.m host rock response for both $\dot{B}z$ and $\dot{B}x$ components.

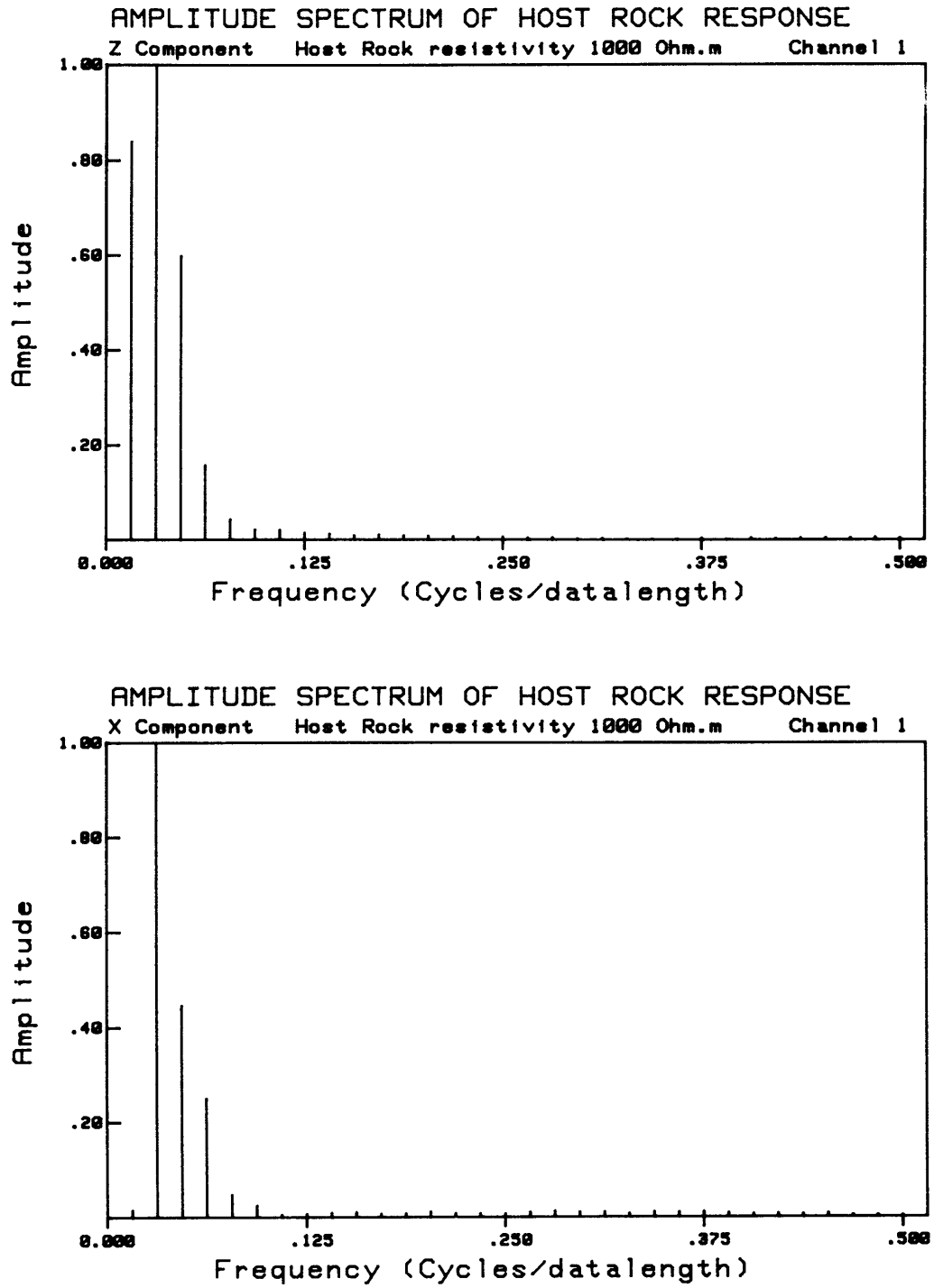

Figure 5.3 Channel 1 amplitude spectra of 1000 ohm.m host rock response for both $\dot{B}z$ and $\dot{B}x$ components.

This gives an indication that the separation of a plate response, with a relative high frequency content, from a high resistivity host rock responses, would be achieved more successfully than to separate the same plate response from a host rock response with a low resistivity. The verification of this will be seen later.

Figure 5.4 to 5.6 shows how the high frequency content of the amplitude spectra of host rock responses of 50, 400 and 1000 ohm.m diminishes as one moves into late channels. The conclusion that is made from this is that this technique would be more successful in late channels. It shall be shown later, that although this is true, the technique does work for early channels under certain constraints.

From the study of the amplitude spectra of the host rock responses it becomes clear that one would not be able to eliminate the frequency content of the host rock responses using a rigid filter. One thus needs a filter that has different characteristics when applied on host rock responses of different channels and resistivities.

5.2 FILTER CHOICE

"(1) Frequency filtering. This type of filtering is applicable as soon as the wave components exhibit enough frequency difference. The success of the filtering depends on the degree of frequency separation between the components. If frequency ranges partially overlap, separation will not be complete and the filtering action will effect the spectrum to be constructed. On the other hand, if frequency separation is virtually complete, then this kind of filtering will be very effective. It is the most usual filtering method in geophysics." (Båth, 1974).

The above describes the essence of the filter technique as studied in this thesis.

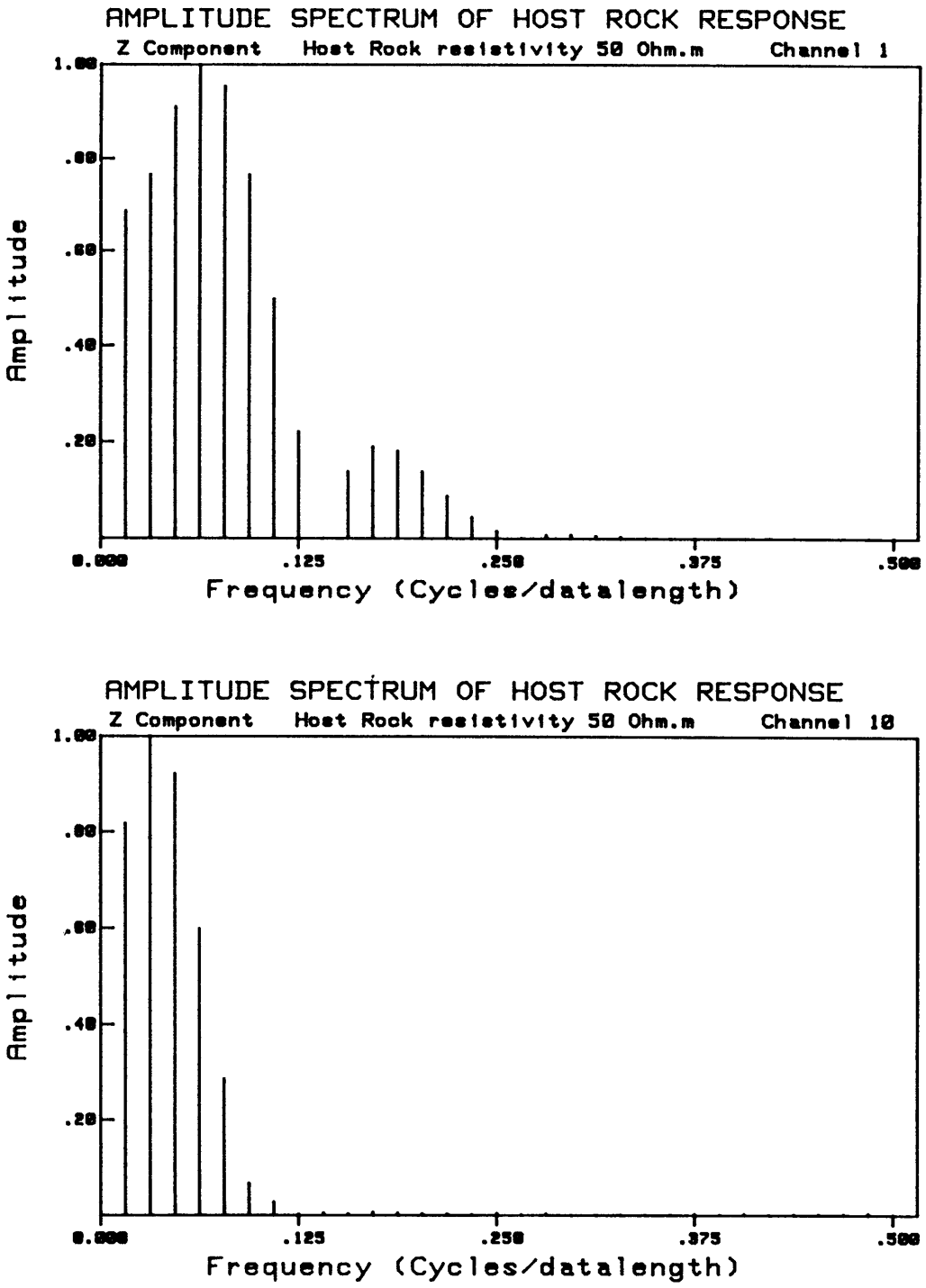

Figure 5.4 Channels 1 and 10 amplitude spectra of 50 ohm.m host rock responses for the $\dot{B}z$ component.

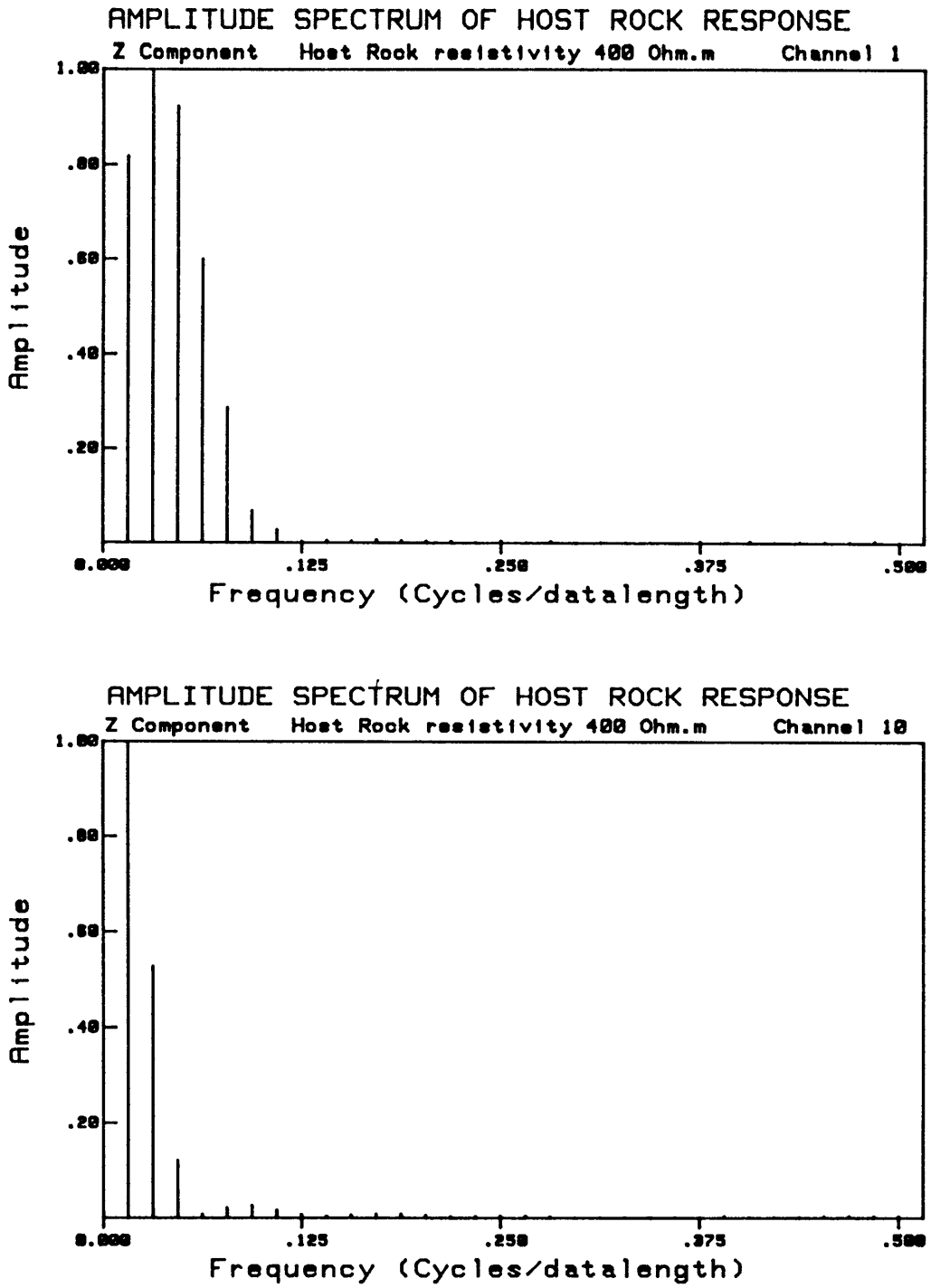

Figure 5.5 Channels 1 and 10 amplitude spectra of 400 ohm.m host rock responses for the $\dot{B}z$ component.

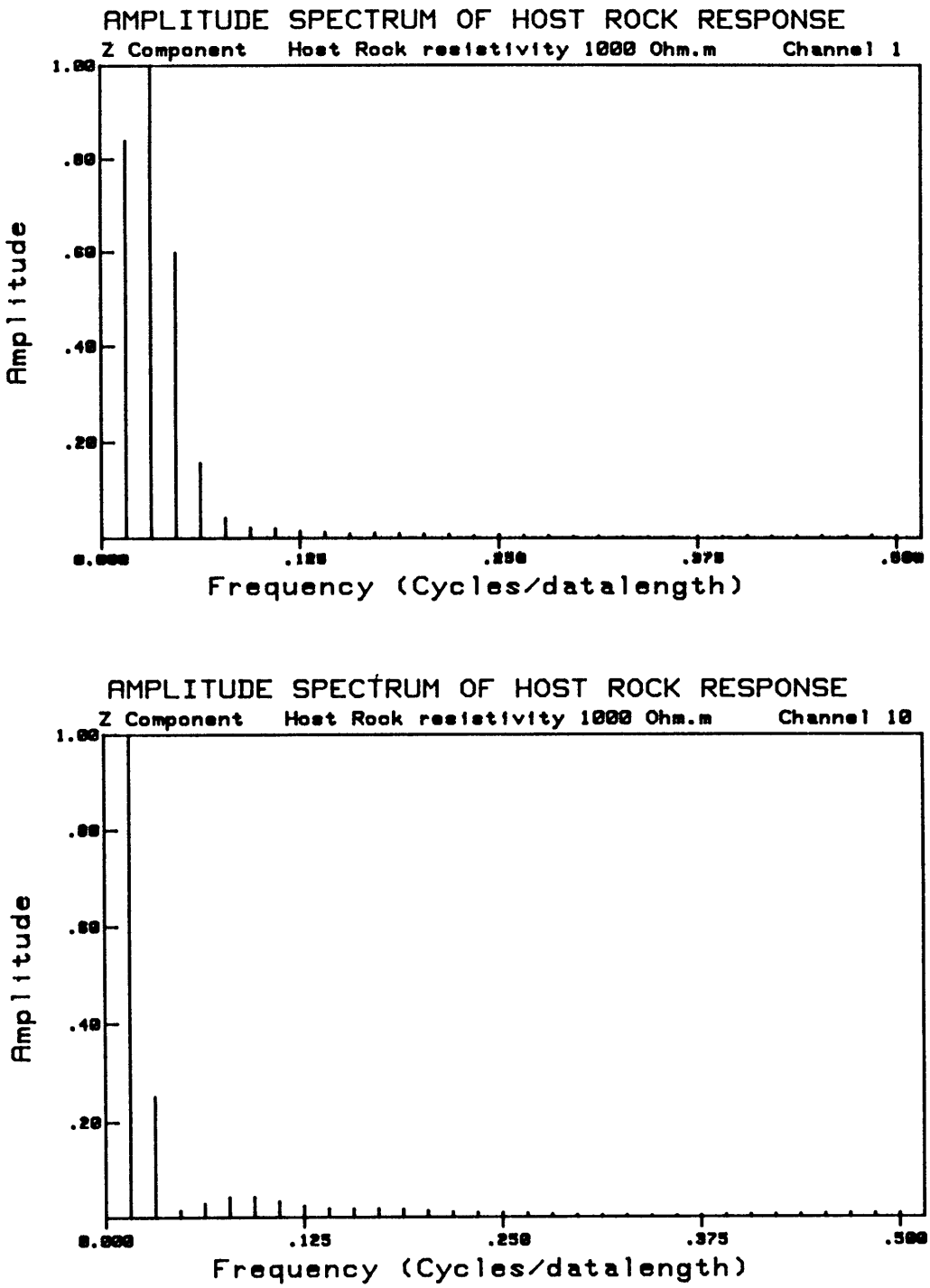

Figure 5.6 Channels 1 and 10 amplitude spectra of 1000 ohm.m host rock responses for the $\dot{B}z$ component.

The host rock response is generally of a lower frequency than the anomalies present, thus it was decided to use a high pass filter of the following sort:

$$e^{-2\pi af^2}$$

with f the cut-off frequency and a the sharpness of the filter.

From the visual examination of the amplitude spectra the shape of the filter, as depicted in Figure 5.7, one can see that the cut-off frequency will have to change for different resistivities and channels. Since cases do exist where the separation of the frequency content is not complete is was decided to choose the sharpness of the filter as steep as possible without causing distortion due to ringing.

5.3 NOMOGRAM FOR CUT-OFF FREQUENCY

As an aid to the choice of which cut-off frequency to use for specific resistivities and channels a nomogram with cut-off frequency versus channel for different resistivities was determined.

This was done by taking each amplitude spectrum of the different host rock responses and then submitting it to a high pass filter with a cut-off frequency of 0,25 cycles/datalength. This maximum was arrived at by visual examination of the amplitude spectra. The result obtained after filtering the data was then examined. The cut-off frequency was then decreased and the filter re-applied on the original data. The cut-off frequency at which the frequency content of the host rock response is no more completely eliminated, were noted. Figure 5.8 depicts a flow diagram that gives a visual explanation of the filitering method.

This was done for both $\dot{B}z$ and $\dot{B}x$ for the entire range of resistivities. The results were plotted on a linear scale and are represented in Figures 5.9 and 5.10.

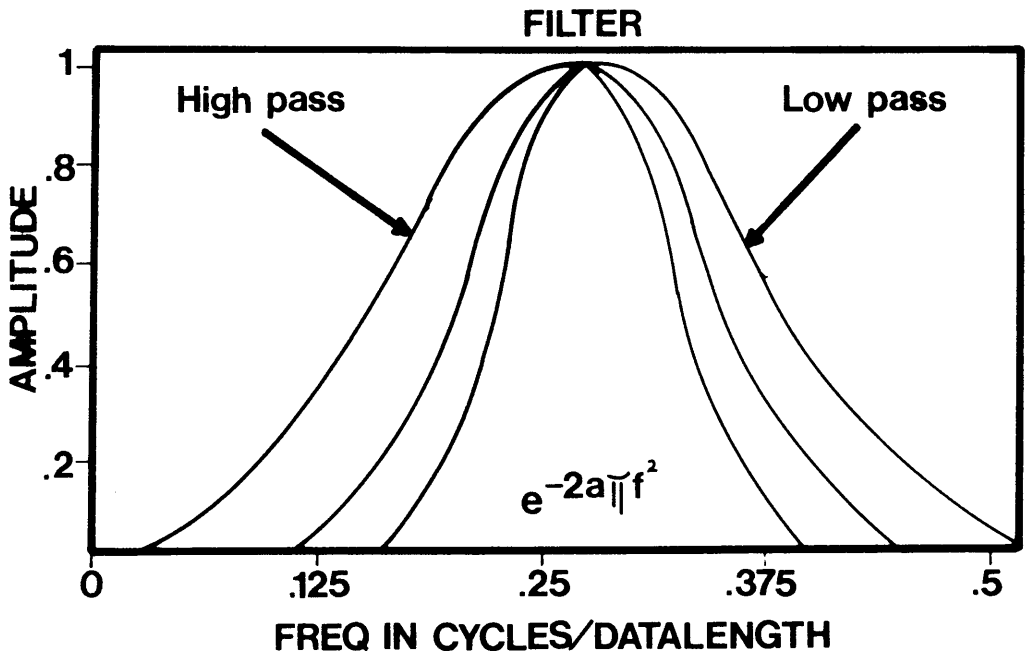

Figure 5.7 Filter shapes for different sharpnesses.

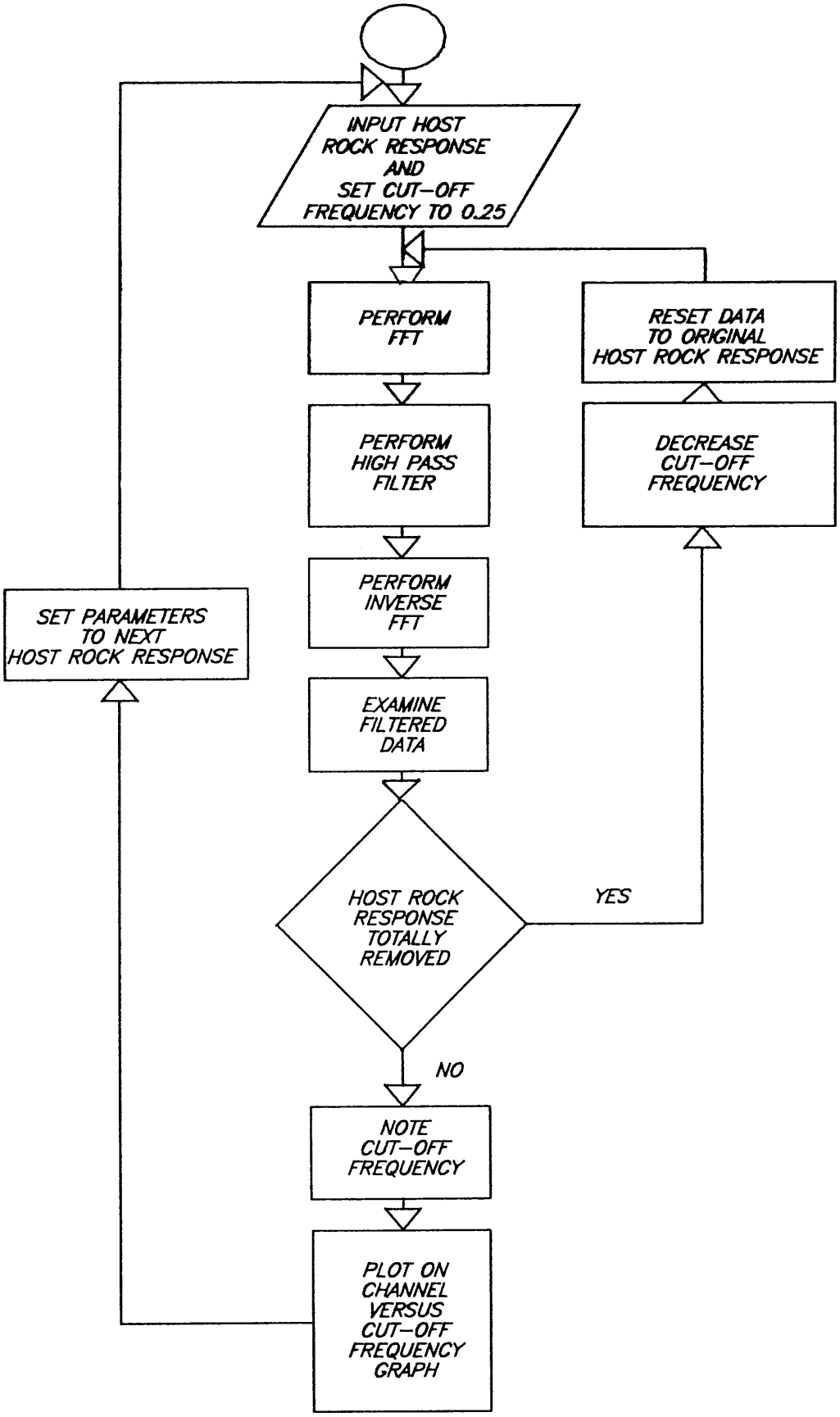

Figure 5.8 Flow diagram to illustrate the determination of the filter cut-off frequency for the removal of the host rock response from theoretical host rock and plate response combinations.

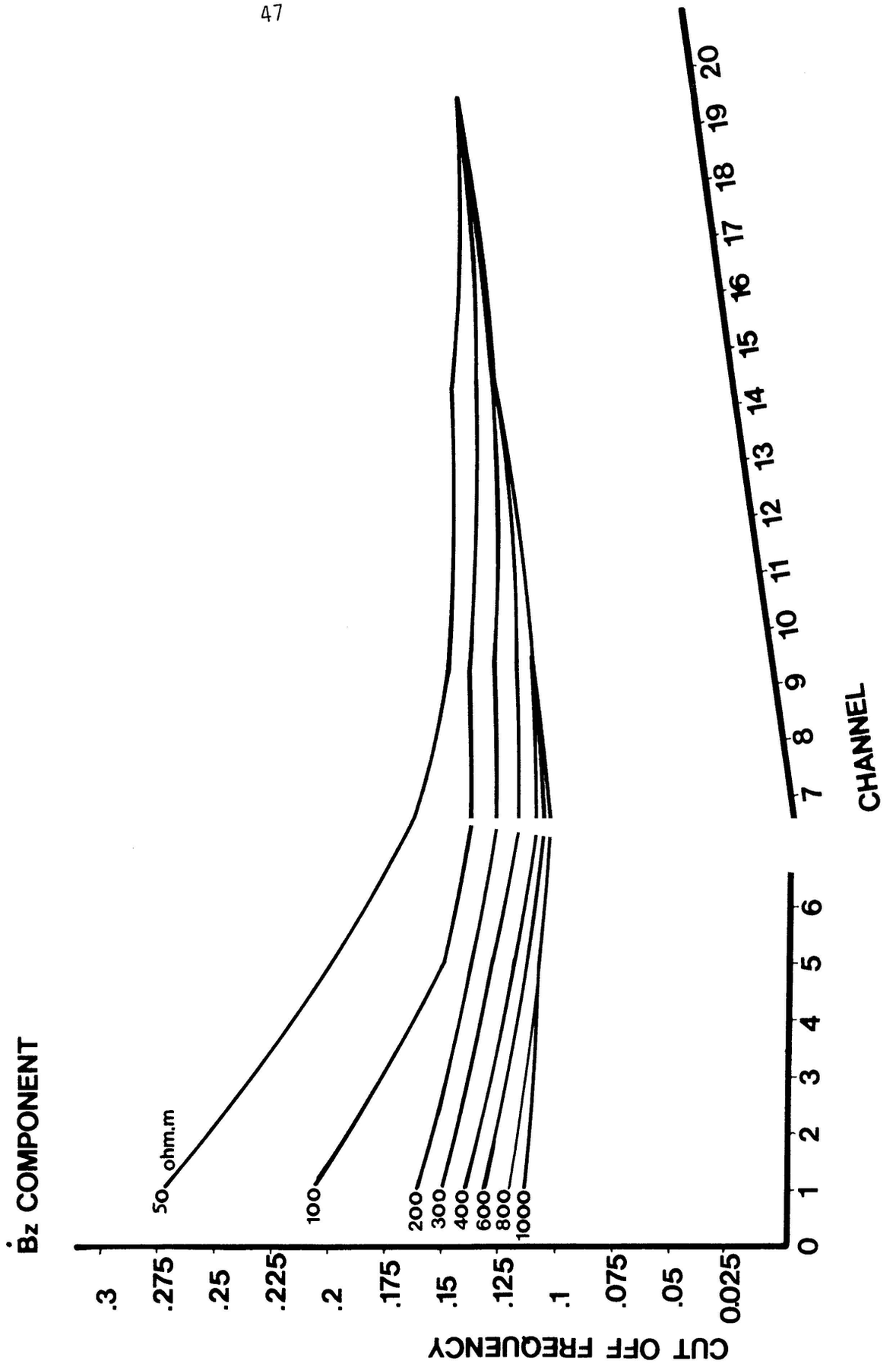

Figure 5.9 Nomogram of cut-off frequency versus time channels for different resistivities for the Ḃz component.

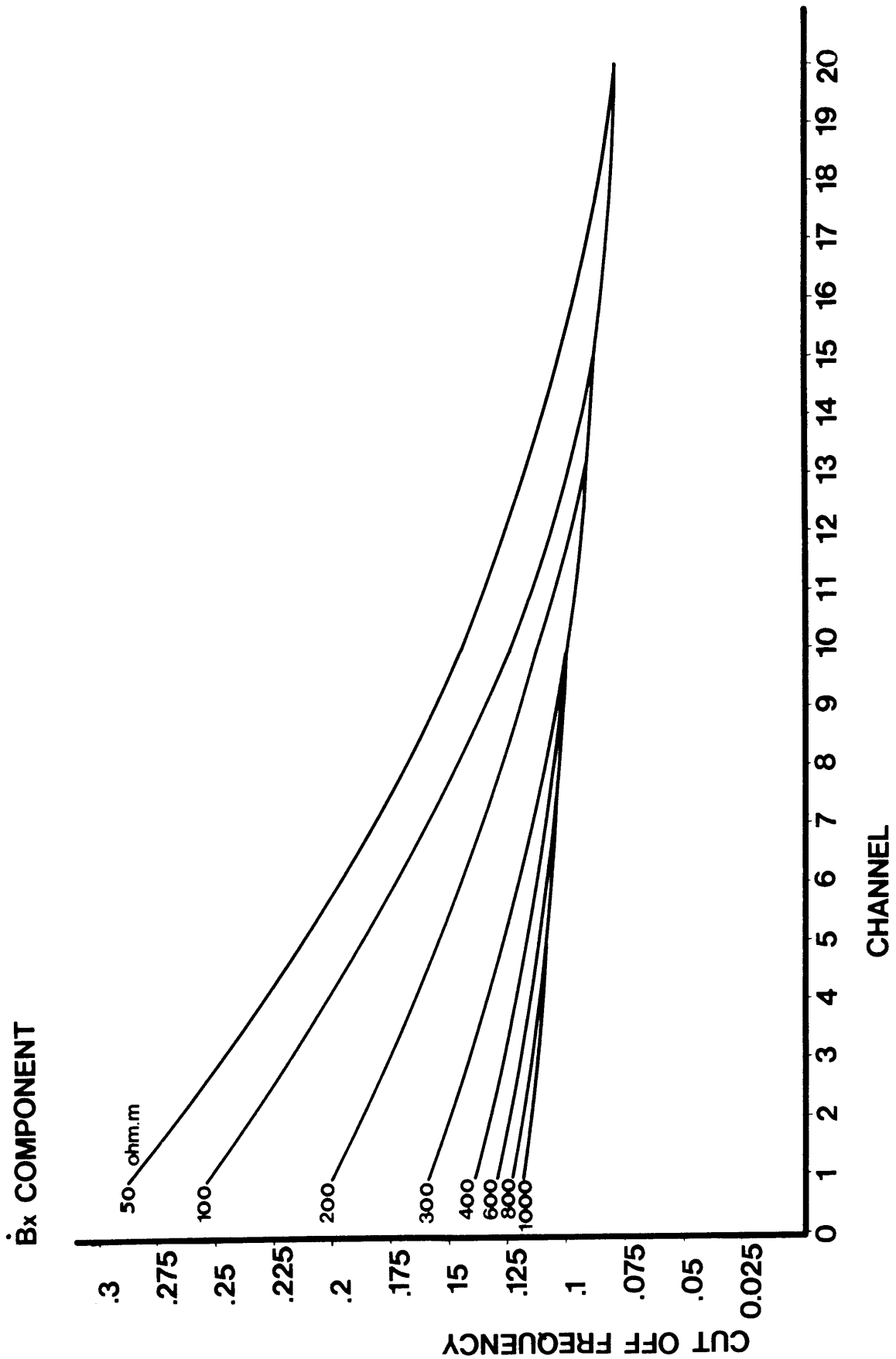

Figure 5.10 Nomogram of cut-off frequency versus time channels for different resistivities for the Ḃx component.

From this nomogram, if a rough estimate can be made of the resistivity of the host rock or survey area, the lowest cut-off frequency needed to empirically filter out the complete host rock response, from a given data set, can be obtained. This can be done for any channel.

5.4 AMPLITUDE SPECTRA OF PLATE RESPONSES

Figures 5.11 and 5.12 depicts amplitude spectra of plate responses with a variety of parameter combinations. From this it is evident that the amplitude spectra of plate responses change very little for different parameter combinations chosen. However, in comparison with amplitude spectra of host rock responses, the spectra of plate responses contains a noticeable high frequency component.

5.5 THE AMPLITUDE RESPONSES OF COMBINATIONS OF HOST ROCK AND PLATE RESPONSES

As explained in Chapter 1 a linear combination of the plate and host rock response can under certain conditions be treated as a fair approximation of the responses as measured in nature (McNeill, 1982; McNeill *et al.*, 1984). By linearly adding host rock responses (low frequencies) to the plate responses (high frequencies) it is expected that one would be able to, in the amplitude spectra of the combined response, distinguish between the frequency contribution of the host rock response and plate response. The visual examination of the spectra of the combined responses confirmed this.

Figure 5.13 shows amplitude spectra of a combination for both $\dot{B}z$ and $\dot{B}x$ components and clearly shows the plate response's high frequency contribution.

However, low resistivity early channel host rock responses have an amplitude spectra with a high frequency content, and for certain combinations of parameters, the two spectra merge and the elimination of the host rock response, by filtering, would result in the removal of a certain part of the plate response's low frequency content.

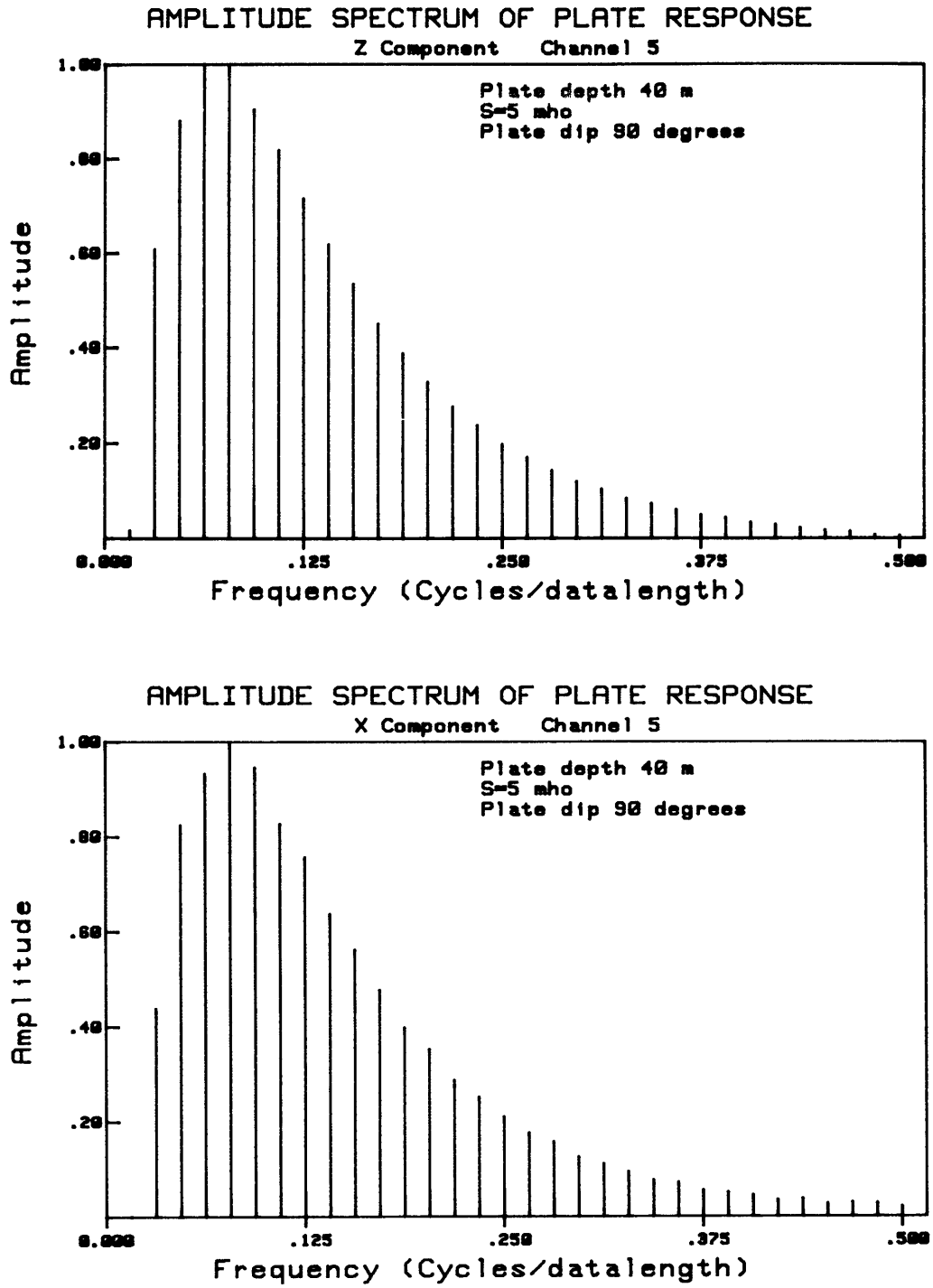

Figure 5.11 $\dot{B}z$ and $\dot{B}x$ component amplitude spectra of the plate response for a 90 degree dipping plate at 40 m depth below surface and a conductivity thickness product of 5 siemens. Channel 5.

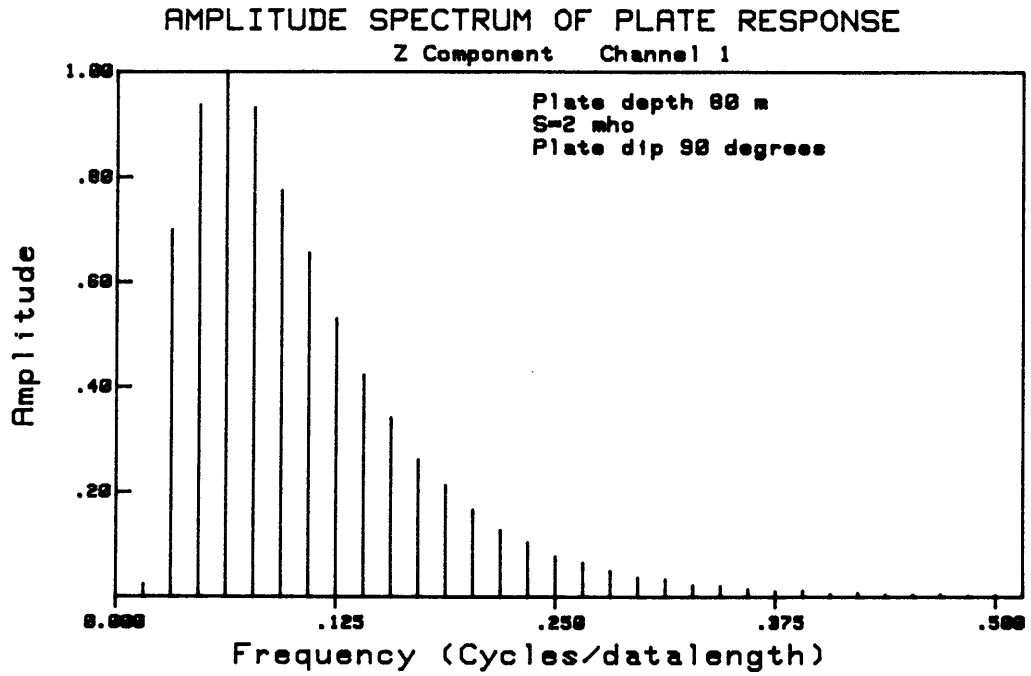

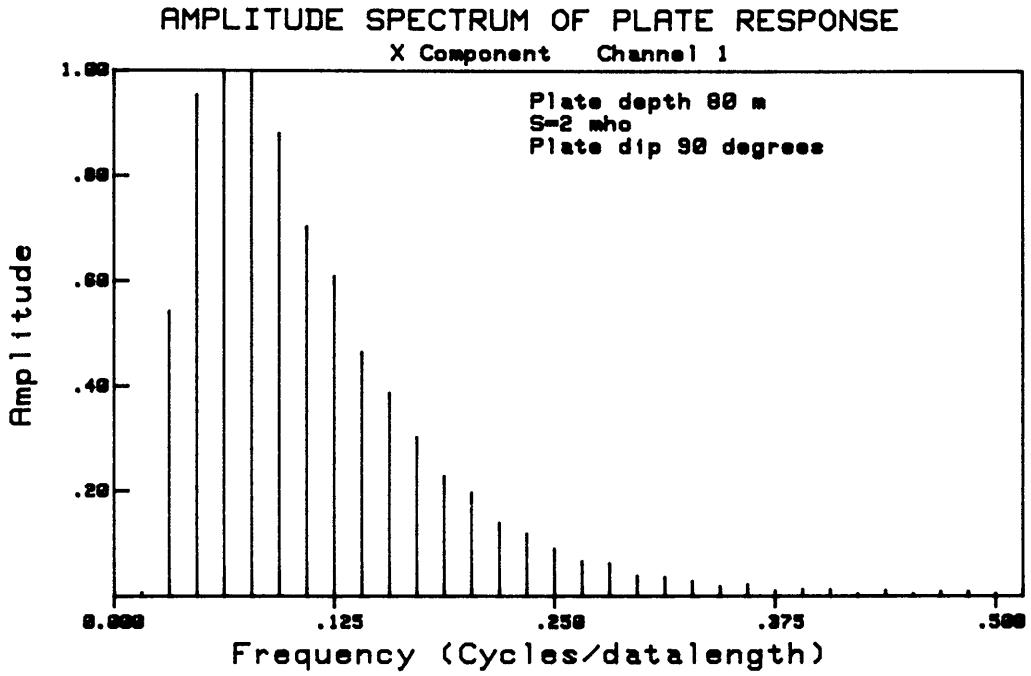

Figure 5.12 $\dot{B}z$ and $\dot{B}x$ component amplitude spectra of the plate response for a 90 degree dipping plate at 80 m depth below surface and a conductivity thickness product of 2 siemens. Channel 1.

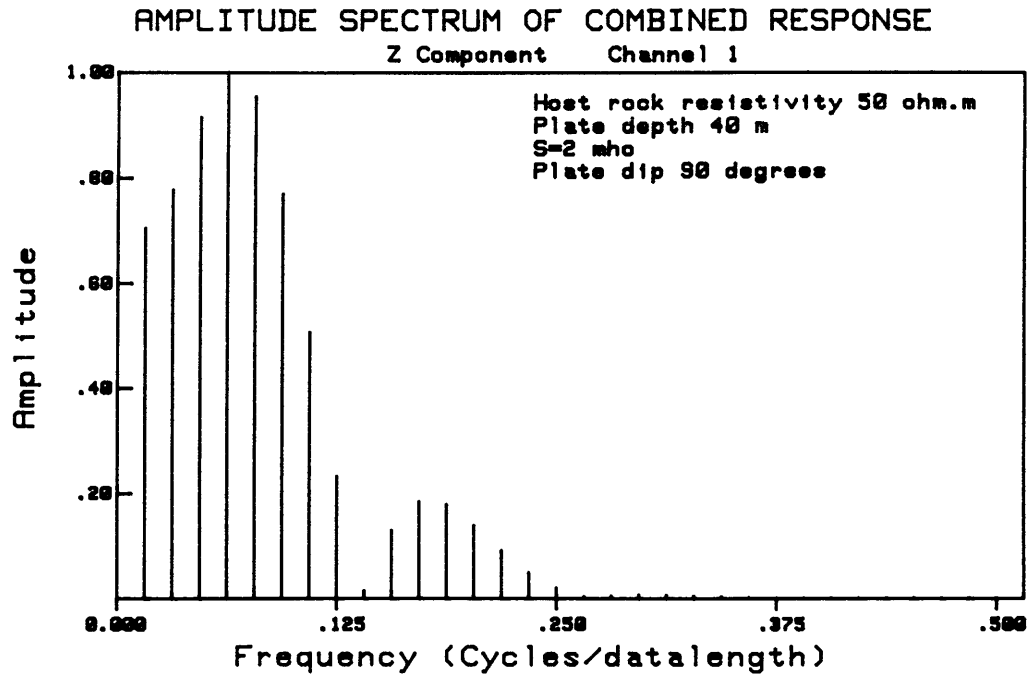

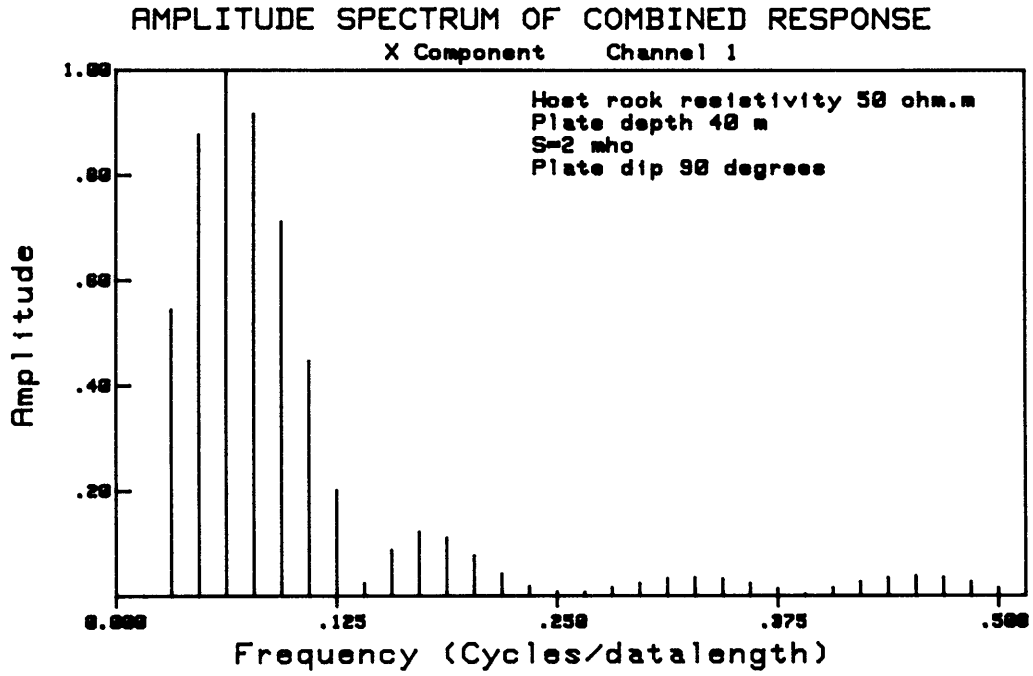

Figure 5.13 $\dot{B}z$ and $\dot{B}x$ component amplitude spectra of 50 ohm.m host rock responses combined with a plate response for a 90 degree dipping plate at 40 m depth below the surface and a conductivity thickness product of 2 siemens.

This then is the major limitation of the technique. It is thus necessary to determine the limit at which this occurs. Figure 5.14 shows the way in which the combinations were added and gives the reader an idea of the amount of combinations that resulted. This confirmed the fact that one needs to restrain the parameters of both host rock and plate responses.

5.6 APPLICATION LIMITS

The limit of the technique was determined by examining constant channel-resistivity combinations. The combinations were submitted to the filter starting at the lower limit of the depth range, and progressing to greater depths. By comparing the pre- and filtered results the model parameters at which the filtered result featured only as noise in comparison to the original response was noted. These model parameters represent the lower limits of applicability. This was again repeated for all the $\dot{B}z$ and $\dot{B}x$ combinations.

Figures 5.15a and 5.16a depict the combination of host rock responses and a deep plate response for $\dot{B}z$ and $\dot{B}x$ respectively. After filtering using the filtering parameters as derived and depicted in figures 5.9 and 5.10 for the specific case, the resulting "isolated anomalies" are depicted in Figures 5.15b and 5.16b. The maximum values of the residual data ($\sim$60mV and $\sim$40mV) only represent 1,6% and 2,7% of the original measured response of 3560mV and 1430mV for respectively the $\dot{B}z$ and $\dot{B}x$ component. Comparing this with Figures 5.15d and 5.16d where the maximum values of the "isolated anomalies" represents 13% for $\dot{B}z$ and 14% for $\dot{B}x$ of the original response.

From the many examples used for this study, it was decided to consider values where the residual is less than 10% of the original values as noise. Where residual values are higher than 10%, as for example in Figures 15d and 16d, the anomaly is clearly recognizable as that of a vertical plate.

Figures 5.17b and 5.17d are repetitions of the isolated anomalies as depicted in Figures 5.15d and 5.16d. Figures 5.17a and 5.17c depict

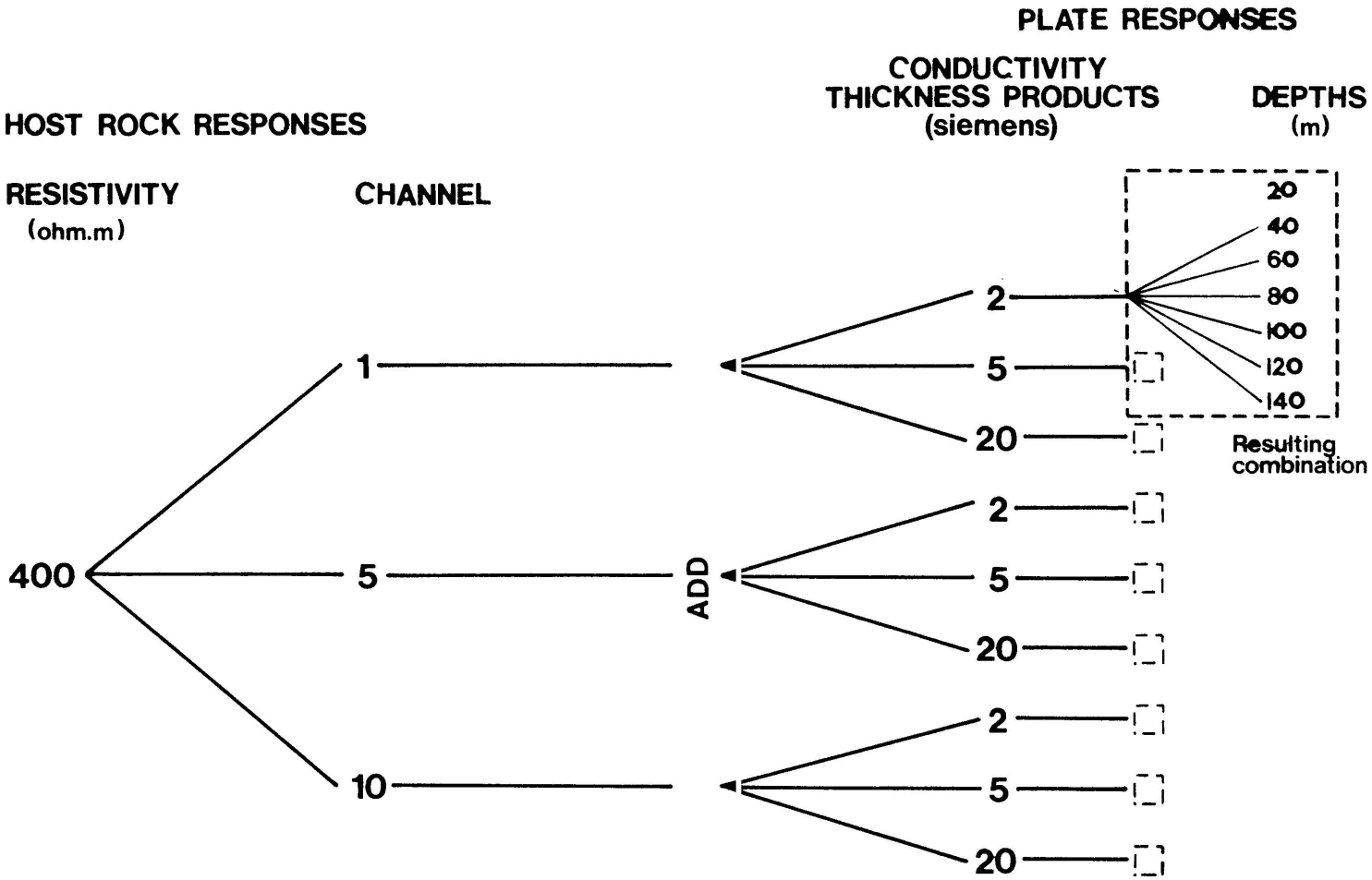

Figure 5.14 Schematic overview of host rock and plate response combination parameters.

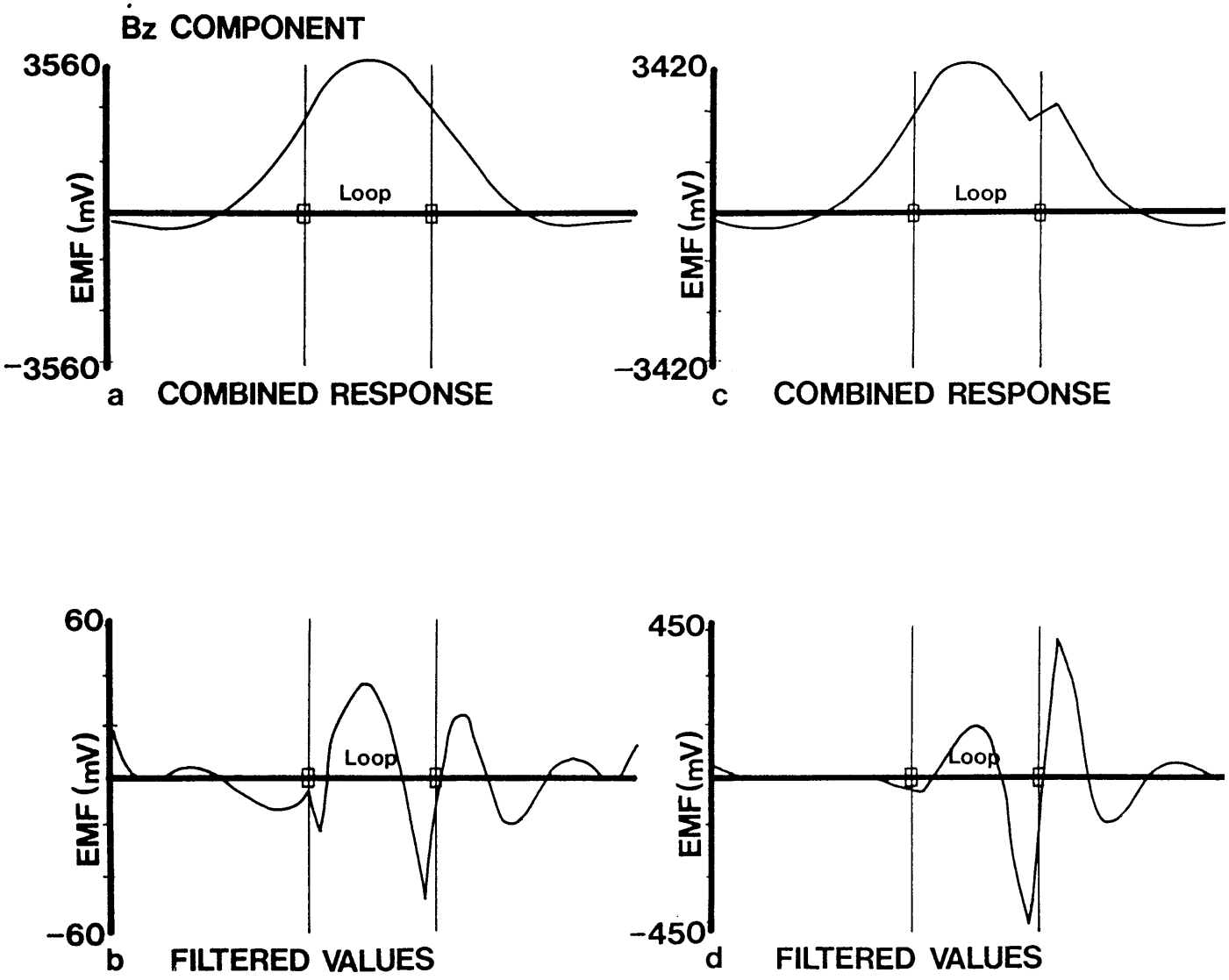

Figure 5.15 Combined host rock and plate responses with isolated anomalies.

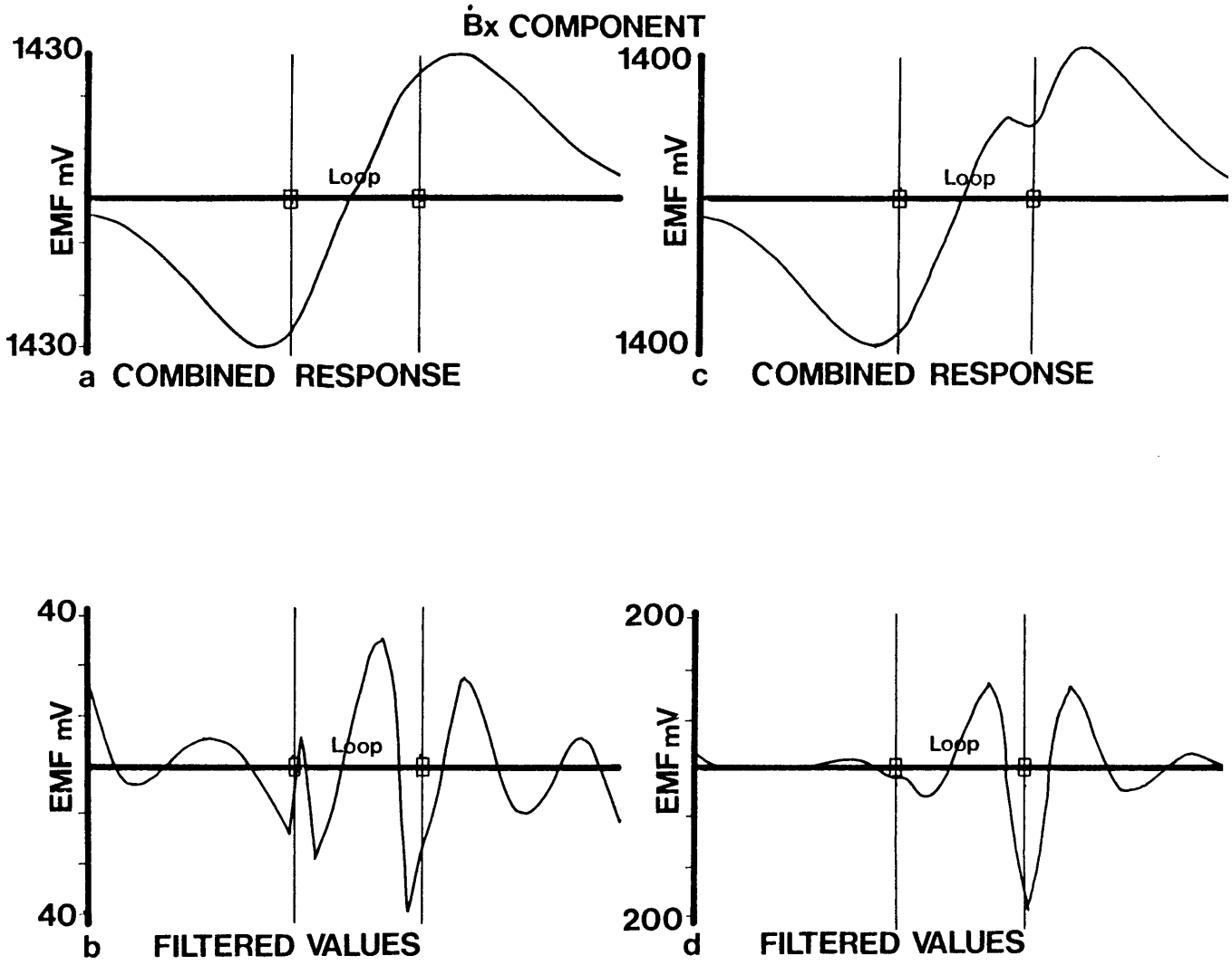

Figure 5.16 Combined host rock and plate responses with isolated anomalies.

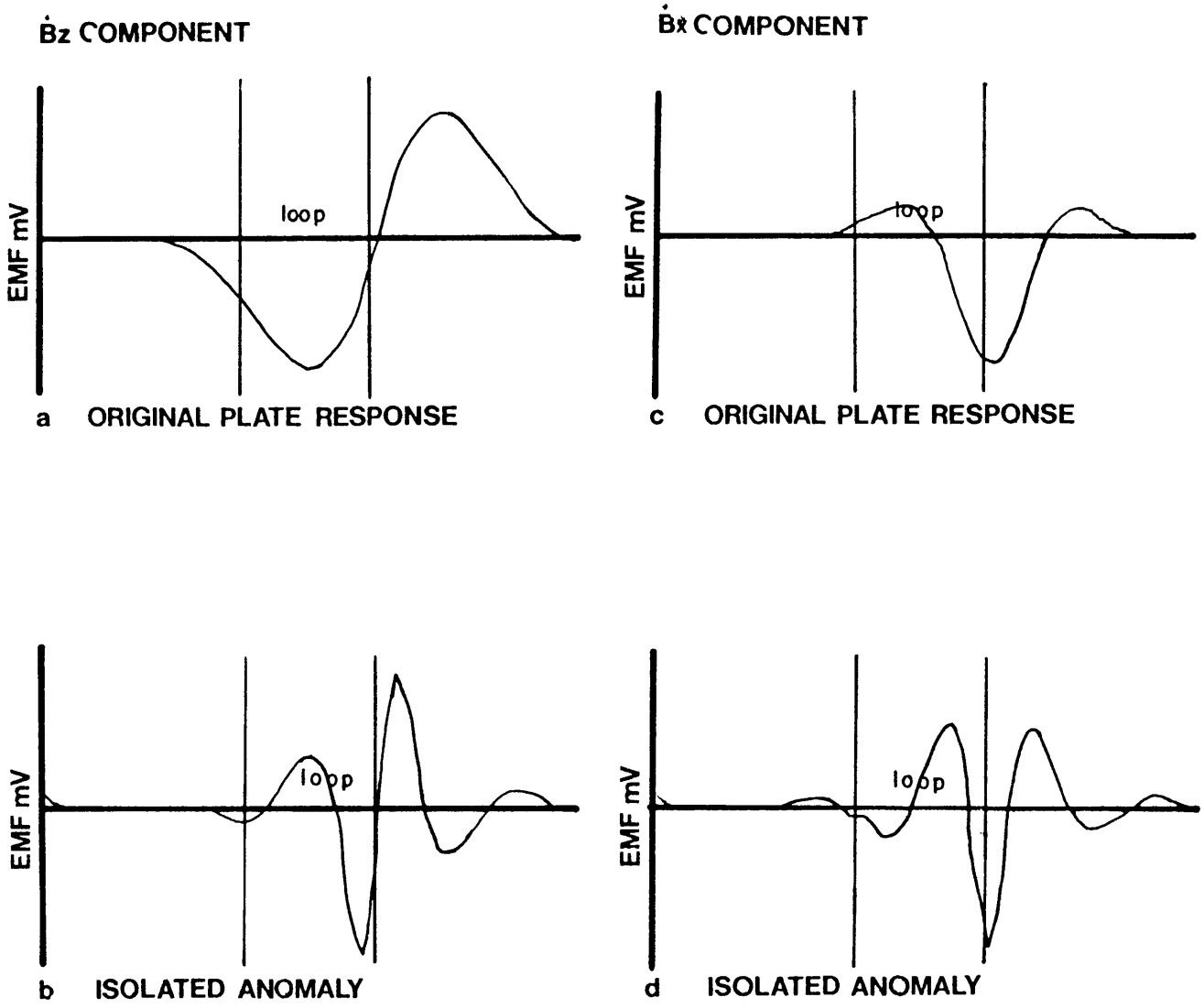

Figure 5.17 Anomalies obtained by the filtering method and compared with the original plate responses added.

the original responses that were added to the host rock responses to yield the combined responses (Figures 5.15c and 5.16c). From this one can see that the position and the shape, with reference to symmetry, of the anomaly have not changed but the frequency of the anomaly is of higher order than that of the original plate response added.

The increase in frequency of the response is a direct result of the filtering and in the interpretation of the anomalies it is thus possible to make an incorrect interpretation as far as depth is concerned. In this specific case the depth to the top of the body would be interpreted as being much closer to the surface by about a factor of 0,5. Furthermore the side lobes that occur would normally be interpreted as reflecting the lower return current, i.e. a depth limited conductor although it may not be the case. The above-mentioned facts should be kept in mind whenever this technique is used.

The data obtained from the investigation were plotted on a log-log scale with the ordinate representing the resistivity range of the host rock and the abscissa the depth to top of plate range (Figure 5.18). The curved lines separate the parameter areas for which the technique works (above the lines) and for which not (below the lines). The use of the graphs is best explained by a few examples.

Case A, channel 1. (Figure 5.18a).

In this case a 100 ohm.m host rock response were added to a plate response with the depth to top of the plate of 60m. Regardless of the conductivity thickness product of the plate, this graph shows that it will not be possible to interpret the residual values after filtering as an anomaly associated with a plate.

Case B, channel 5. (Figure 5.18b).

In this case a 100 ohm.m host rock response was added to a plate response with depth to top of plate 40m. If the conductivity thickness product of the plate is less than 2 siemens it would not be possible to isolate the response by the filter technique since the position in terms of parameters of the combination was below the 2

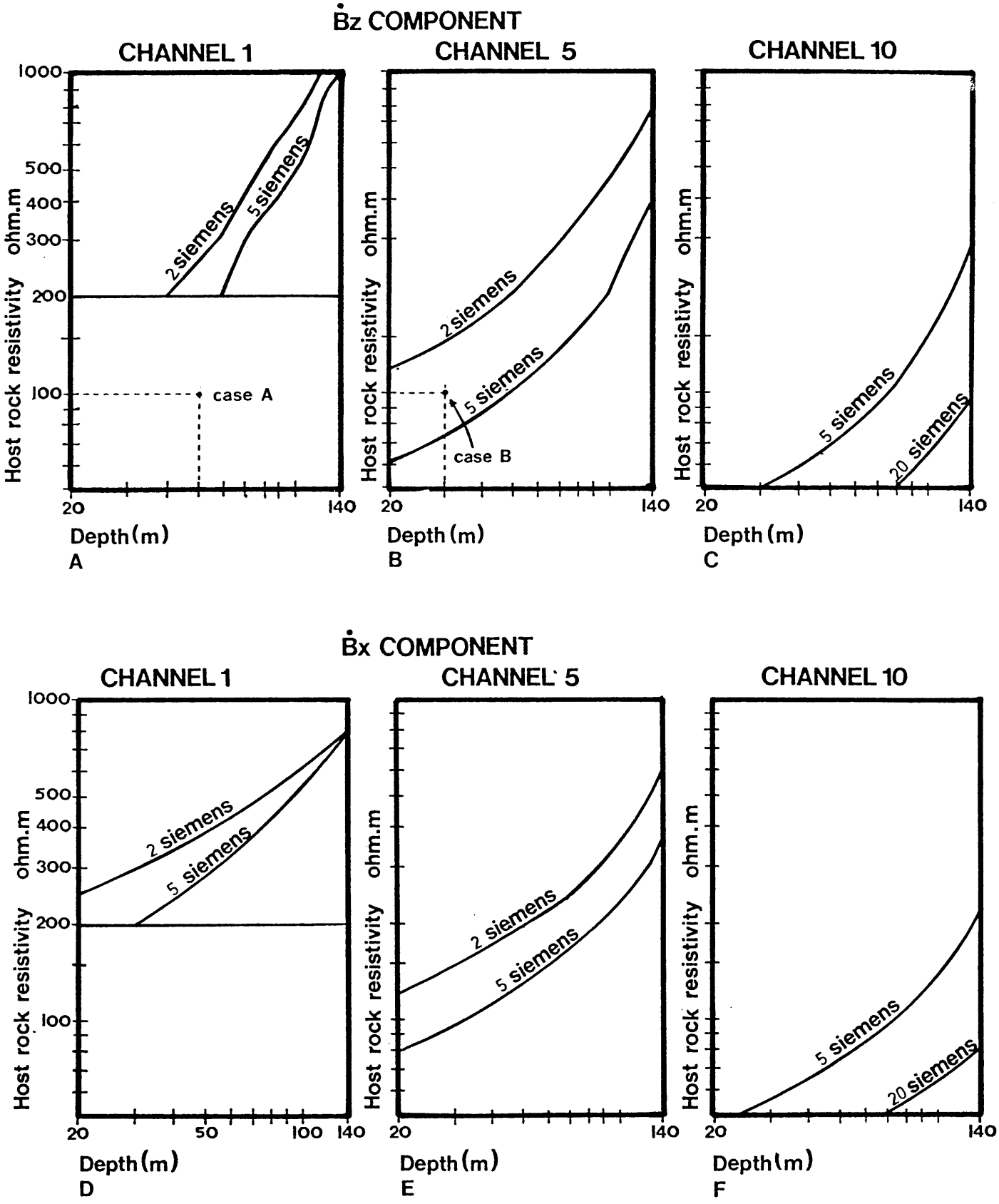

Figure 5.18 Applicability graphs for the Ḃz and Ḃx components.

siemens limit line. However, if the conductivity thickness product is greater than 5 siemens, the response could be isolated since the parameter plot of the combination lies in the area above the 5 siemens limit line.

It should be kept in mind that the graphs depicted in Figure 5.18 are only valid for the host rock and plate parameters as specified previously. Although the graphs are the result of theoretical calculated combinations, it should be possible to use them to determine whether the filter technique would work in a practical case. With a knowledge of the host rock resistivity, possible depth of the plate and an approximation of the conductivity thickness product it should be possible to plot the point according to the parameters on the appropriate graph and see whether the point falls in the applicability range or not.

From the above it follows that:

i. For the plate parameters considered in this study, it would not be possible to isolate any plate anomaly in channel 1 for a host rock resistivity of less than 200 ohm.m.

ii. Due to the fact that the results of the plate program are only valid in late time, (Gallagher *et al.*, 1985) it was found that a conductivity thickness product of 20 siemens lead to erroneous data for channels 1 and 5. The same applied to 2 siemens for channel 10. This then is the reason why the graphs for channels 1 and 5 show applicability areas for plates with a conductivity thickness product of 1 and 5 siemens and the graph for channel 10 only areas for 5 and 20 siemens plates.

iii. For later times the areas of applicability are larger. This phenomena was expected because the host rock response has decayed considerably, shifting it further to the low frequency spatial frequency content.

iv. As expected one can now clearly see from the graph that the method will work for high host rock resistivities and late

times (channels) and with certain constraints it will yield results in the low resistivity early time areas.

v. Areas exist where the amplitude spectra of the host rock and plate responses are merged to such an extend that successful filtering is impossible. These areas are depicted as the areas under the lower depth limit lines on Figure 5.18.

vi. The frequency of the anomalies obtained after filtering is of higher frequency than that of the original plate responses added as can be seen on Figure 5.16. This is explained by the fact that the amplitude spectra of the host rock response and the plate response are not of the band limited type and that "contamination" occurs in the lower frequency part of the spectra. By removing this part in order to remove the host rock response, one removes the low frequency content of the plate response, resulting in a higher frequency.

vii. By taking into consideration the fact that the areas of applicability enlarge as one moves to the later channels, one can assume that for channels greater than channel 10 the technique will almost always work.

viii. Although the quantitative interpretation of an anomaly obtained by the filter technique could be distorted as far as depth and size of conductor are concerned, a fair approximation of the dip and position of the conductor can be made.

CHAPTER 6

CASE HISTORIES

In this chapter two case histories are studied namely:

(i) The lake Ngami copper prospect in northern Botswana where a good confined conductor occurs in a fairly resistive host rock medium.

(ii) The mapping of faults and dolerite dykes on the coal fields in the vicinity of Sasolburg (South Africa). This represents a case of poor conductors in a low resistivity environment.

6.1 DATA ACQUISITION

All data were acquired using a GEONICS EM37 transient system. A 400m x 400m transmitter loop was laid out to obtain maximum coupling with the suspected conductor. The transmitter carried a 30 Hz step-function with peak amplitude of between 15 and 17 amps. Three sets of measurements, as explained in Chapter 3, at each station were taken with the portable receiver.

6.2 THE LAKE NGAMI COPPER PROSPECT

6.2.1 Location

The area of interest lies some 120km southwest of Maun in the northern part of Botswana as shown on a locality map in Figure 6.1.

6.2.2 Geology

In the area under investigation information from three boreholes is available. The information indicates a contact zone between siltstones and sandstones of the Karoo sediments that dips at an angle

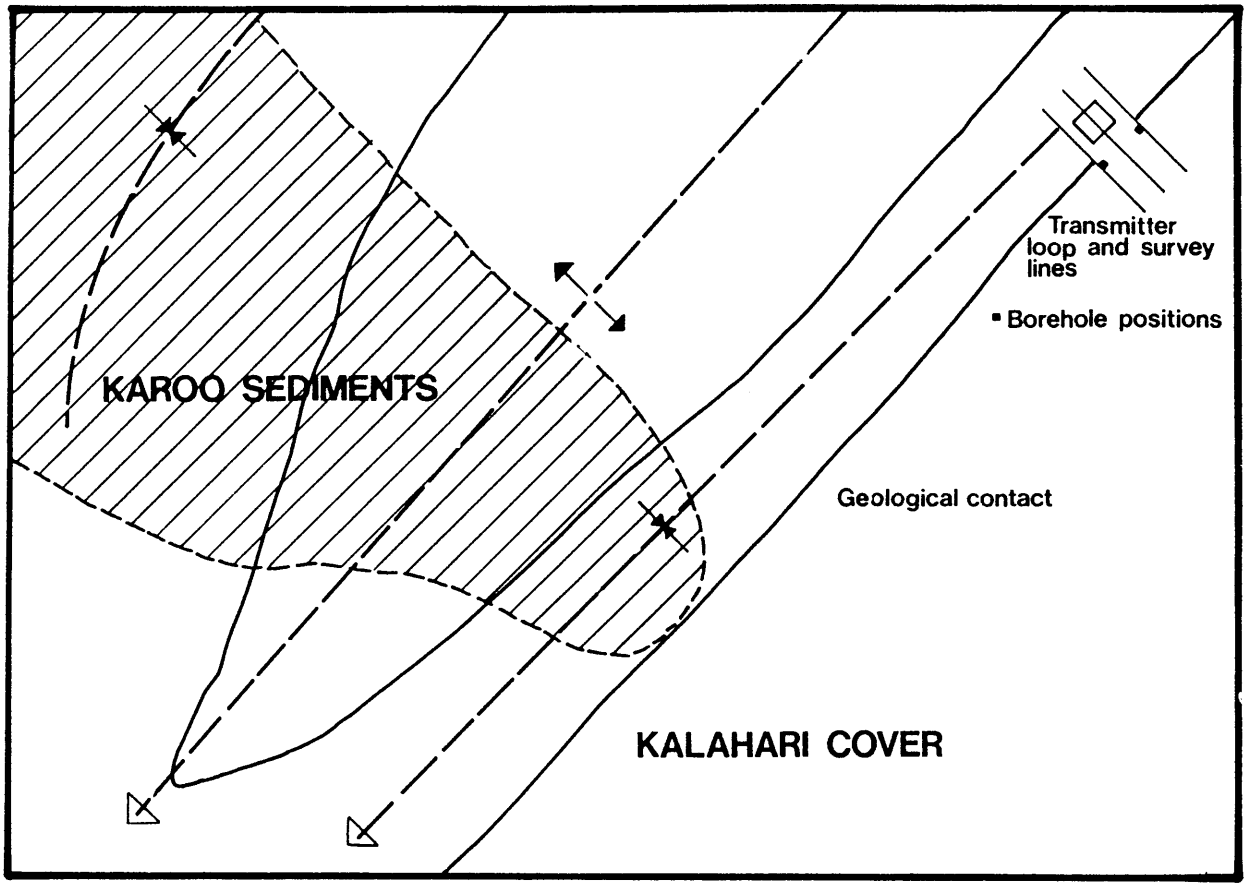

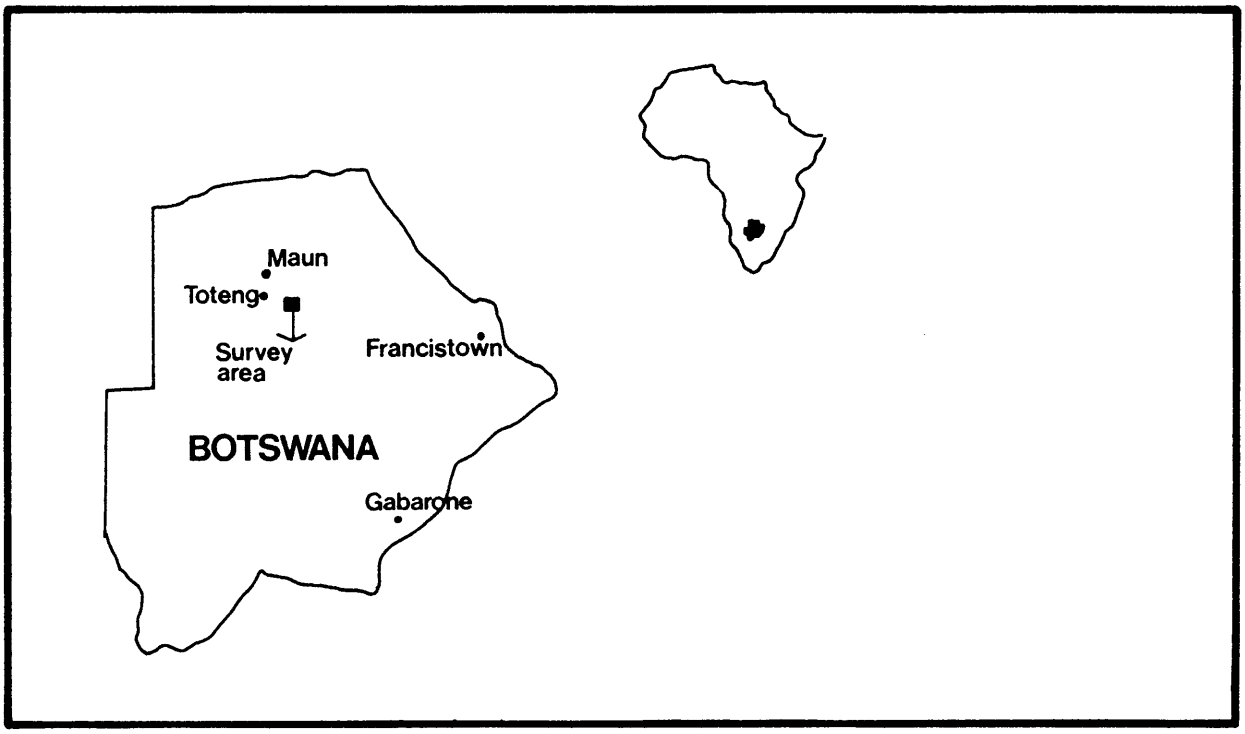

Figure 6.1 Locality map of Lake Ngami Copper prospect.

of 70 to 80 degrees northwest. Copper sulphide mineralisation of up to 2,5% Cu occurs in this contact zone at a depth of between 100 and 125 meters. The borehole profiles are shown in Figure 6.2.

6.2.3 Field lay-out

Figure 6.3 depicts the field lay-out. The mapped position of the contact zone, the transmitter loop and station positions are also shown. Three lines, LNG-GN1, LNG-GN3 and LNG-GN5, were surveyed with a station spacing of 40m.

6.2.4 Interpretation

In order to interpret the anomalies, the traditional method for host rock removal, viz. by calculating a best fitting host rock response and subsequent subtraction, was applied to the data. The filtering technique was also applied to the data and the resulting anomalies compared.

i. Line LNG-GN1

Figure 6.4 depicts examples of the field data of the line LNG-GN1 for different channels and the accompanying host rock responses as calculated to obtain a best fit with the non-anomalous side of the profiles. The occurrence of anomalies on the suspected non-anomalous side of the profile makes the task of achieving a best fit between the calculated host rock and the non-anomalous side extremely difficult. This clearly illustrates the problem that occur if the anomaly is not limited to the one side of a symmetrical field profile.

The $\dot{B}z$ component anomalies isolated by means of subtracting the host rock response from the field data are depicted in Figures 6.5 and 6.6.

In order to compare these anomalies with anomalies obtained from using the frequency domain filter technique, the line was filtered using the

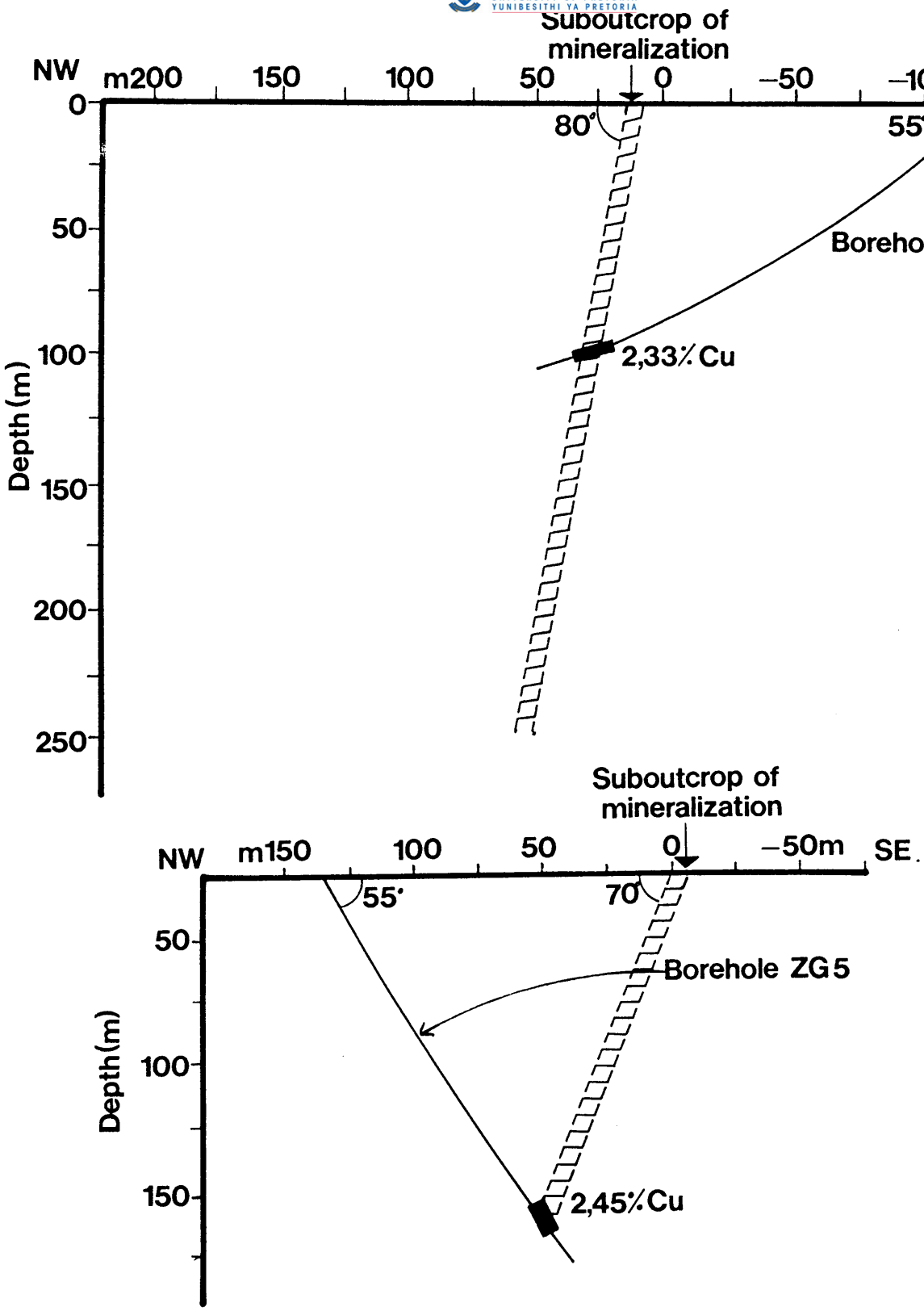

Figure 6.2 Borehole profiles of boreholes ZG19 and ZG5.

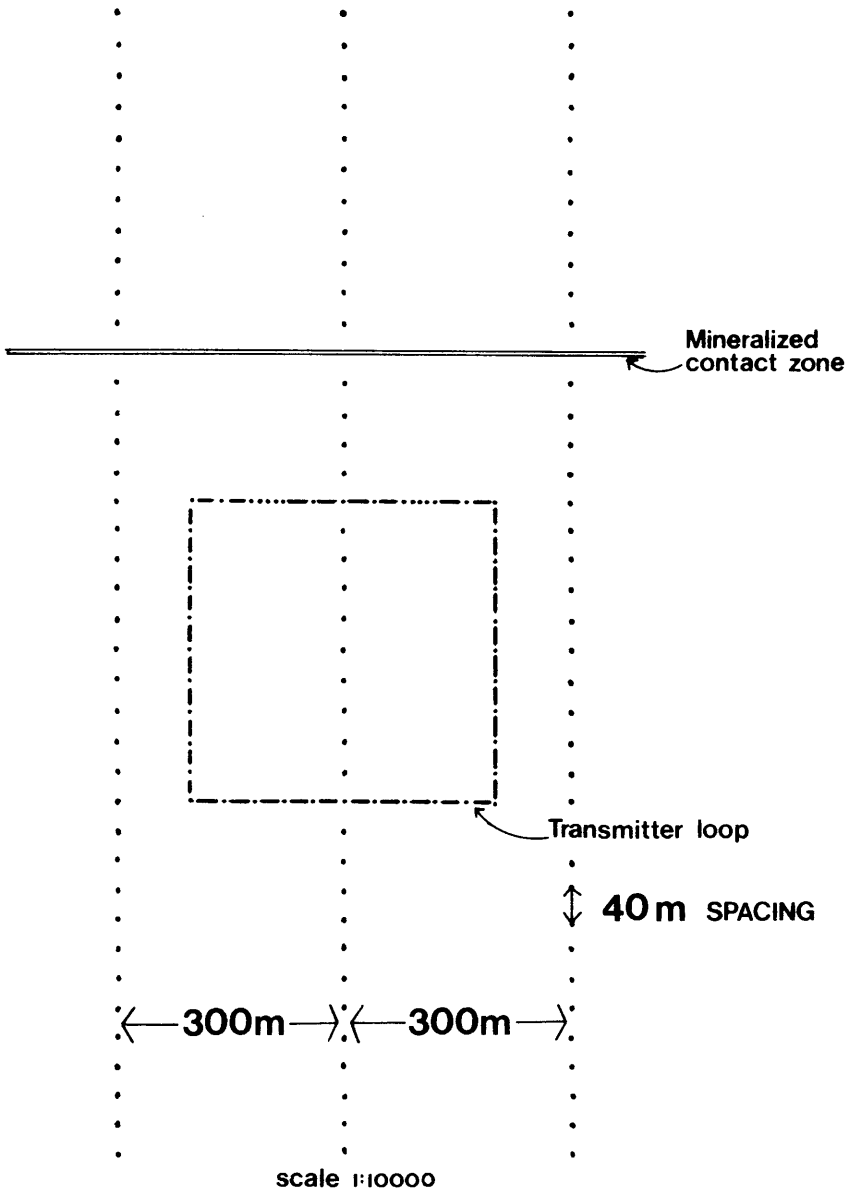

Figure 6.3 Field lay-out for the Lake Ngami Copper prospect.

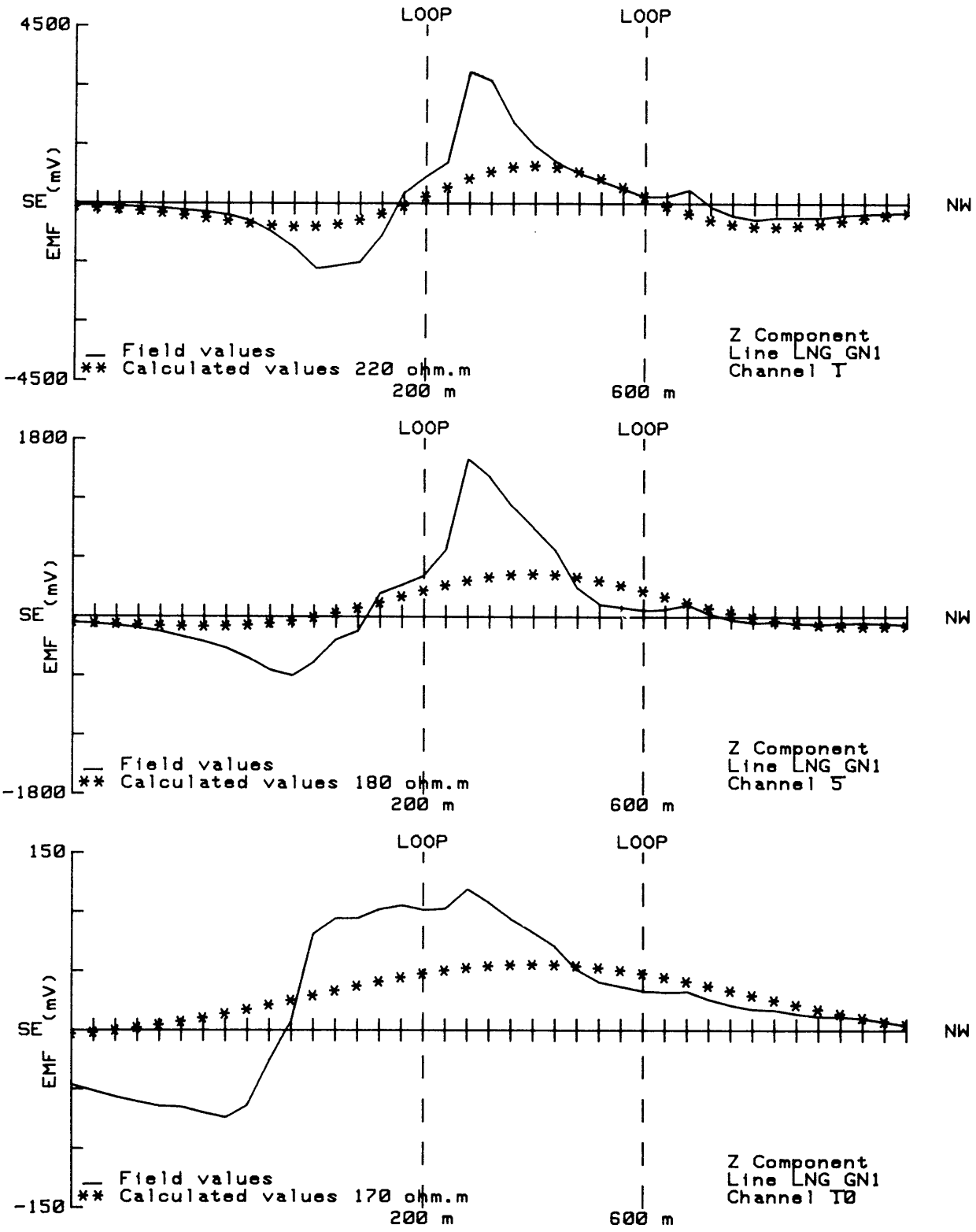

Figure 6.4 Line LNG-GN1 field data for channels 1, 5 and 10 together with the best fitting calculated host rock responses.

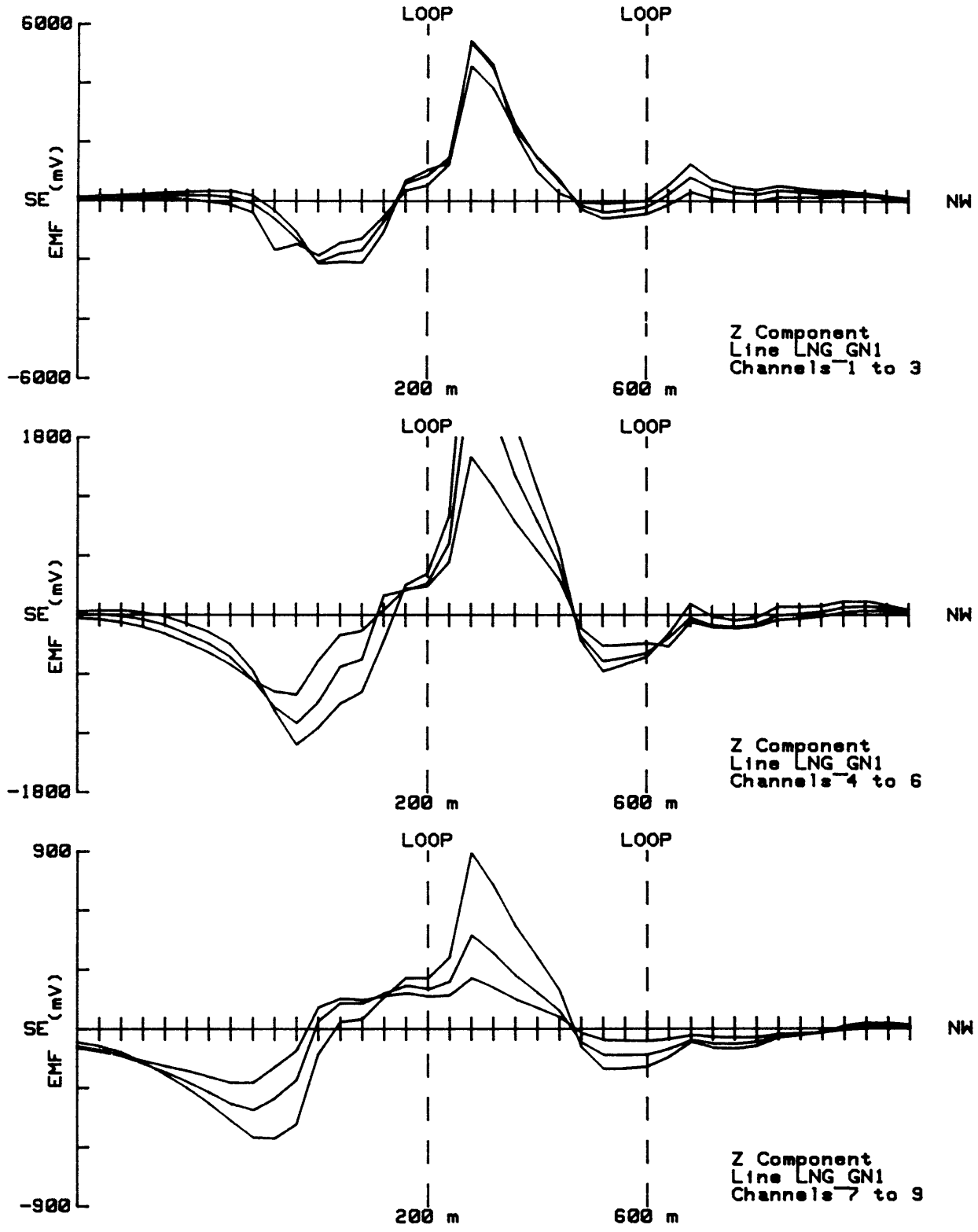

Figure 6.5 Isolated anomalies for channels 1 to 9 of line LNG-GN1 obtained by the traditional host rock removal method. $\dot{B}z$ component.

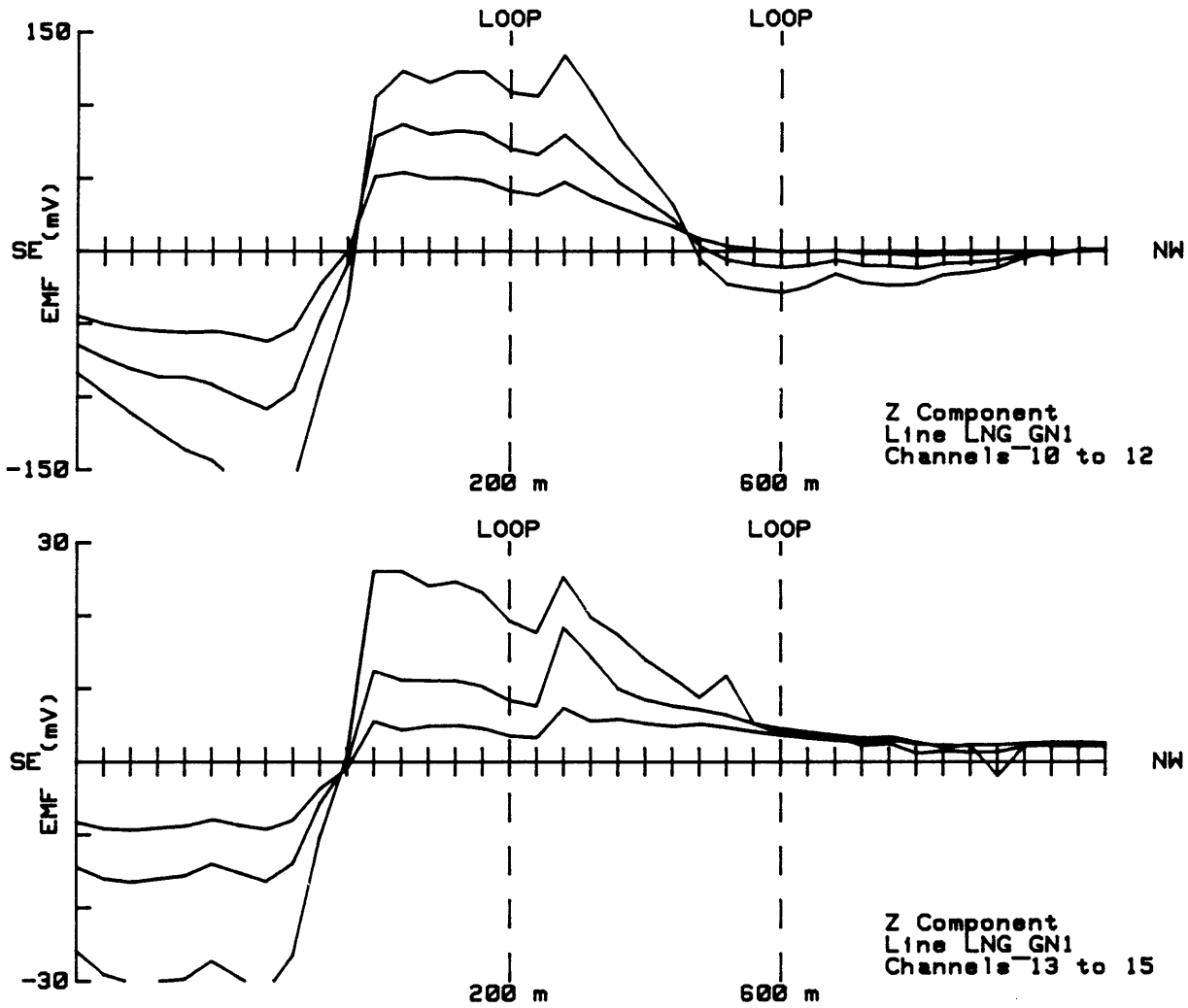

Figure 6.6 Isolated anomalies for channels 10 to 15 of line LNG-GN1 obtained by the traditional host rock removal method. $\dot{B}z$ component.

program included in Appendix B. Both $\dot{B}z$ and $\dot{B}x$ components for channels 1 to 15 were filtered. The cut-off frequency for the filter was derived from the nomograms given in Figures 5.9 and 5.10. The isolated anomalies are depicted in Figures 6.7 to 6.10.

By comparing this with the anomalies obtained from the calculating and subtracting the host rock response (Figure 6.5) one can see that the same interpretation on the computed and subtracted data could not be made due to the fact that a clear cross-over position is not evident.

A second anomaly situated between station 540 to 680 was isolated by the filtering method. This anomaly is not clearly noticeable on the calculated profiles (Figures 6.5 to 6.6) and it is not possible to interpret the anomaly in this case. However, from the filtered profiles this anomaly is interpreted as being caused by a possible wide weathered conductive zone situated between stations 560 and 640.

By examining the late time channels (channels 10 to 15) it can be seen that the anomaly situated at station 0 can be isolated by both the calculation and subtraction of host rock response and by means of the filter technique. This anomaly is associated with the suspected mineralised contact zone. The top of the contact zone, as derived from the crossover and peak positions on $\dot{B}z$ and $\dot{B}x$ respectively, correlates very closely with the geologically mapped position. From the shape of the anomalies a steep northwest dipping conductor is interpreted. This also correlates well with the geology.

A decay plot is obtained by plotting the emf (mV) values for each channel for a specific station and a log-linear graph where the log scale represents the emf values and the linear scale the time for each channel. If the late time segment of such a log-linear plot (decay plot) approaches a straight line the decay constant of the conductor can be estimated from the slope of the straight line segment. The significance of the decay constant is that it contains valuable diagnostic information about the electrical properties of the target (McNeill *et al.*, 1984).

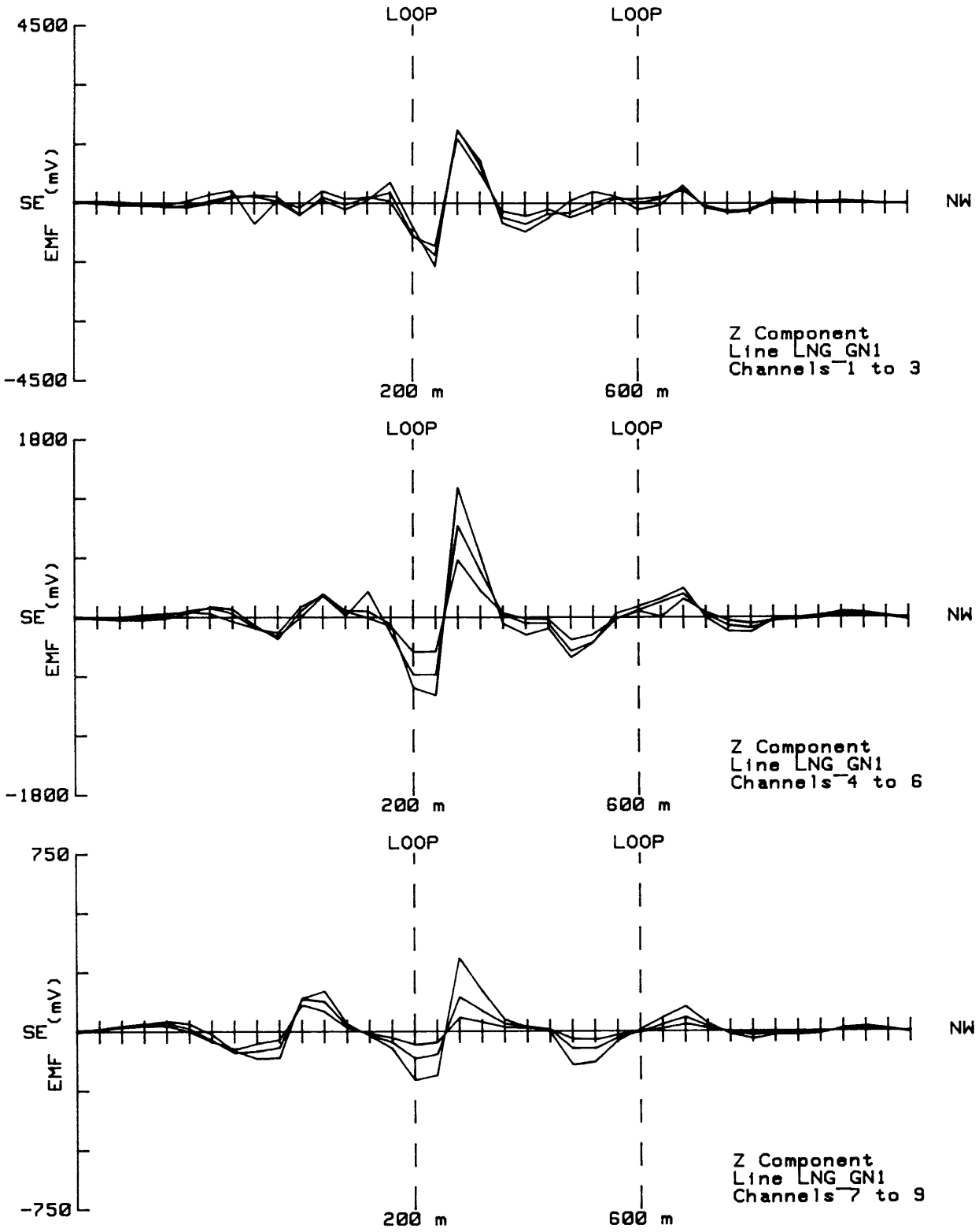

Figure 6.7 Isolated anomalies for channels 1 to 9 of line LNG-GN1 obtained by the filtering method. $\dot{B}z$ component.

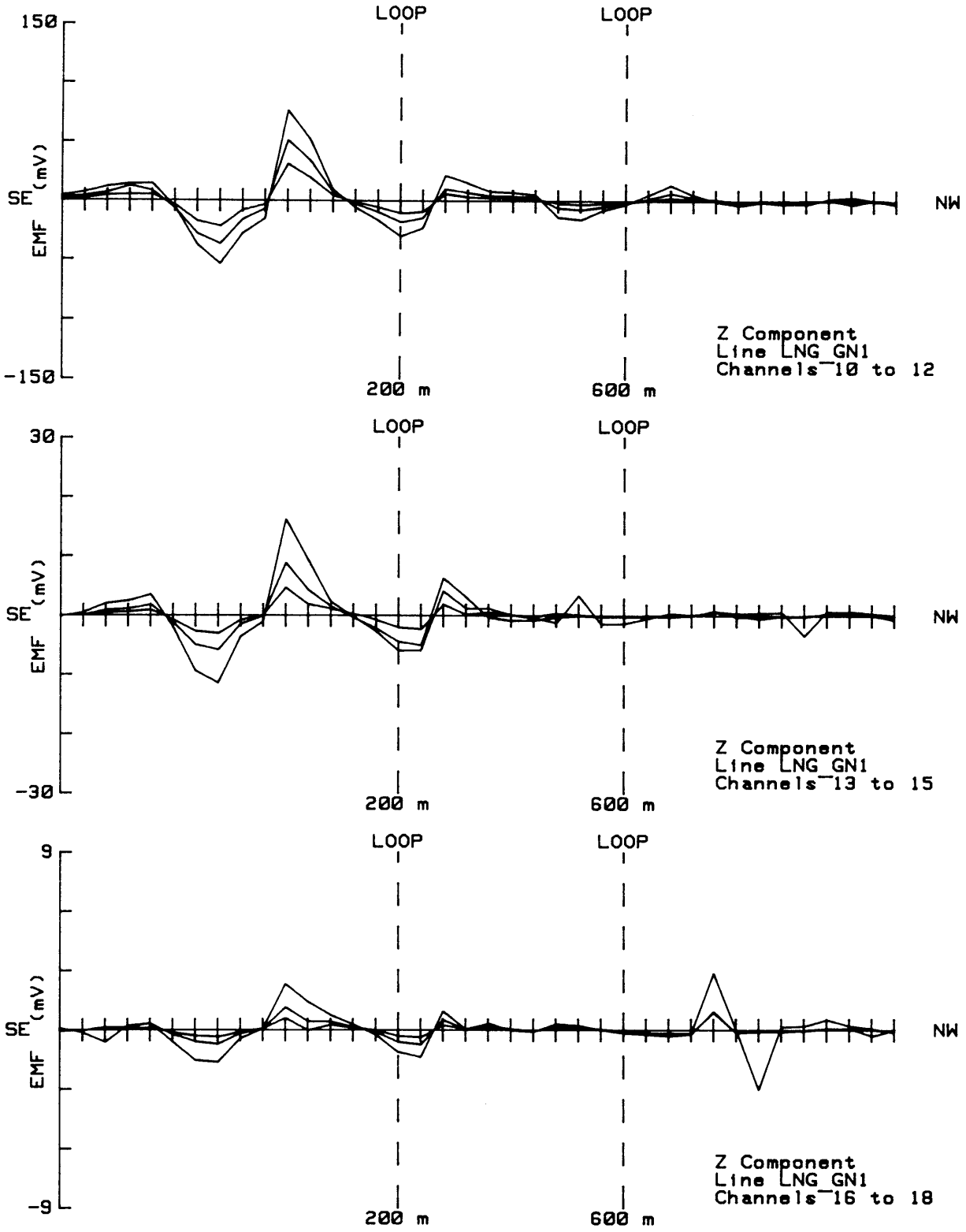

Figure 6.8 Isolated anomalies for channels 10 to 18 of line LNG-GN1 obtained by the filtering method. $\dot{B}z$ component.

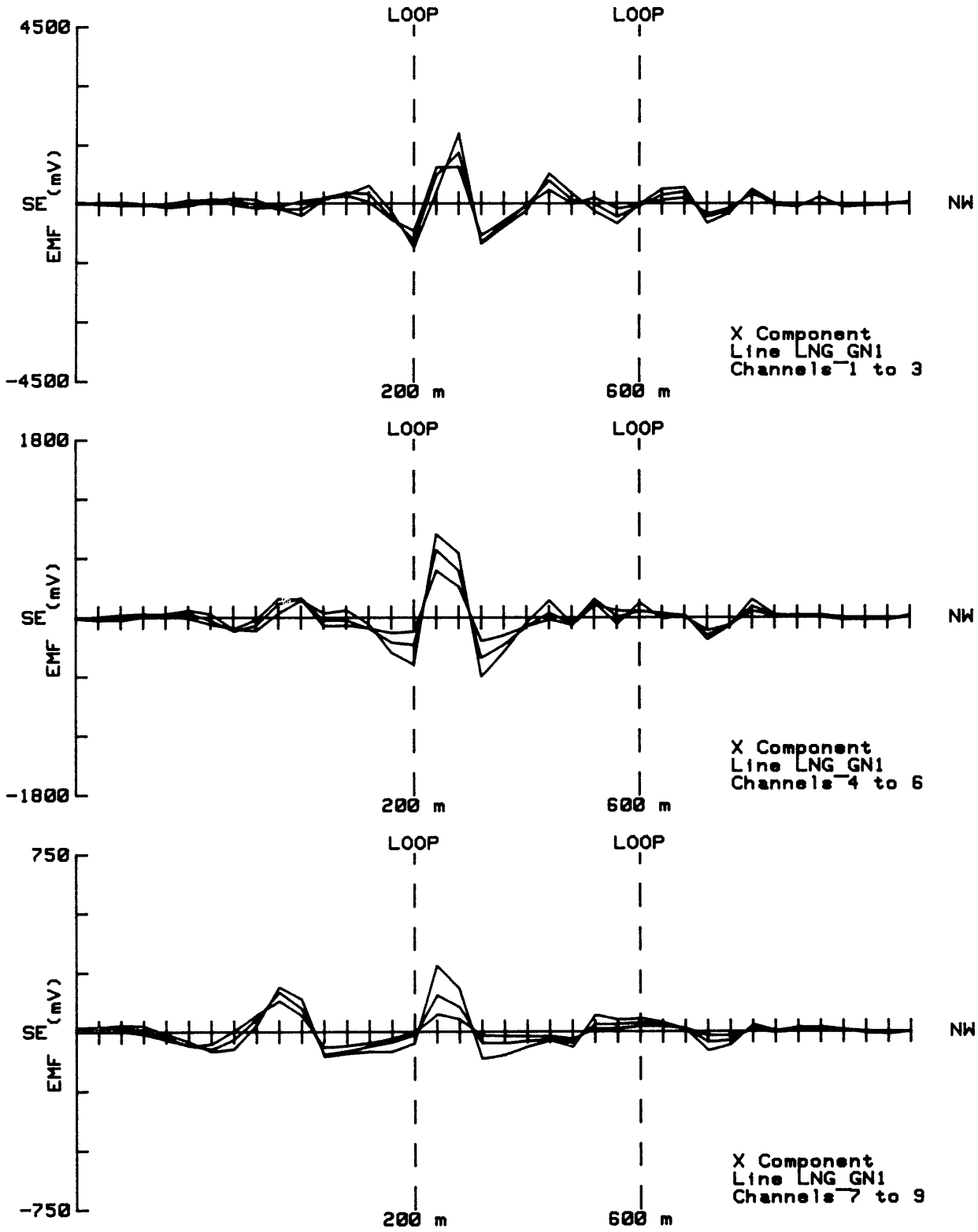

Figure 6.9 Isolated anomalies for channels 1 to 9 of line LNG-GN1 obtained by the filtering method. $\dot{B}x$ component.

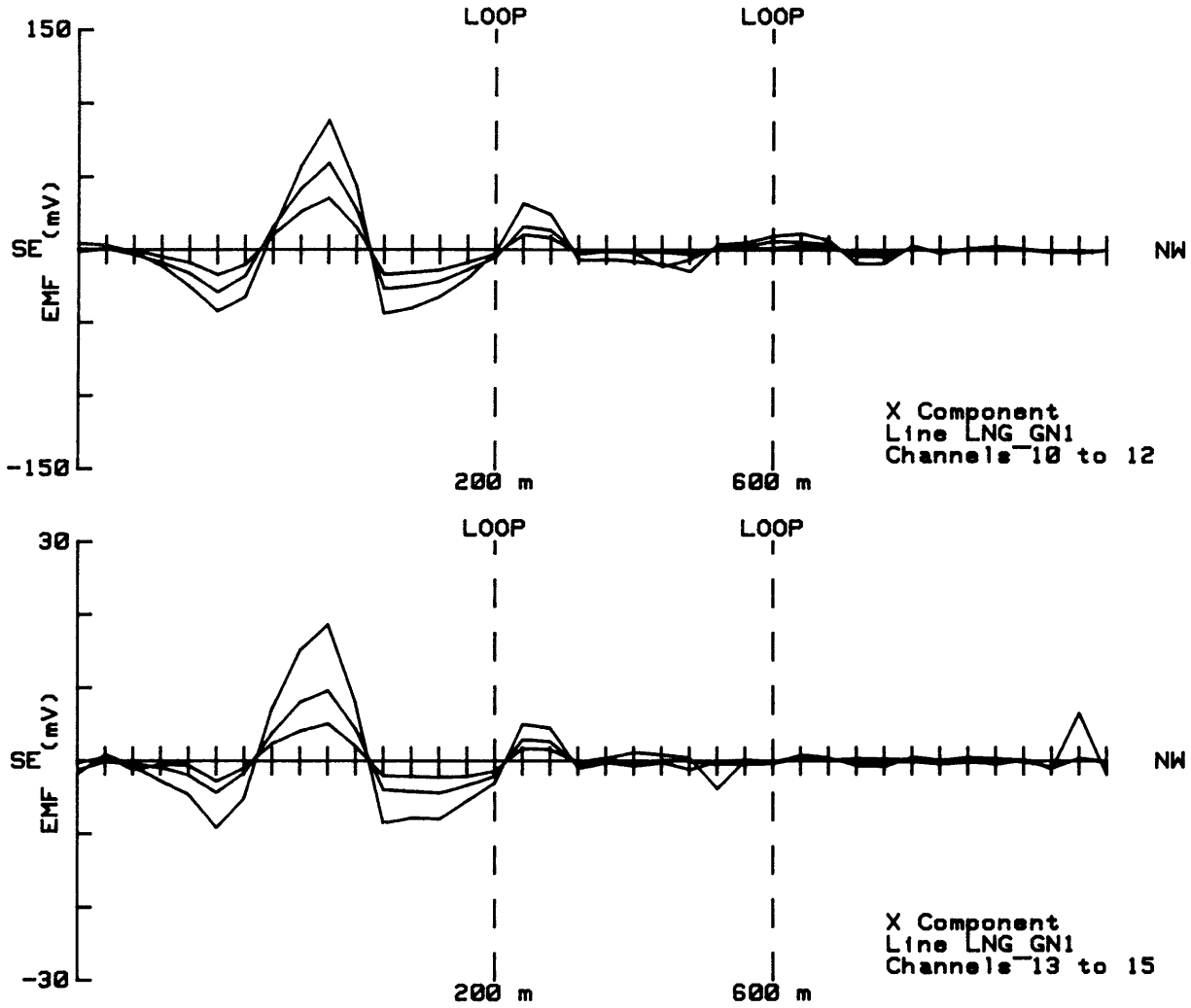

Figure 6.10 Isolated anomalies for channels 10 to 15 of line LNG-GN1 obtained by the filtering method. $\dot{B}x$ component.

A comparison between the decay plots for the anomaly associated with the contact zone and the anomaly situated between stations 160 and 340 isolated by the traditional host rock response removal technique (Figure 6.11) and the new filtering technique (Figure 6.12) reveals that the decay constants, derived from the slope of the straight line segment, correlate very well as can be seen from the following:

The following decay constants were calculated for the anomalies obtained by the filtering method.

Contact zone anomaly (station 0): 1,09ms ($\dot{B}z$) 1,29ms ($\dot{B}x$)

Confined conductor
anomaly (station 280): 0,28ms ($\dot{B}z$) 0,36ms ($\dot{B}x$)

Weathered zone
anomaly (station 680): 0,48ms ($\dot{B}z$) 0,59ms ($\dot{B}x$)

The corresponding $\dot{B}z$ component decay constants for the anomalies as obtained from the traditional host rock response removal method are, (station 0) 1,03ms, (station 320) 0,3ms and (station 640) 0,45ms.

From this fact it is concluded that in this case the decay constants obtained by the filtering technique is an accurate approximation of the real decay constants and that the filtering technique is ideal for host rock removal.

Decay plots of the anomalies obtained with the filtering technique were plotted for representative stations for all three anomalies that were isolated. The appropriate plots are given in Figures 6.13, 6.14 and 6.15.

ii. Line LNG-GN3

Both methods for the removal of the host rock response were applied on this line.

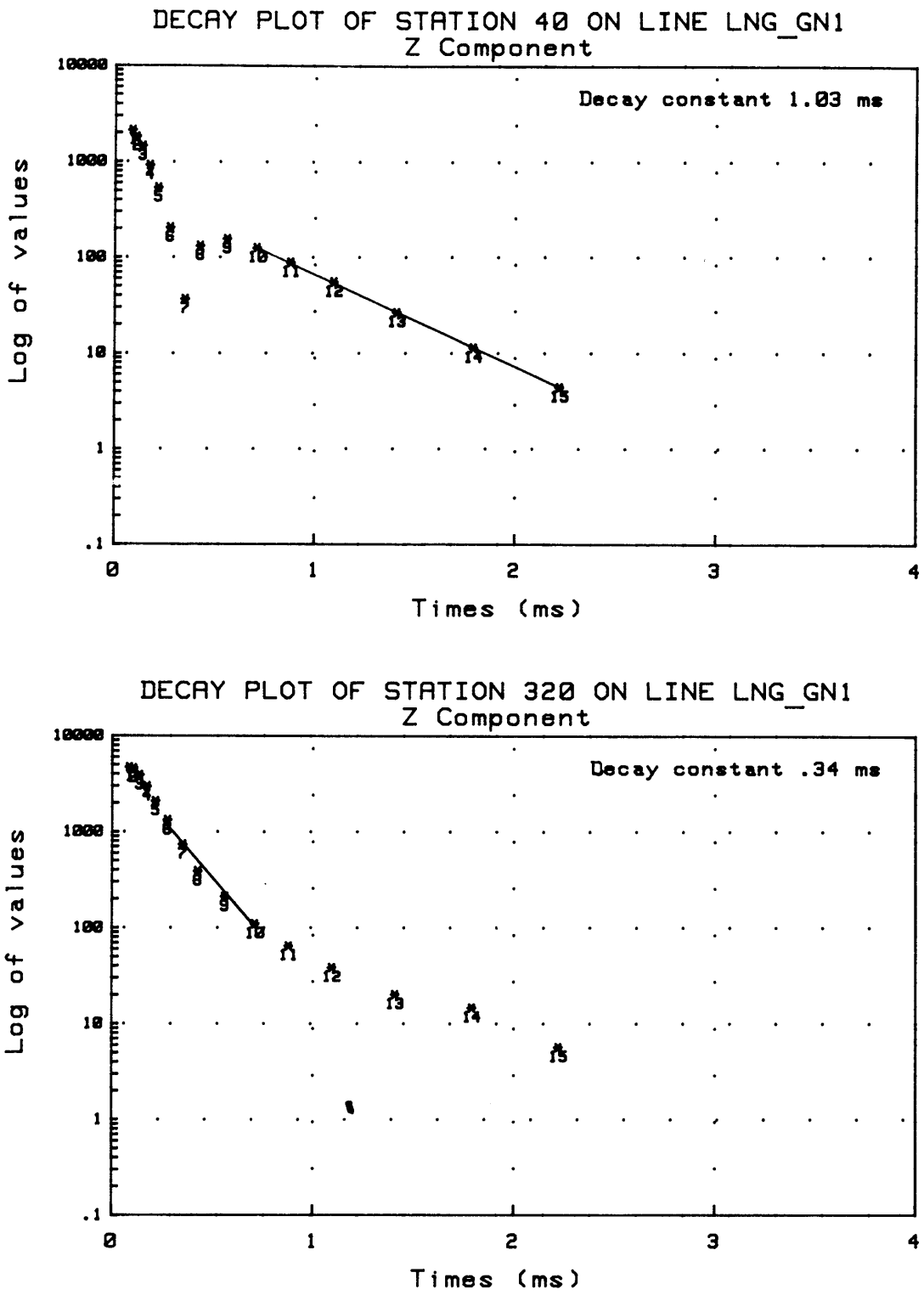

Figure 6.11 Stations 40 and 320 decay plots for anomalies obtained by the traditional host rock removal method. Ḃz component.

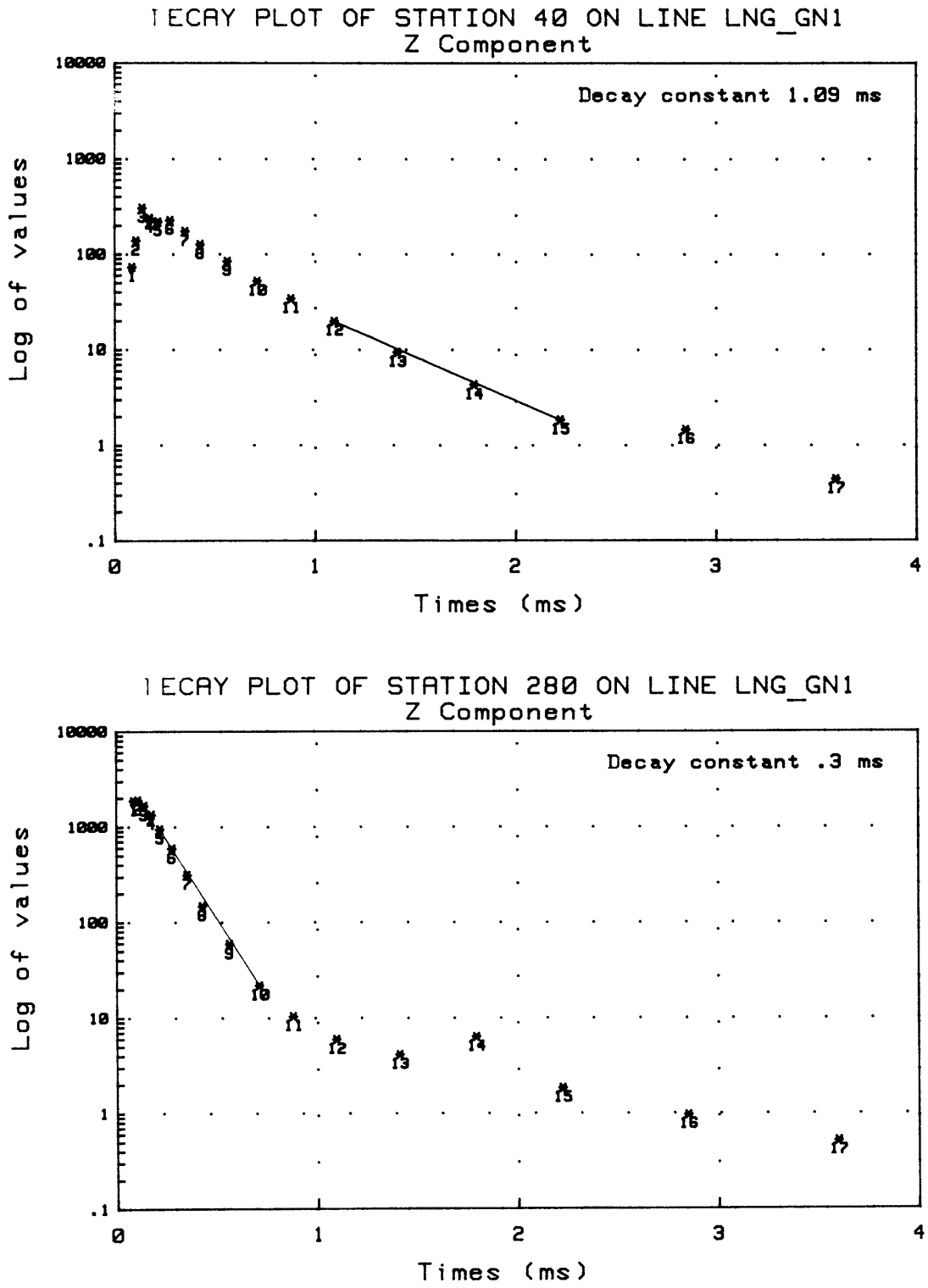

Figure 6.12 Stations 40 and 280 decay plots for anomalies obtained by the filtering method. $\dot{B}z$ component.

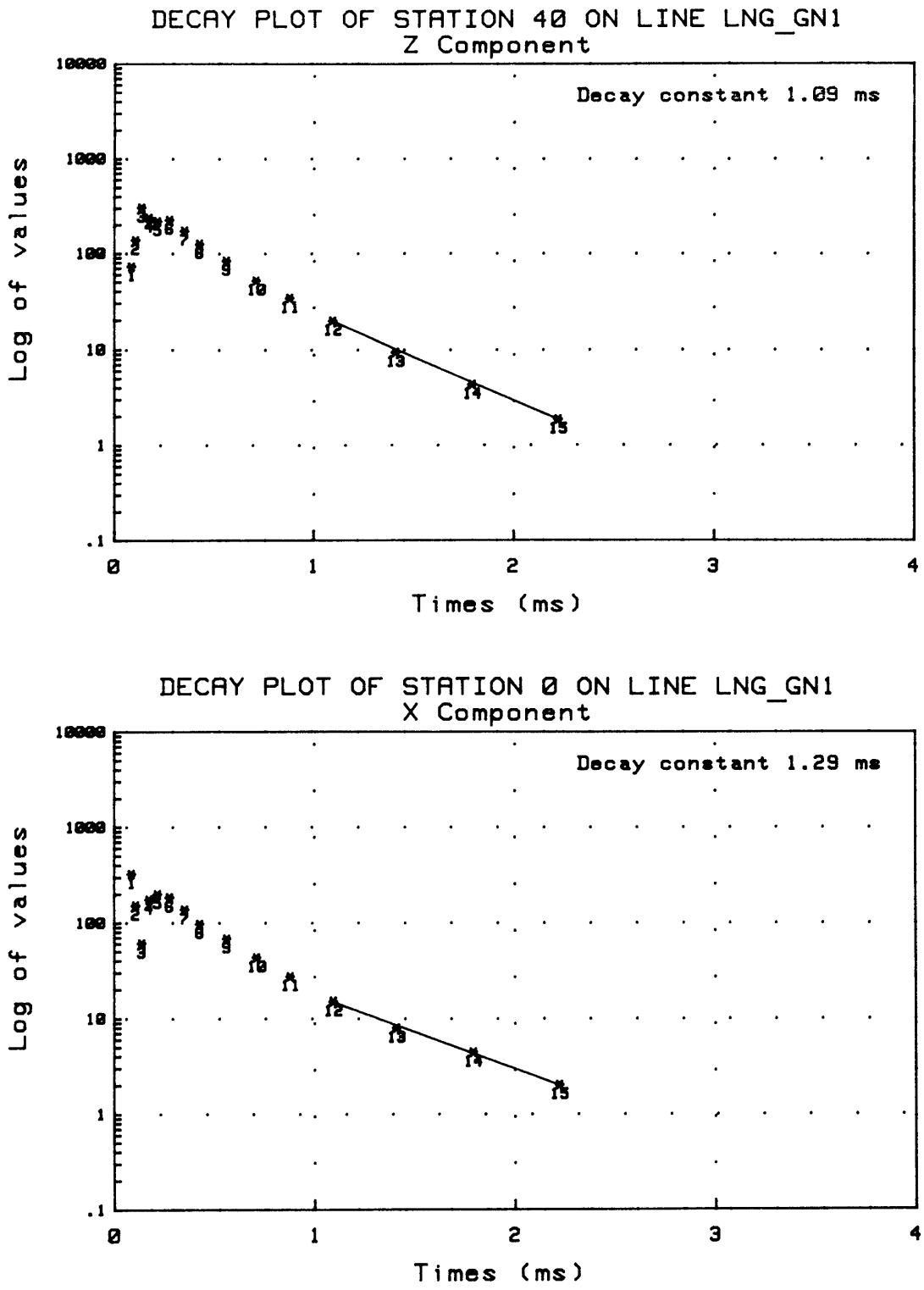

Figure 6.13 Stations 40 and 0 decay plots for anomalies obtained by the filtering method for both Bz and Bx components.

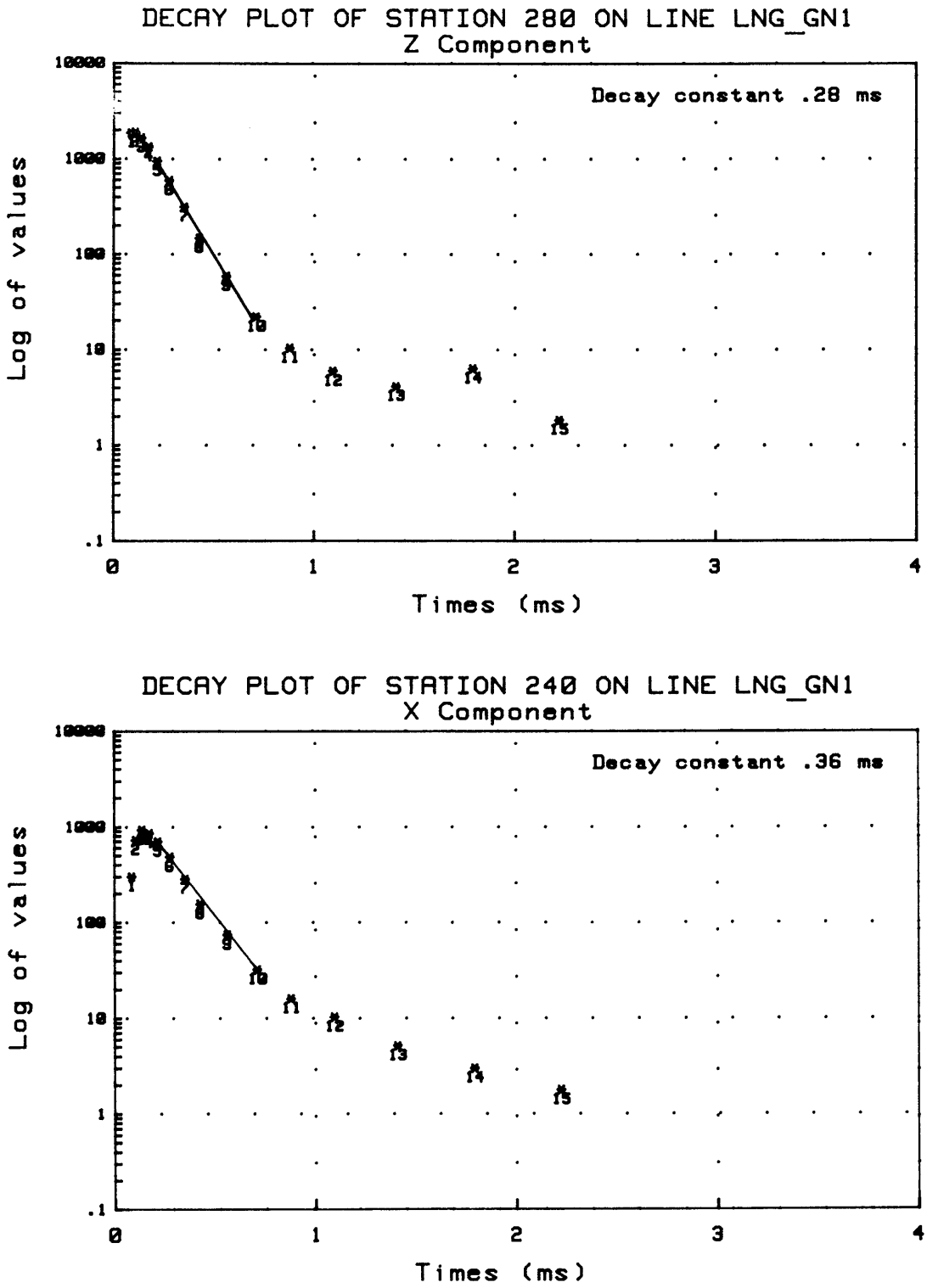

Figure 6.14 Stations 280 and 240 decay plots for anomalies obtained by the filtering method for both $\dot{B}z$ and $\dot{B}x$ components.

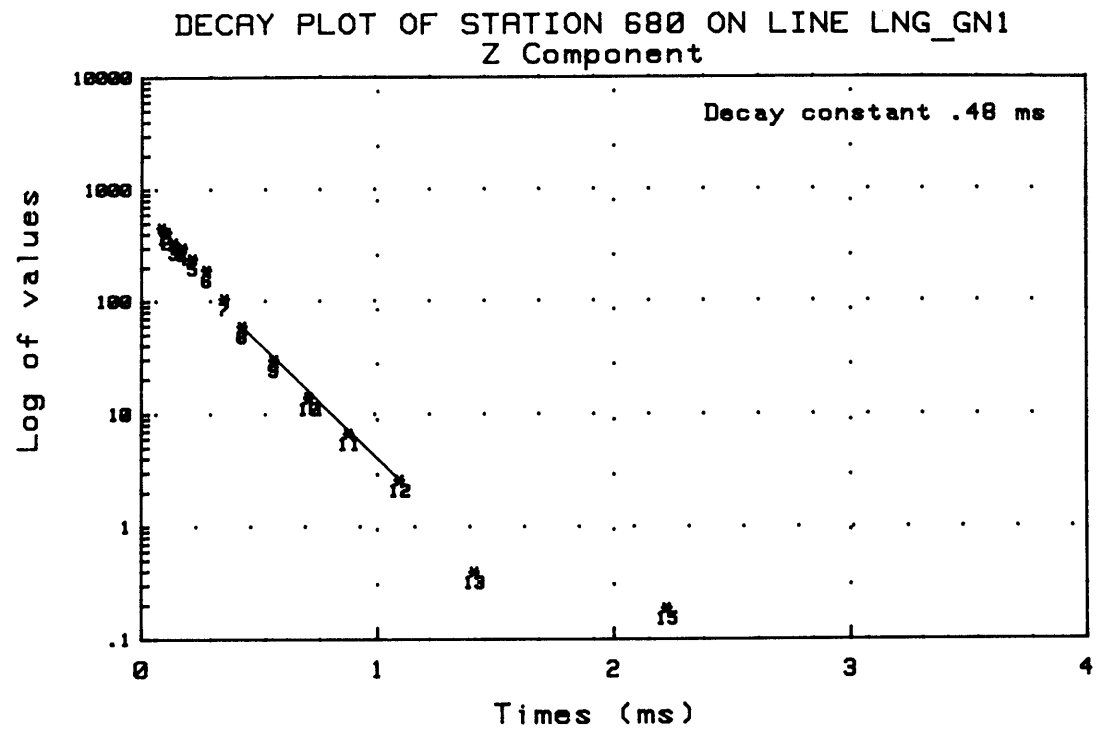

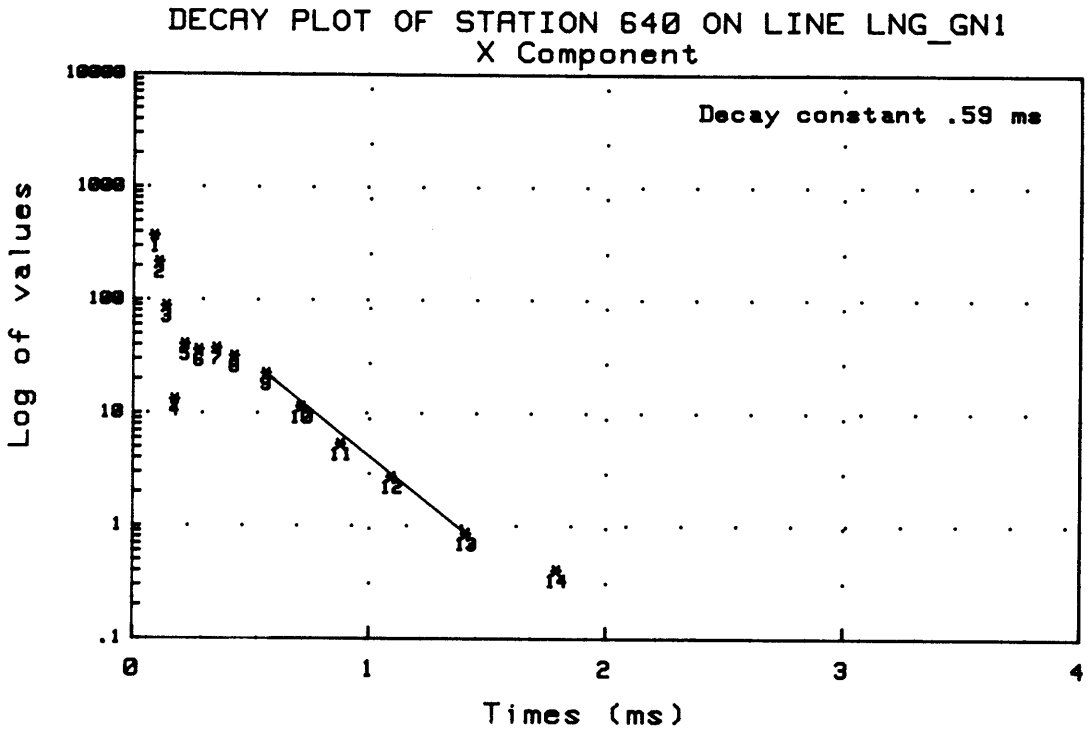

Figure 6.15 Stations 680 and 640 decay plots for anomalies obtained by the filtering method for both $\dot{B}z$ and $\dot{B}x$ components.

Figures 6.16 and 6.17 depicts the $\dot{B}z$ component anomalies for channels 1 to 17 obtained by means of calculation and subtraction of the host rock response. Figure 6.18 shows the $\dot{B}x$ component anomalies for channels 10 to 17 also using the traditional method.

The anomalies obtained from filtering the data are depicted in Figures 6.19 to 6.22. These again show that the rapid decaying anomalies situated at approximately station 200 and 600 are isolated more effectively in early time by the filter technique.

The anomalies on this line are associated with the same conductors as the corresponding anomalies on the LNG-GN1. This is confirmed by the decay constants as calculated from decay plots depicted in Figures 6.23 to 6.25.

The decay constants as calculated are:

Contact zone anomaly (station 0): 1,38ms ($\dot{B}z$) 1,63ms ($\dot{B}x$)

Confined conductor
anomaly (station 280): 0,19ms ($\dot{B}z$) 0,36ms ($\dot{B}x$)

Weathered zone
anomaly (station 640): 0,34ms ($\dot{B}z$) 0,39ms ($\dot{B}x$)

The $\dot{B}z$ component decay constants obtained from the anomalies isolated by the traditional host rock removal technique are:

Station 0 1,15ms
Station 280 0,21ms
Station 640 0,21ms

iii. Line LNG-GN5

The $\dot{B}z$ component anomalies obtained from the traditional host rock response removal technique are depicted in Figures 6.26 and 6.27.

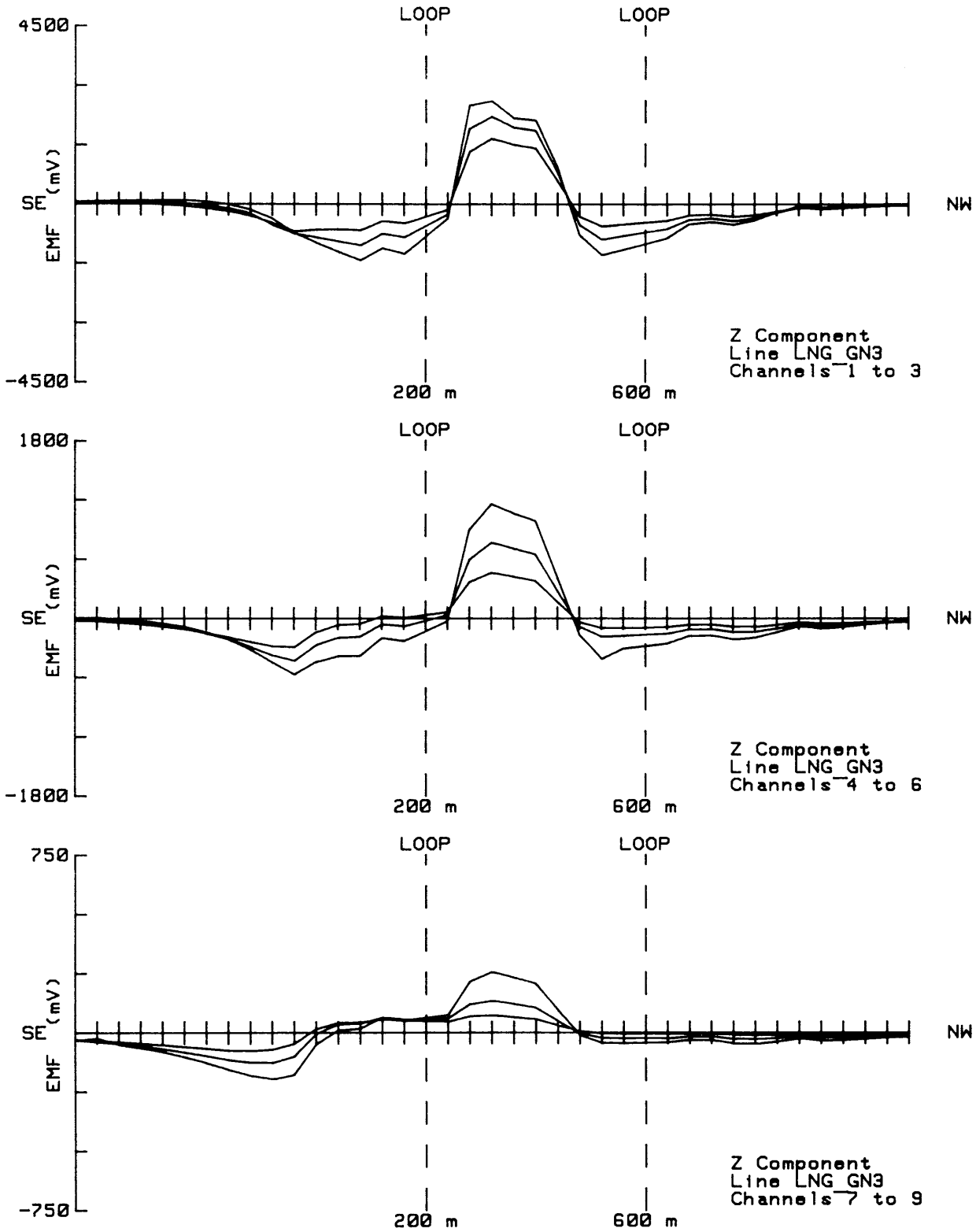

Figure 6.16 Isolated anomalies for channels 1 to 9 of line LNG-GN3 obtained by the traditional host rock removal method. Bz component.

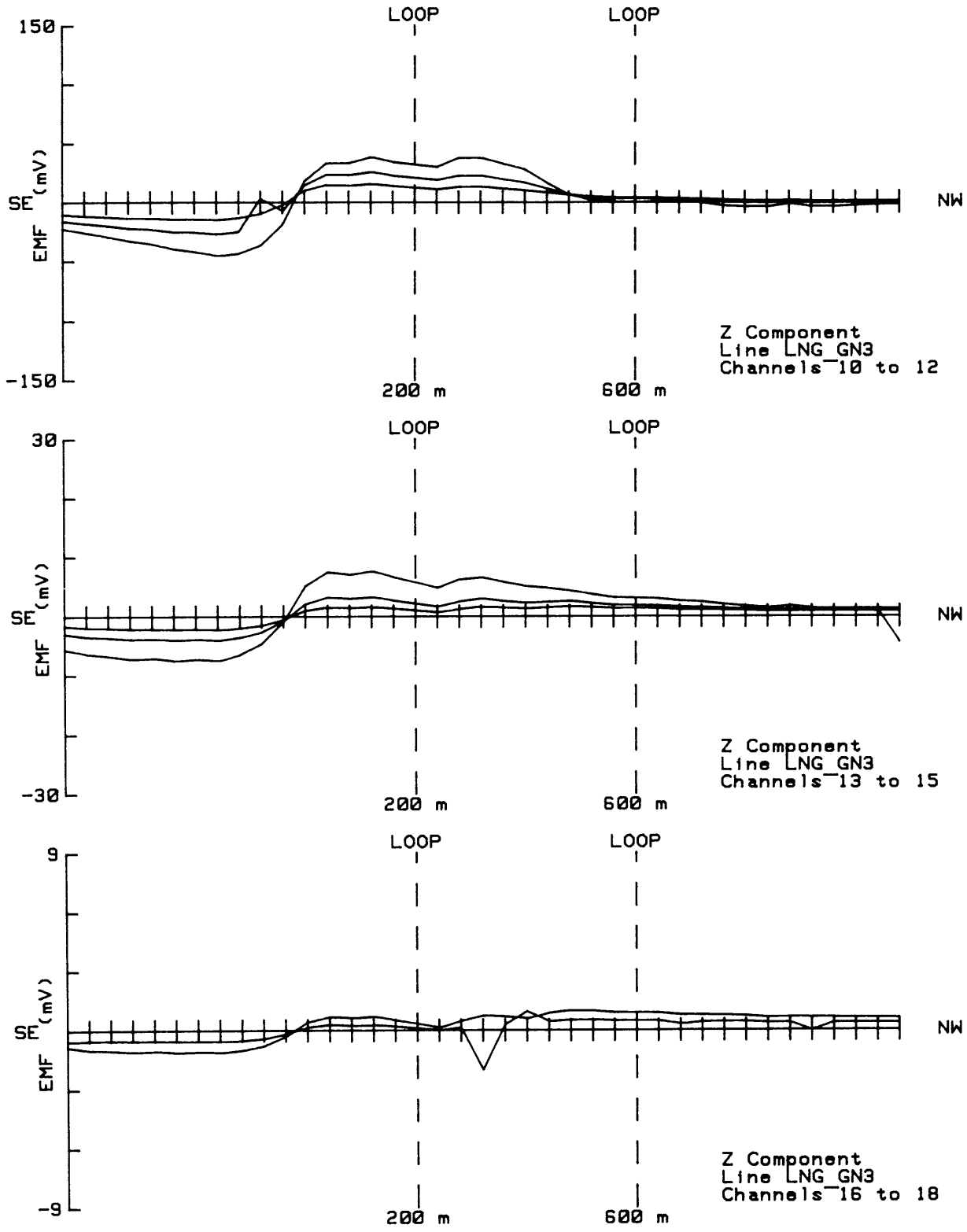

Figure 6.17 Isolated anomalies for channels 10 to 17 of line LNG-GN3 obtained by the traditional host rock removal method. $\dot{B}z$ component.

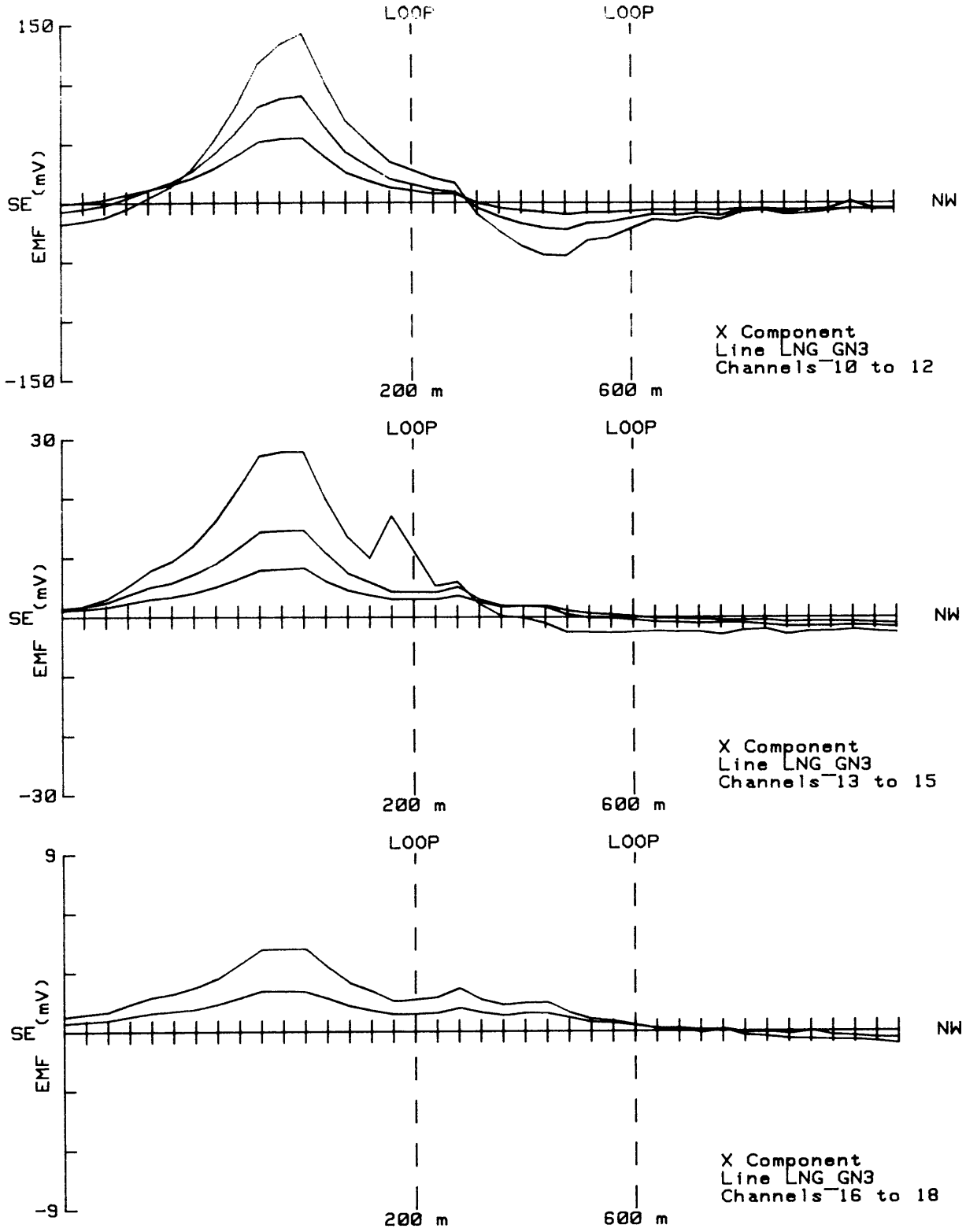

Figure 6.18 Isolated anomalies for channels 10 to 17 of line LNG-GN3 obtained by the traditional host rock removal method. $\dot{B}x$ component.

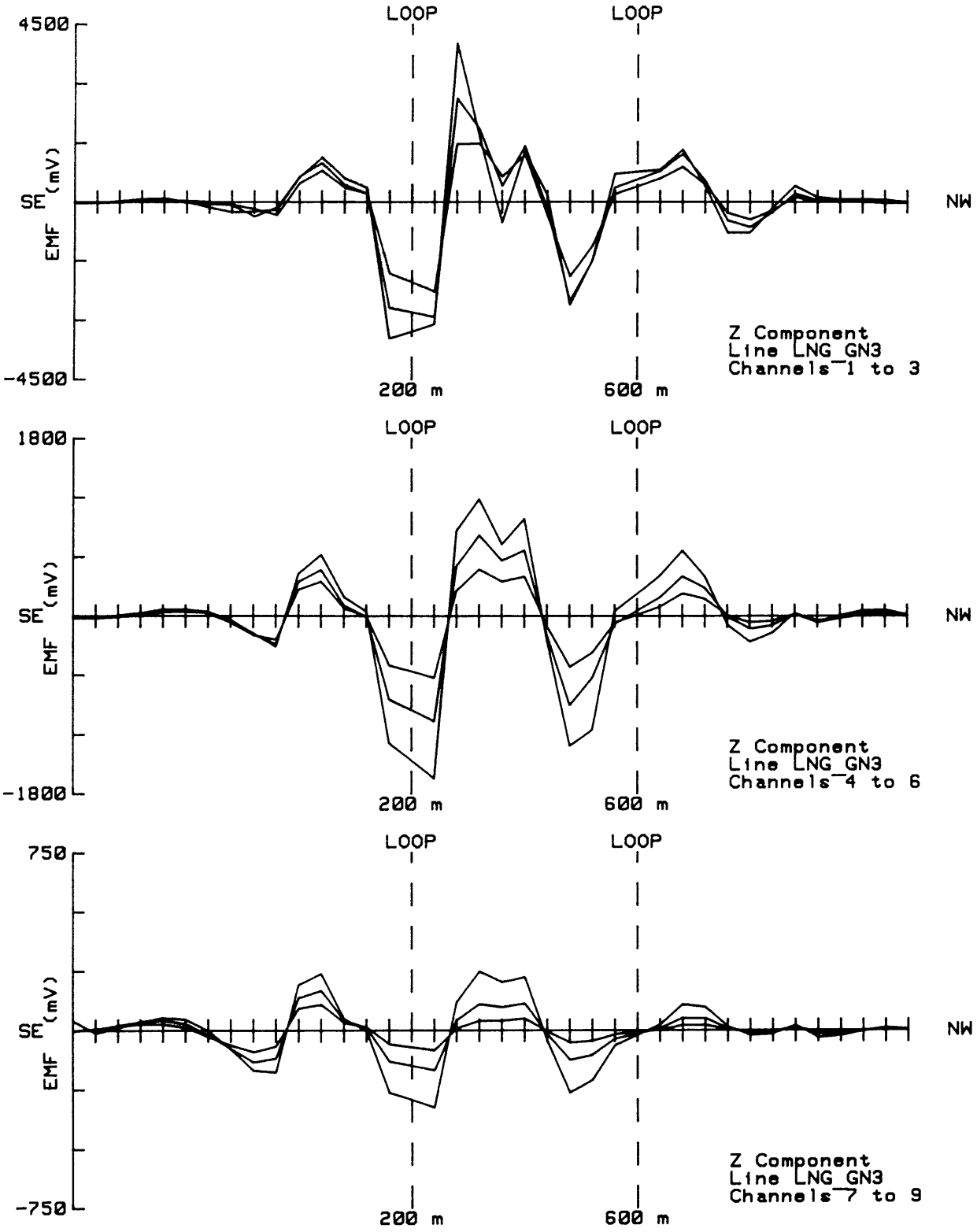

Figure 6.19 Isolated anomalies for channels 1 to 9 of line LNG-GN3 obtained by the filtering method. $\dot{B}z$ component.

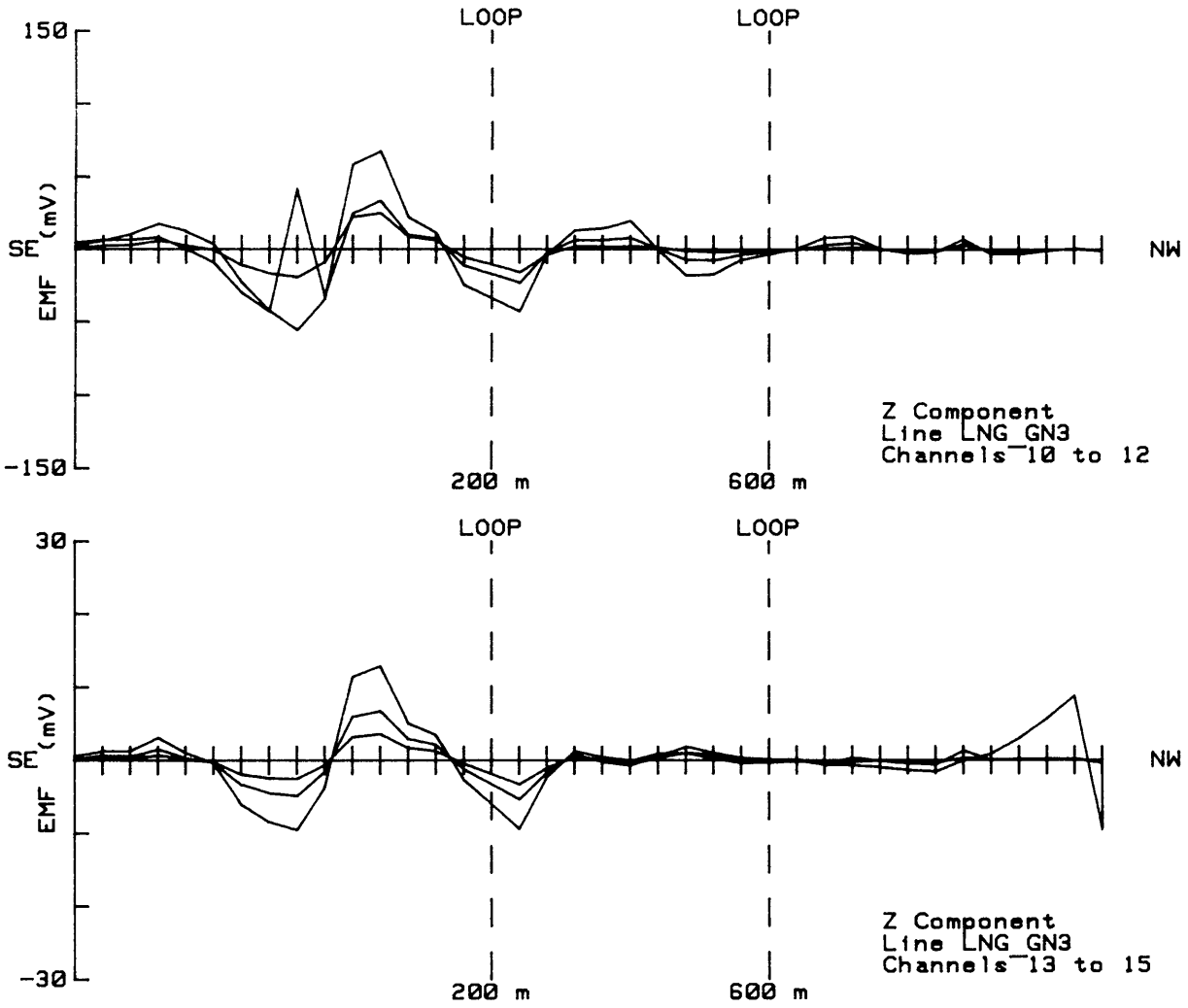

Figure 6.20 Isolated anomalies for channels 10 to 15 of line LNG-GN3 obtained by the filtering method. $\dot{B}z$ component.

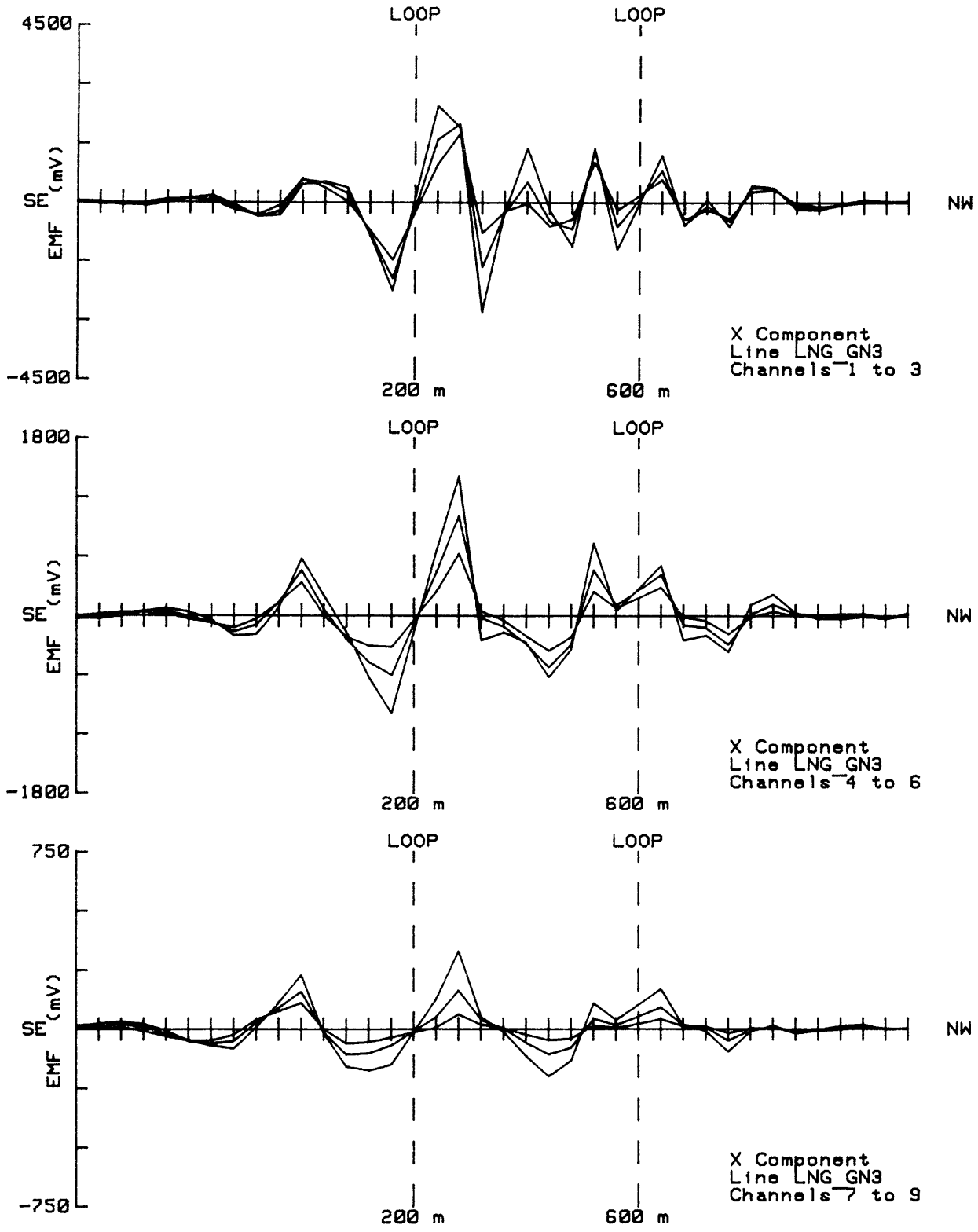

Figure 6.21 Isolated anomalies for channels 1 to 9 of line LNG-GN3 obtained by the filtering method. $\dot{B}x$ component.

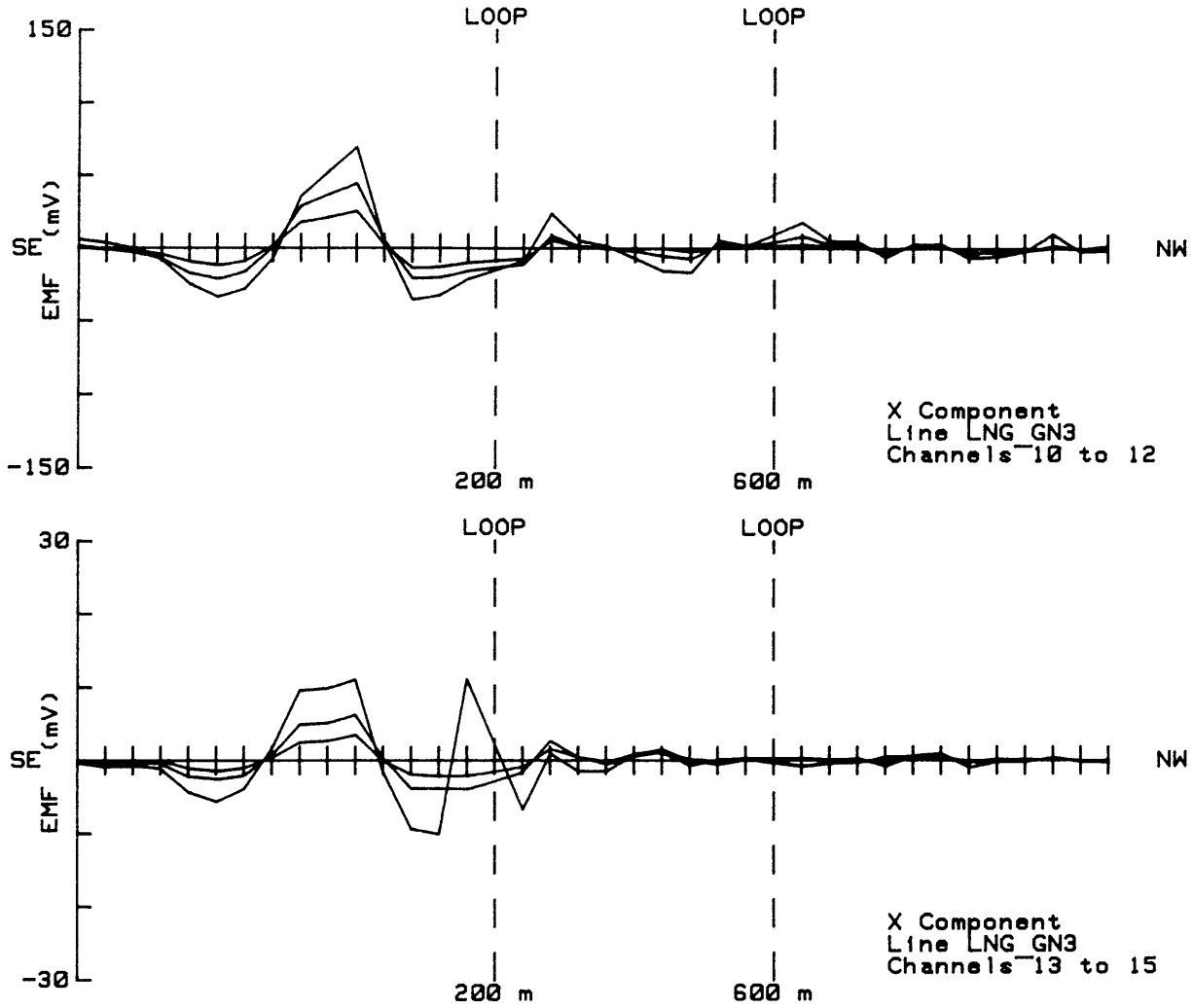

Figure 6.22 Isolated anomalies for channels 10 to 15 of line LNG-GN3 obtained by the filtering method. $\dot{B}x$ component.

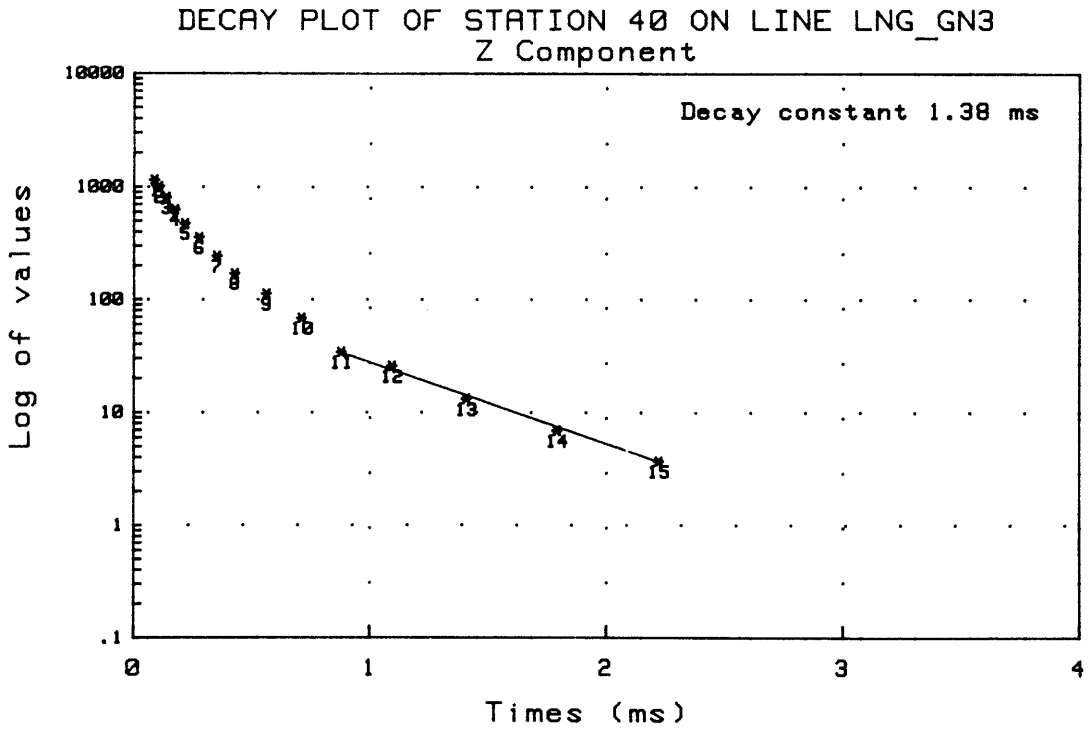

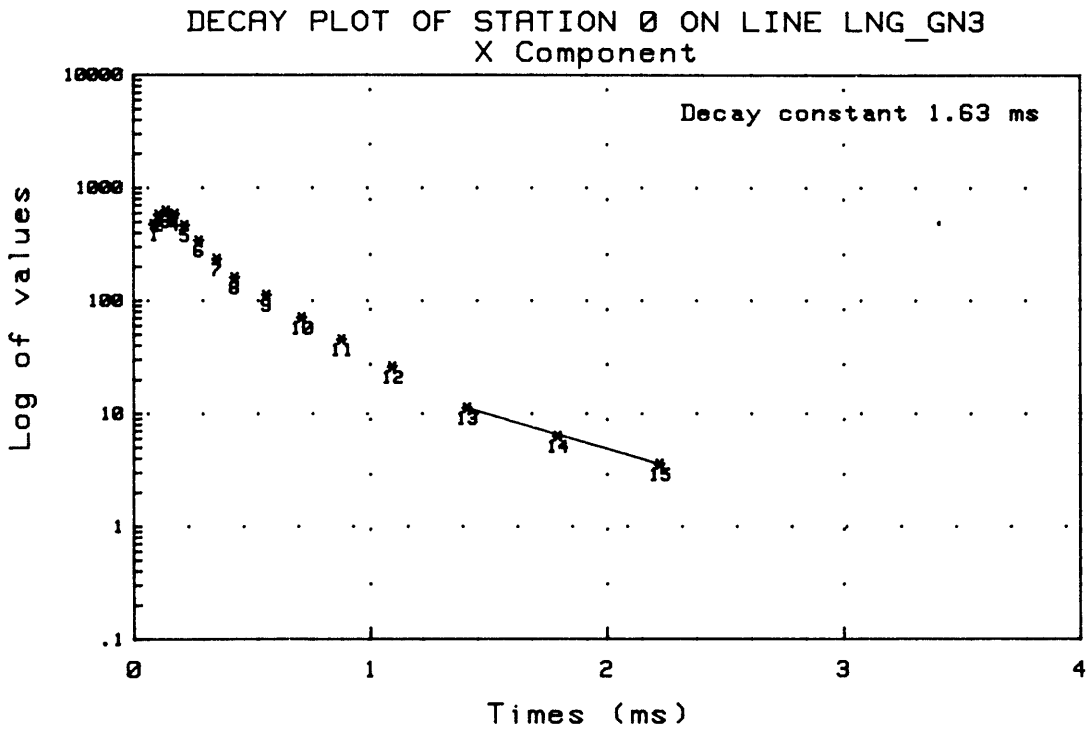

Figure 6.23 Stations 40 and 0 decay plots for anomalies obtained by the filtering method for both $\dot{B}z$ and $\dot{B}x$ component.

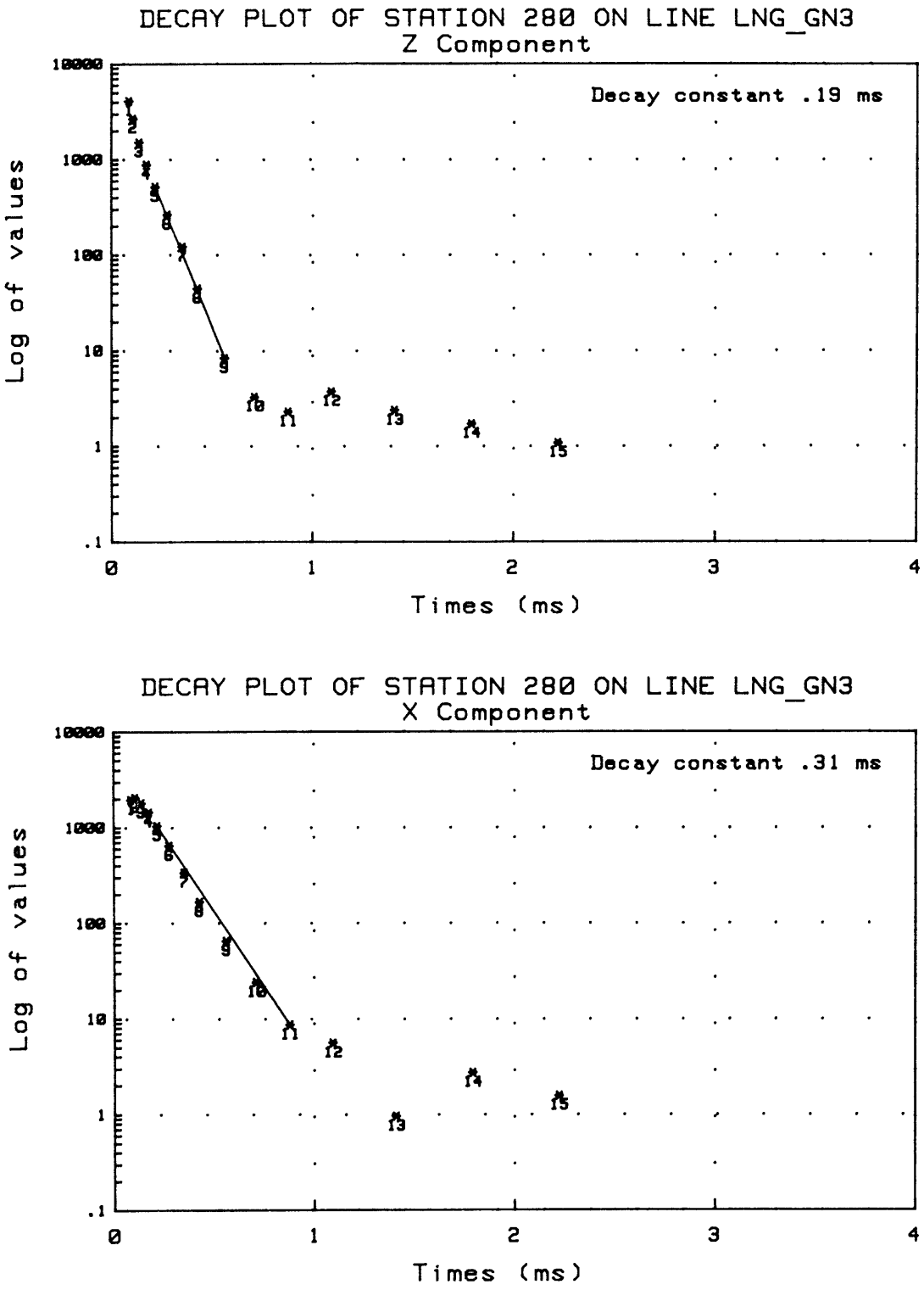

Figure 6.24 Station 280 decay plots for anomalies obtained by the filtering method for both $\dot{B}z$ and $\dot{B}x$ component.

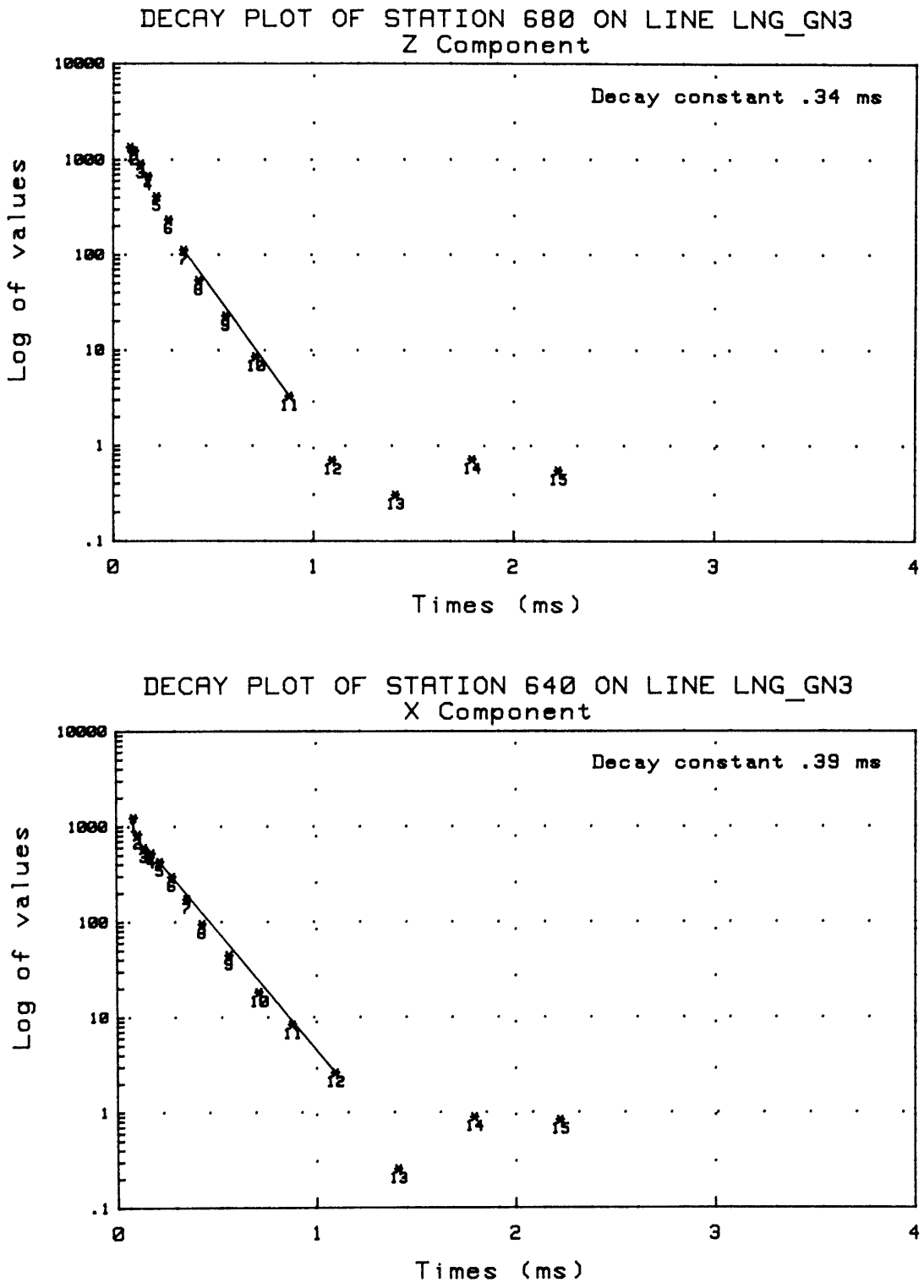

Figure 6.25 Stations 680 and 640 decay plots for anomalies obtained by the filtering method for both $\dot{B}z$ and $\dot{B}x$ component.

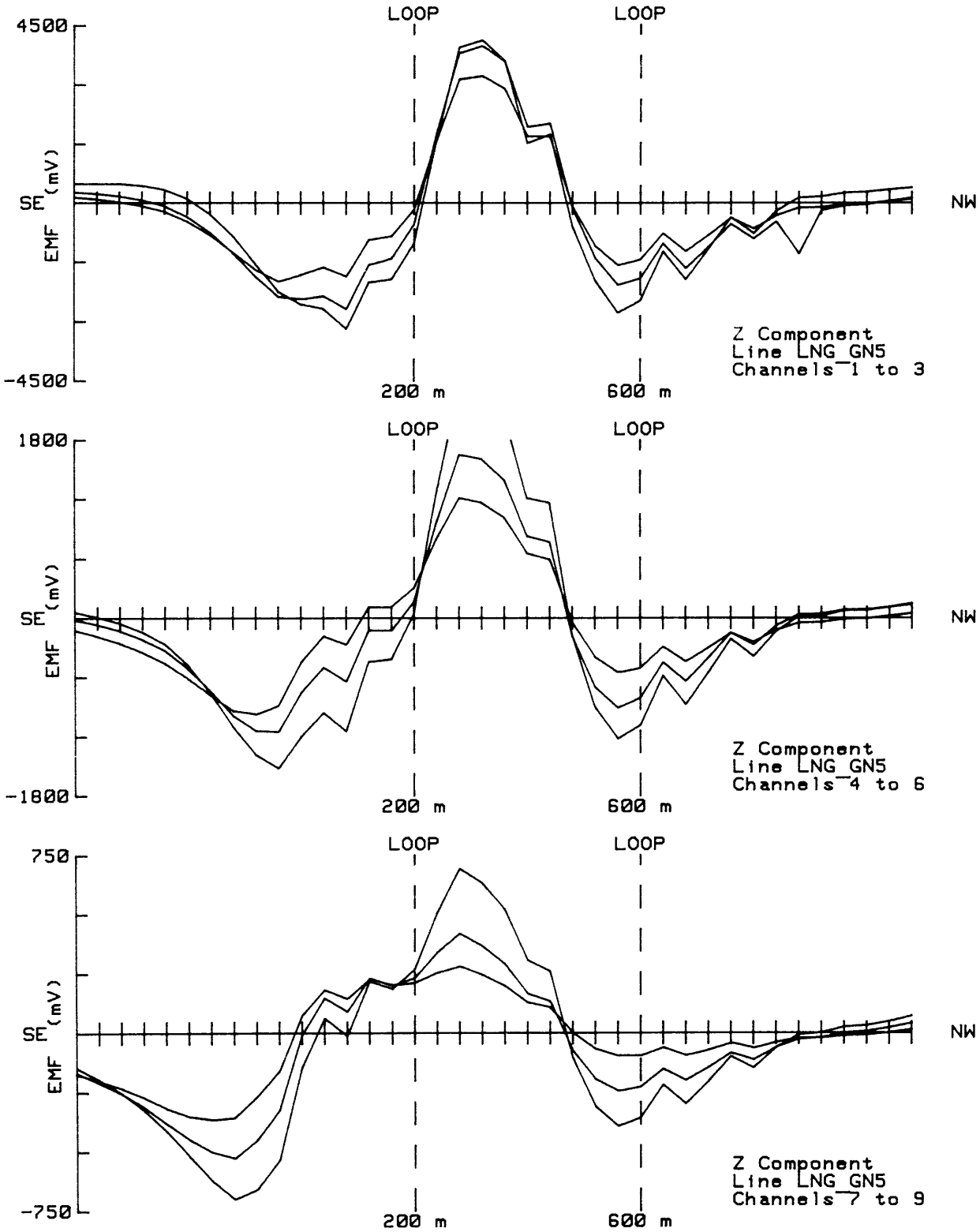

Figure 6.26 Isolated anomalies for channels 1 to 9 of line LNG-GN5 obtained by the traditional host rock removal method. Ḃz component.

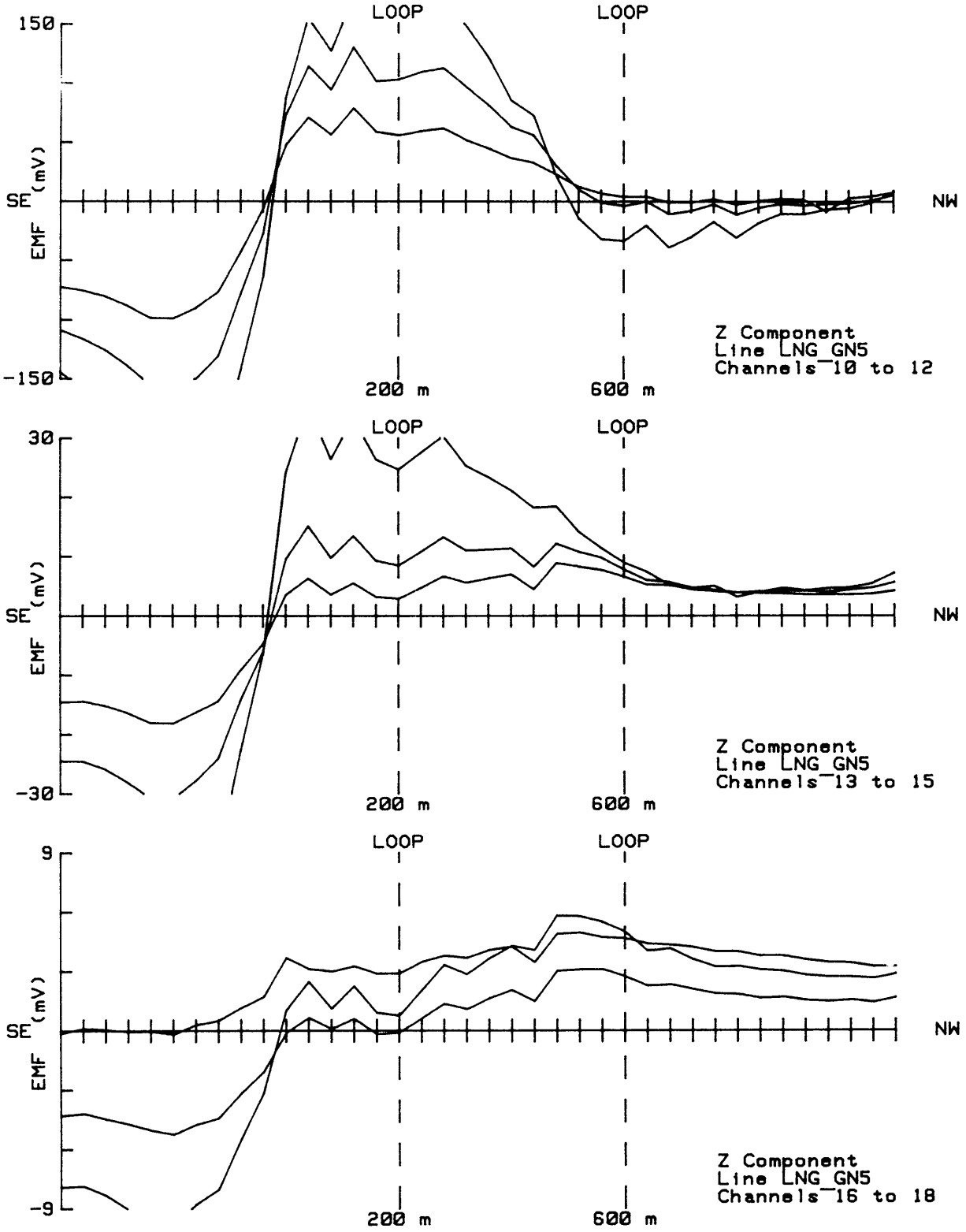

Figure 6.27 Isolated anomalies for channels 10 to 17 of line LNG-GN5 obtained by the traditional host rock removal method. $\dot{B}z$ component.

The filtered anomalies for the $\dot{B}z$ component are given in Figures 6.28 and 6.29. From this one sees that the early channel anomalies that were easily recognisable on the previous two lines are not obvious on this line. An examination of the field data reveals that the data is very noisy and this explains the high frequency anomalies that were obtained during host rock removal where the low frequency content of the spectrum is removed. In order to overcome this problem the data was smoothed by removing the ultra high frequency component of the spectrum by means of a low pass filter with a gradual slope. Figures 6.30 to 6.33 depict the anomalies obtained from the smoothed data. A low pass filter with cut-off frequency of 0,2 cycles/datalength and sharpness of 20 was applied to the data before the removal of the host rock response.

By comparing this result with Figures 6.28 and 6.29 it can be seen that all the single station anomalies were removed for the early channels thus making it far more easy to define the true shape of the anomalies. It is also noticeable that the smoothing had a reduced effect in the late channels.

A comparison between the decay curves for stations 40,280 and 640 before and after smoothing reveals that the smoothing had very little effect on the decay constants (Figures 6.34 to 6.36).

The decay constants for the three anomalies are as follows:

Contact zone anomaly (station 40): 1,45ms ($\dot{B}z$) 1,34ms ($\dot{B}x$)

Confined conductor
anomaly (station 280): 0,23ms ($\dot{B}z$) 0,31ms ($\dot{B}x$)

Weathered zone
anomaly (station 640): 0,37ms ($\dot{B}z$) 0,50ms ($\dot{B}x$)

From the shape and the positions of the anomalies and modelling with the plate program the same qualitative interpretation as for line

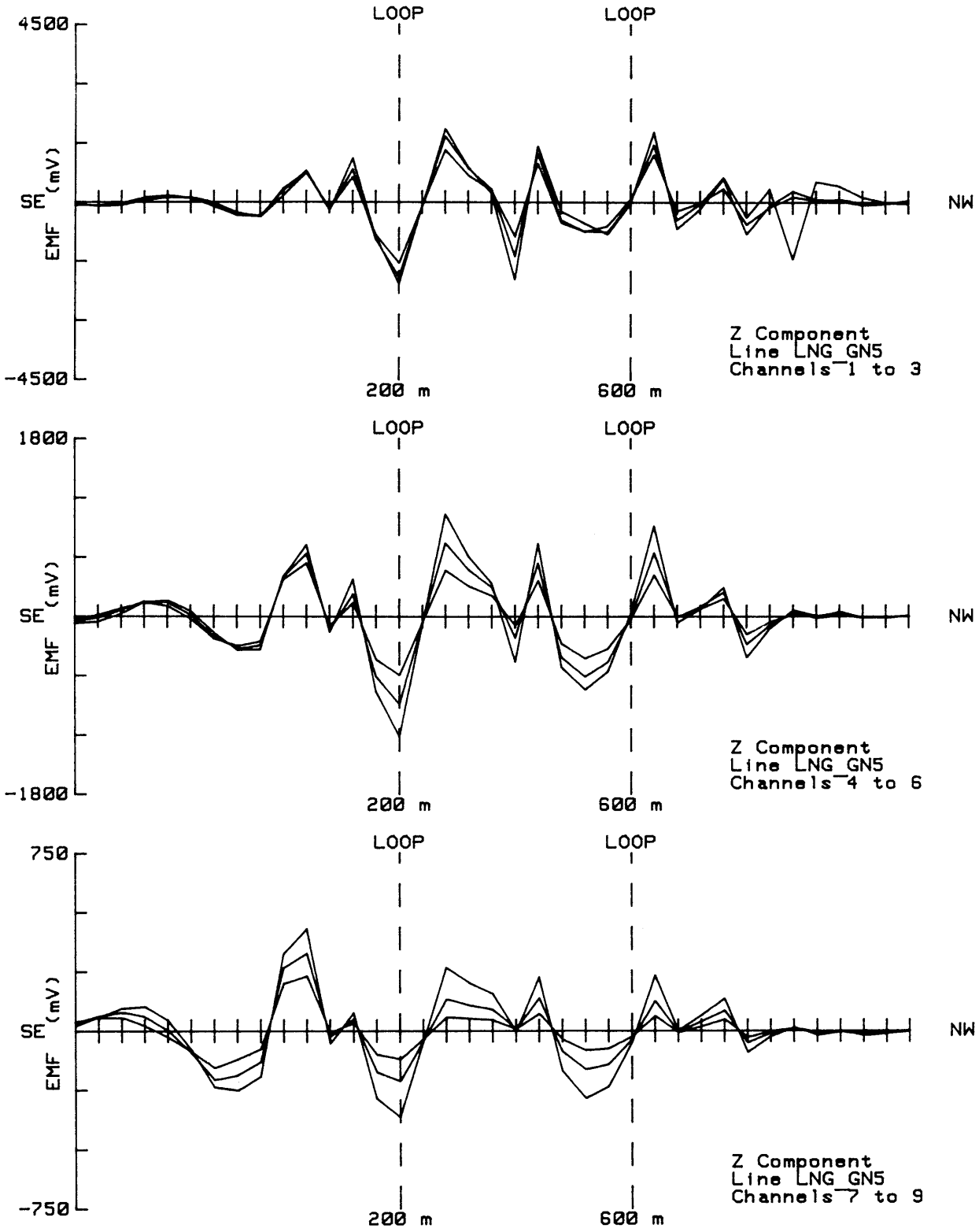

Figure 6.28 Isolated anomalies for channels 1 to 9 of line LNG-GN5 obtained by the filtering method. $\dot{B}z$ component.

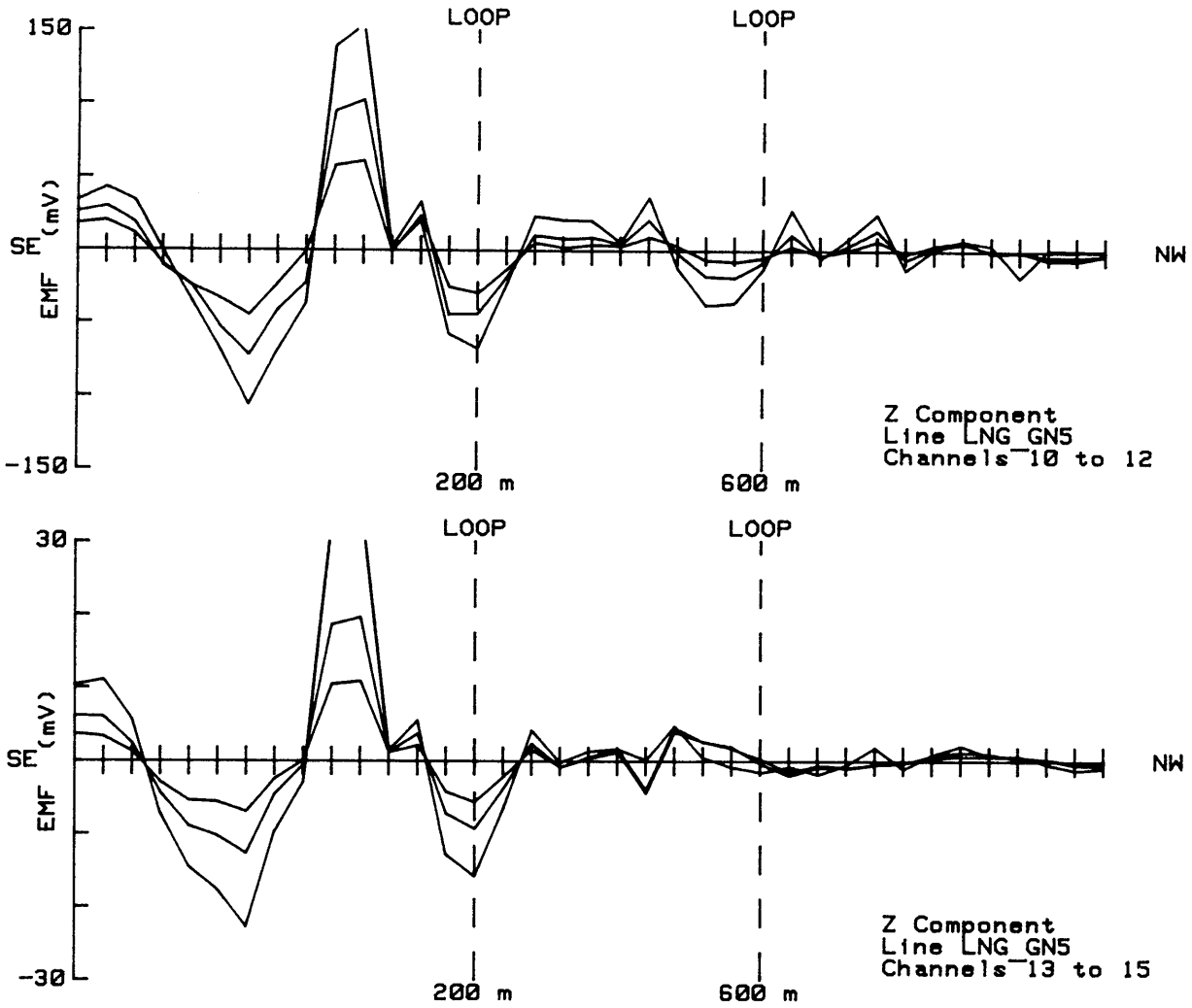

Figure 6.29 Isolated anomalies for channels 10 to 15 for line LNG-GN5 obtained by the filtering method. $\dot{B}z$ component.

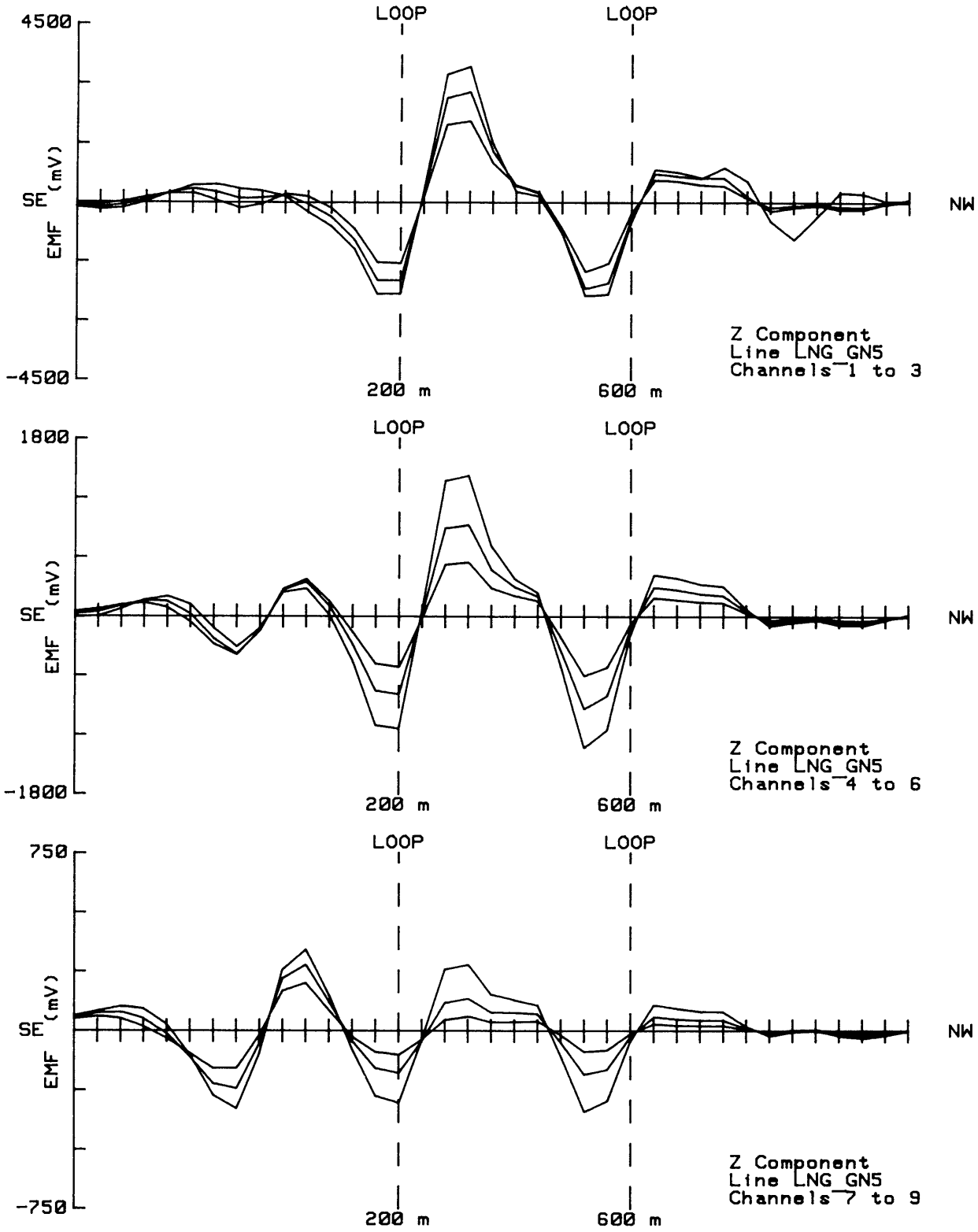

Figure 6.30 Smoothed isolated anomalies for channels 1 to 9 for line LNG-GN5 obtained by the filtering method. $\dot{B}z$ component.

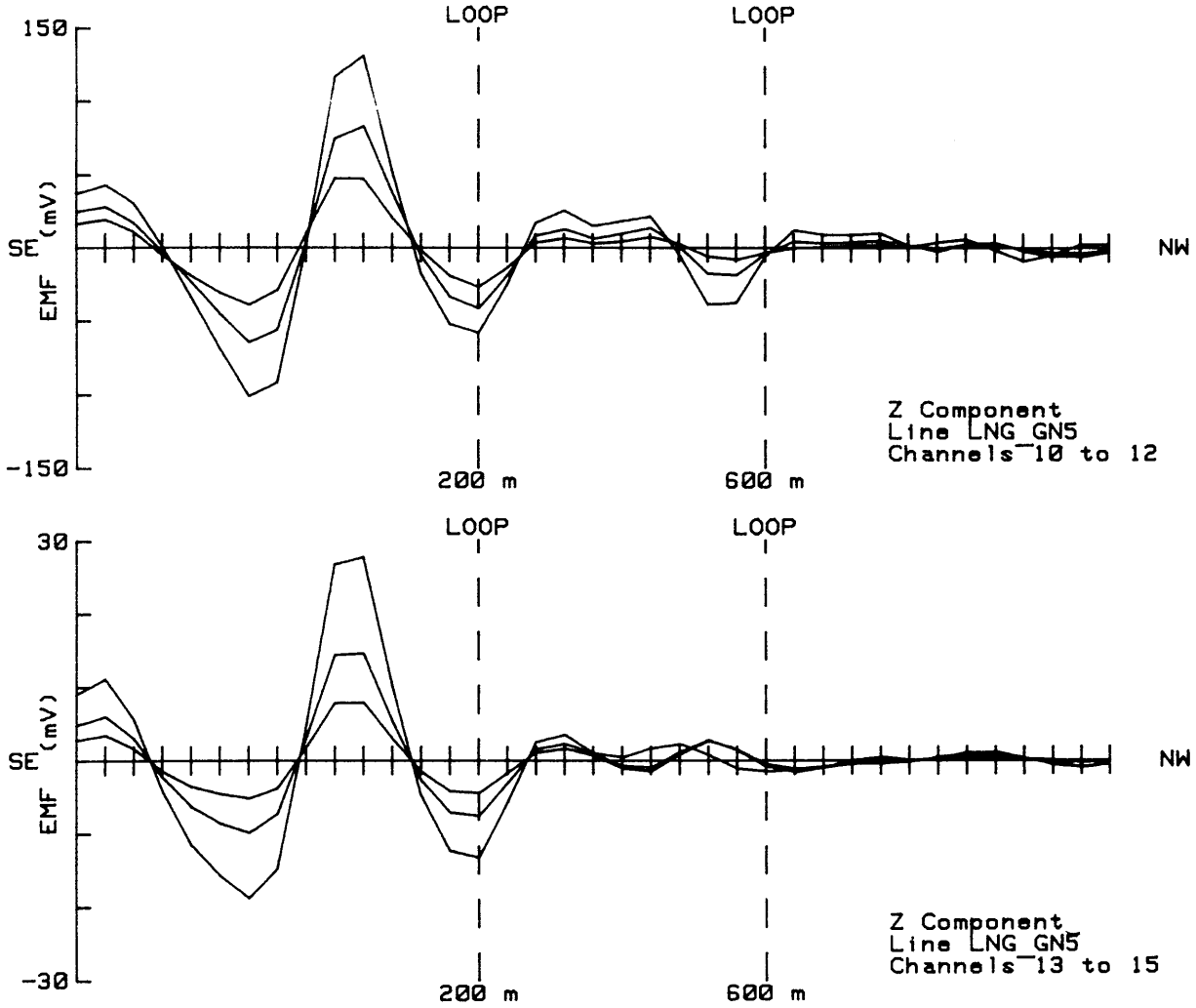

Figure 6.31 Smoothed isolated anomalies for channels 10 to 15 for line LNG-GN5 obtained by the filtering method. $\dot{B}z$ component.

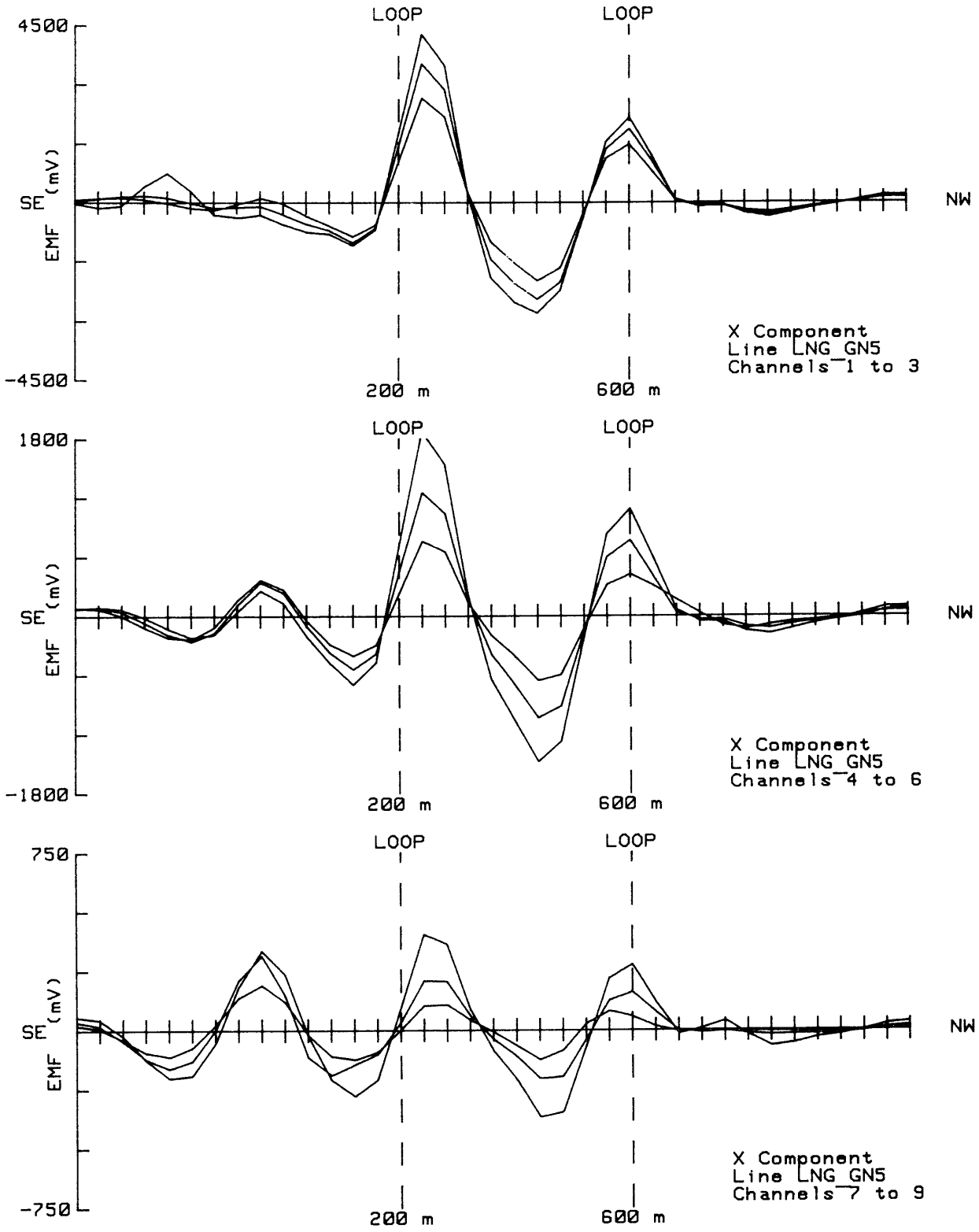

Figure 6.32 Smoothed isolated anomalies for channels 1 to 9 for line LNG-GN5 obtained by the filtering method. $\dot{B}x$ component.

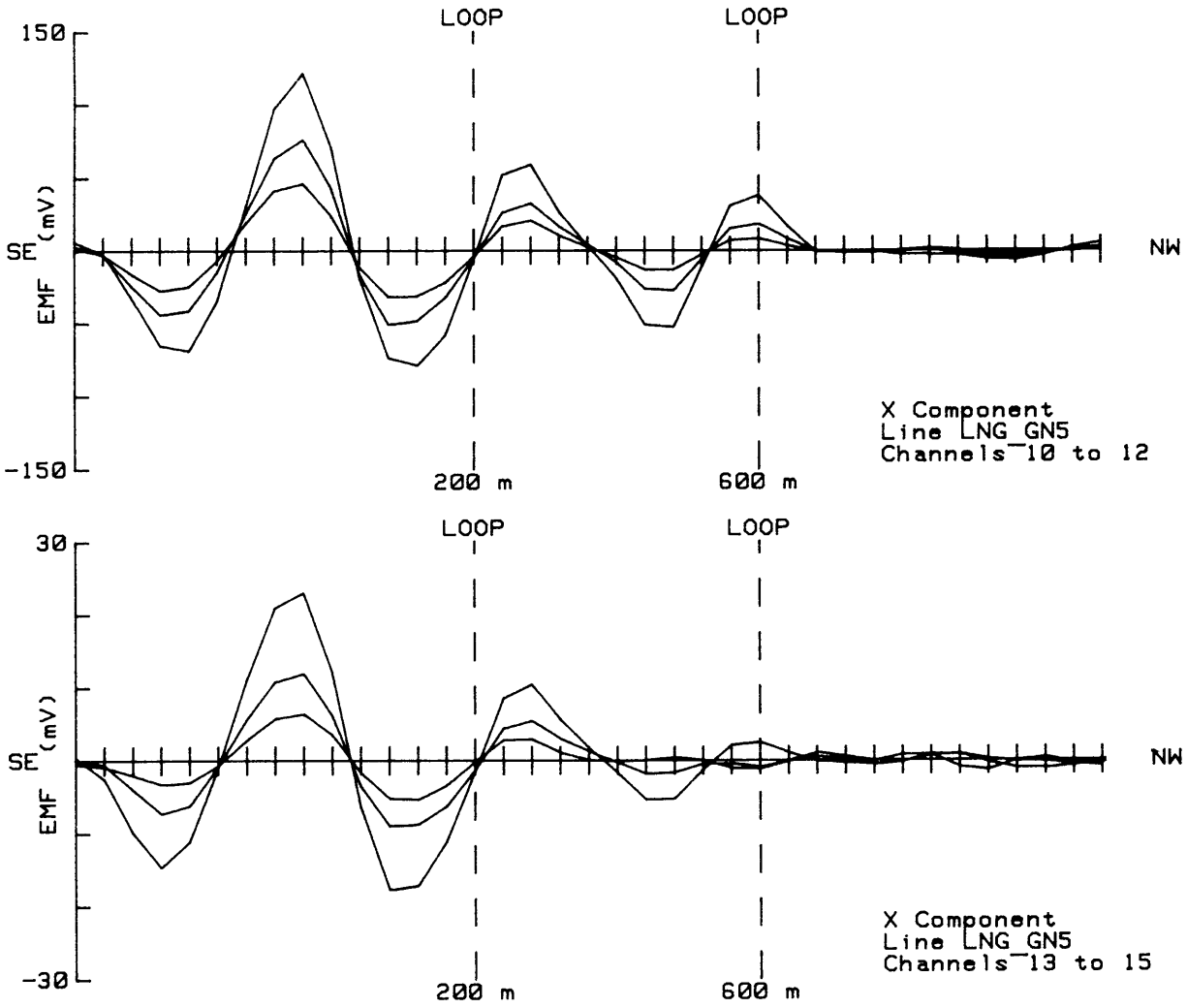

Figure 6.33 Smoothed isolated anomalies for channels 10 to 15 for line LNG-GN5 obtained by the filtering method. $\dot{B}x$ component.

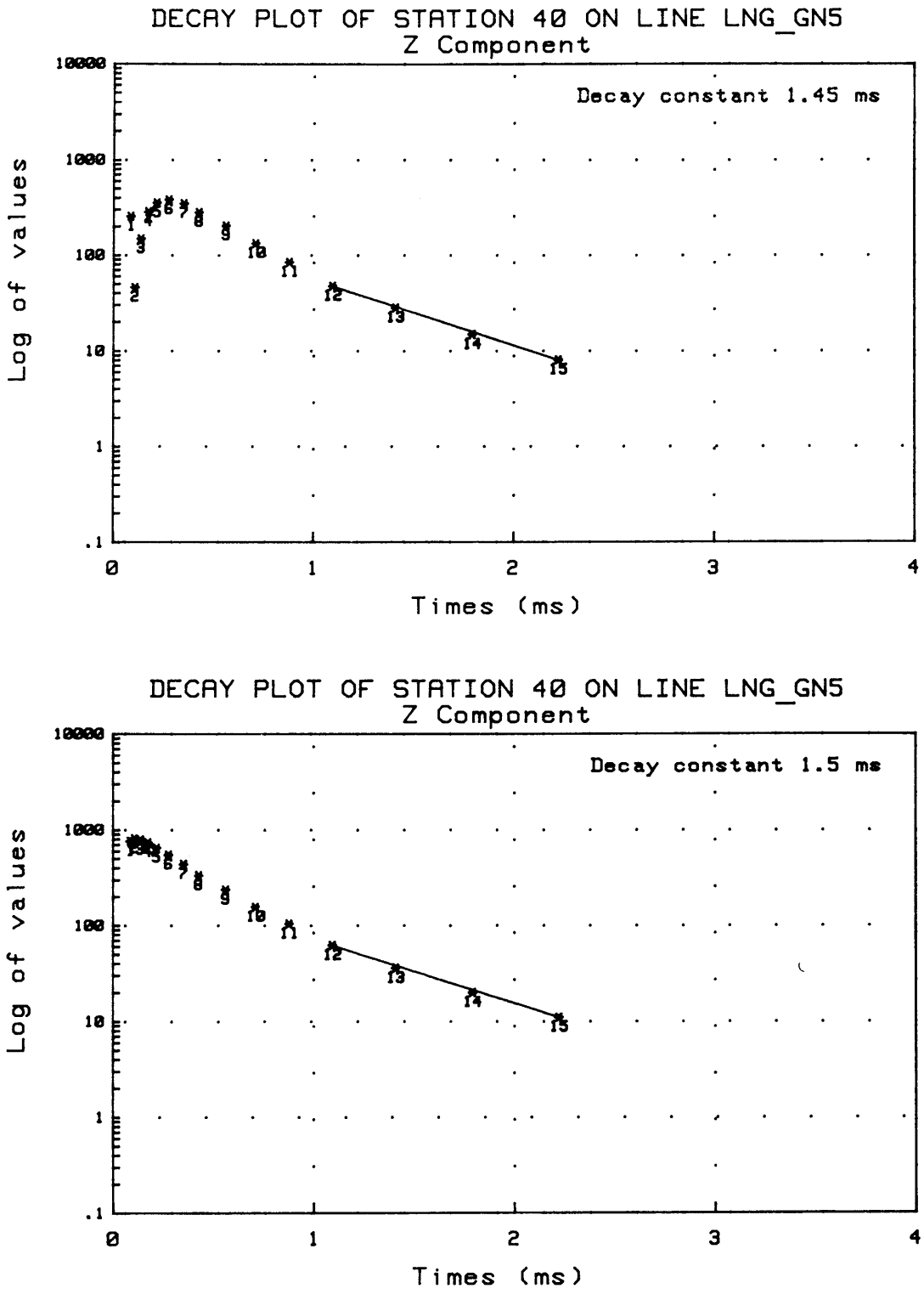

Figure 6.34 Station 40 decay plots for the unsmoothed and smoothed anomalies obtained by the filtering method for the Ḃz component.

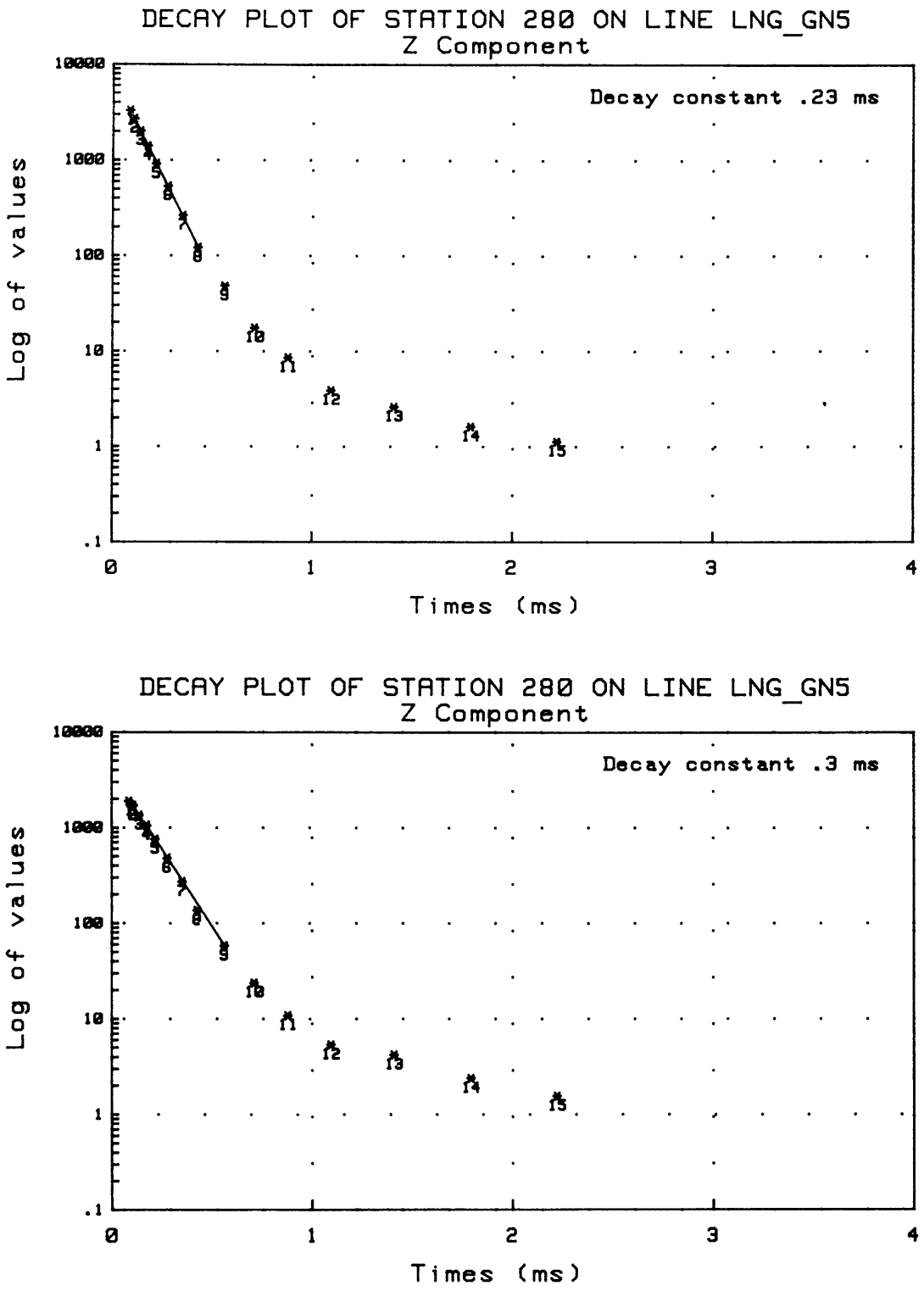

Figure 6.35 Station 240 decay plots for anomalies obtained by the filtering method for both $\dot{B}z$ and $\dot{B}x$ components.

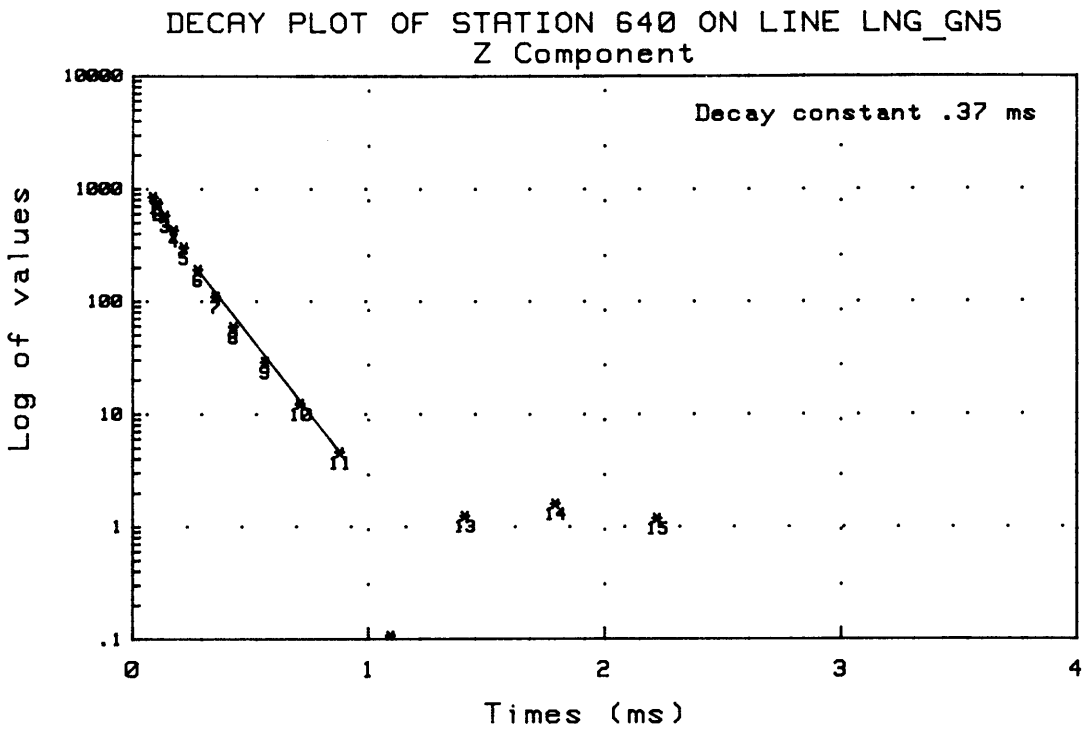

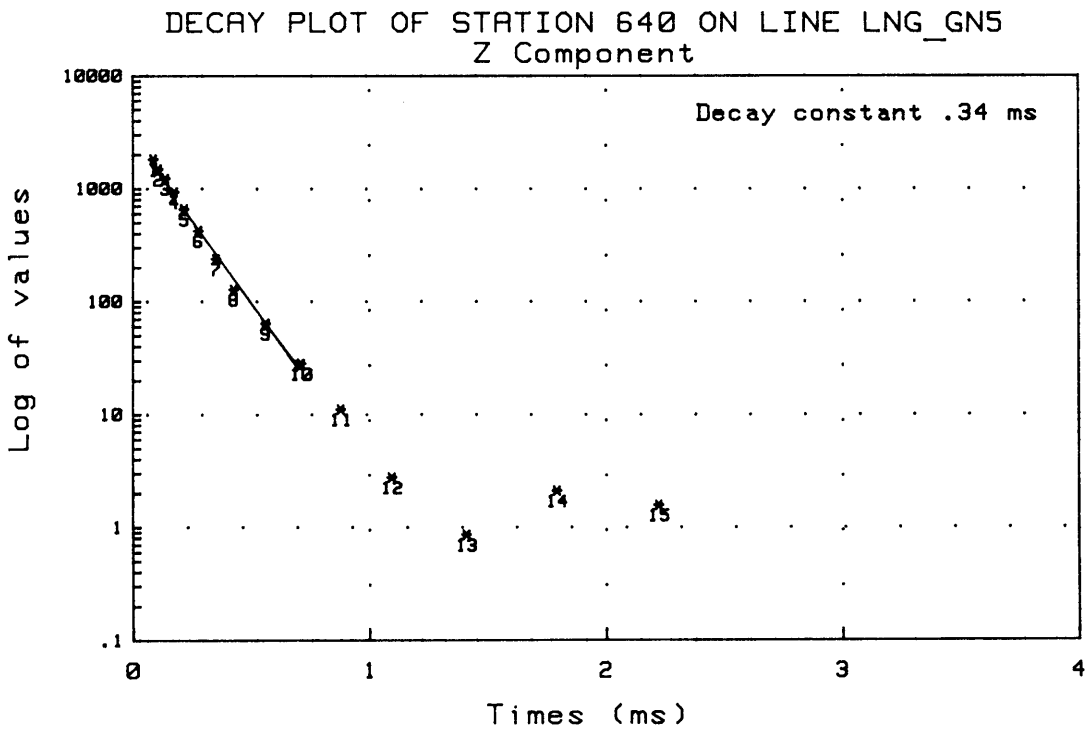

Figure 6.36 Station 640 decay plots for anomalies obtained by the filtering method for both $\dot{B}z$ and $\dot{B}x$ components.

LNG-GN1 and LNG-GN3 are made, with the exception that the anomaly of the weathered zone has changed from that of a vertical structure to that of a horizontal structure. A possible explanation for this can be that the depth of weathering has decreased and that the broad weathered zone now behaves like a shallow horizontal plate.

6.2.5 Summary

A summary of the interpretation of the three lines is given in Figure 6.37. This shows the anomaly locations and the decay constants as calculated for the different anomalies by the filter technique. A qualitative interpretation in the form of a profile is also depicted in this figure.

6.3 SASOLBURG CASE HISTORY

6.3.1 Location

The survey area under investigation is situated on the farm Petershoogte some 10km southwest of Sasolburg. Figure 6.38 depicts the locality map together with the transmitter loop position. A single line (SAS-00) through the centre of the transmitter loop was surveyed. Data acquisition was done in a similar manner as for the Lake Ngami survey.

6.3.2 Geology

The coal fields of this area are part of the Sigma basin. This basin is underlain by Ventersdorp lavas and dolomites of the Transvaal Supergroup. The pre-Karoo palaeotopography was characterized by hills and valleys. This uneven palaeotopography was partially smoothed by the deposition of the Dwyka tillites. The coal zone is up to 30m thick with the lowest layer near or on top of the Dwyka tillites. The coal zone can be evenly divided into 3 layers. Interbedded between the lower and middle layer deposits of up to 2m thick gritty

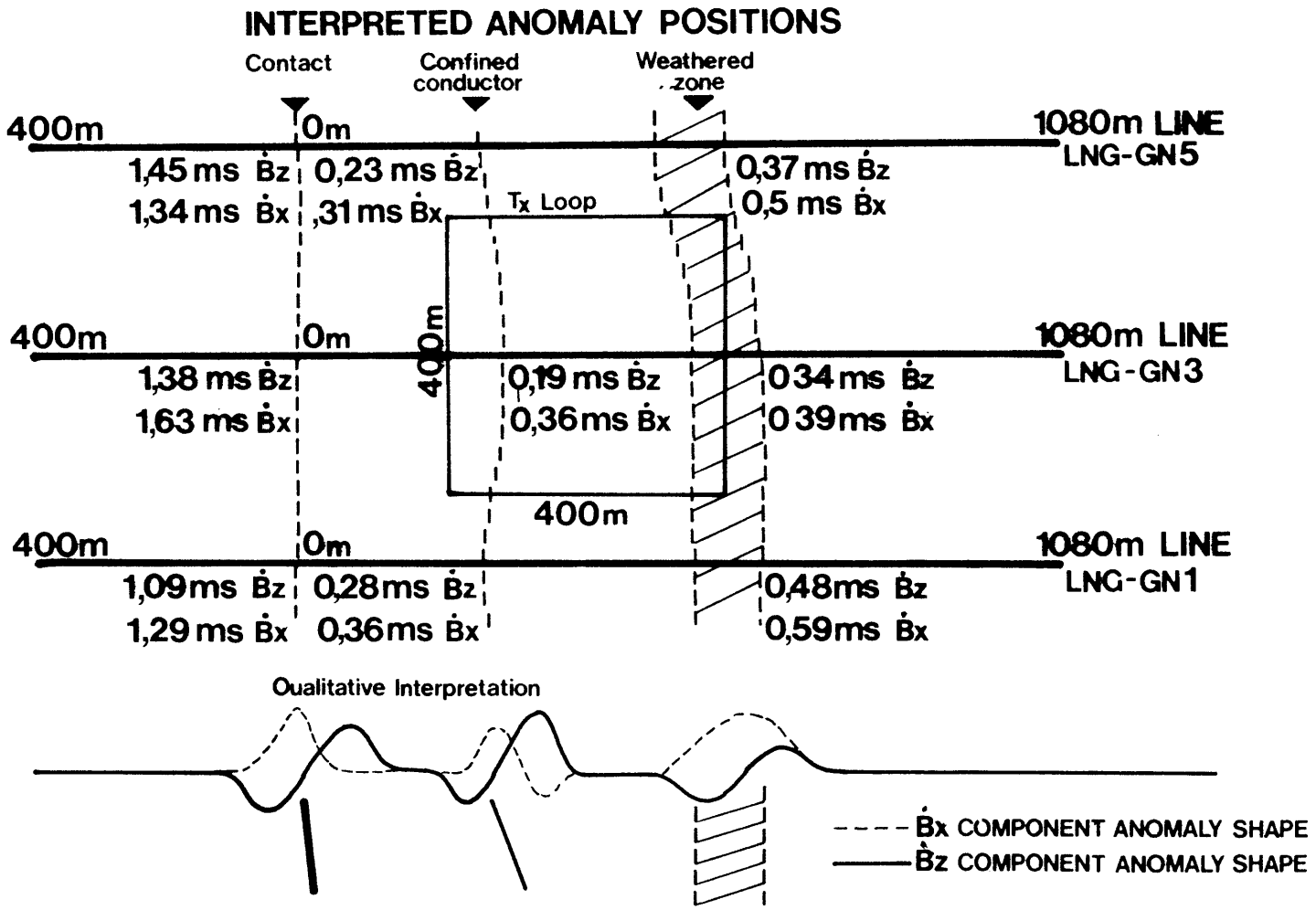

Figure 6.37 Summary of interpretation including qualitative interpretation and decay constants.

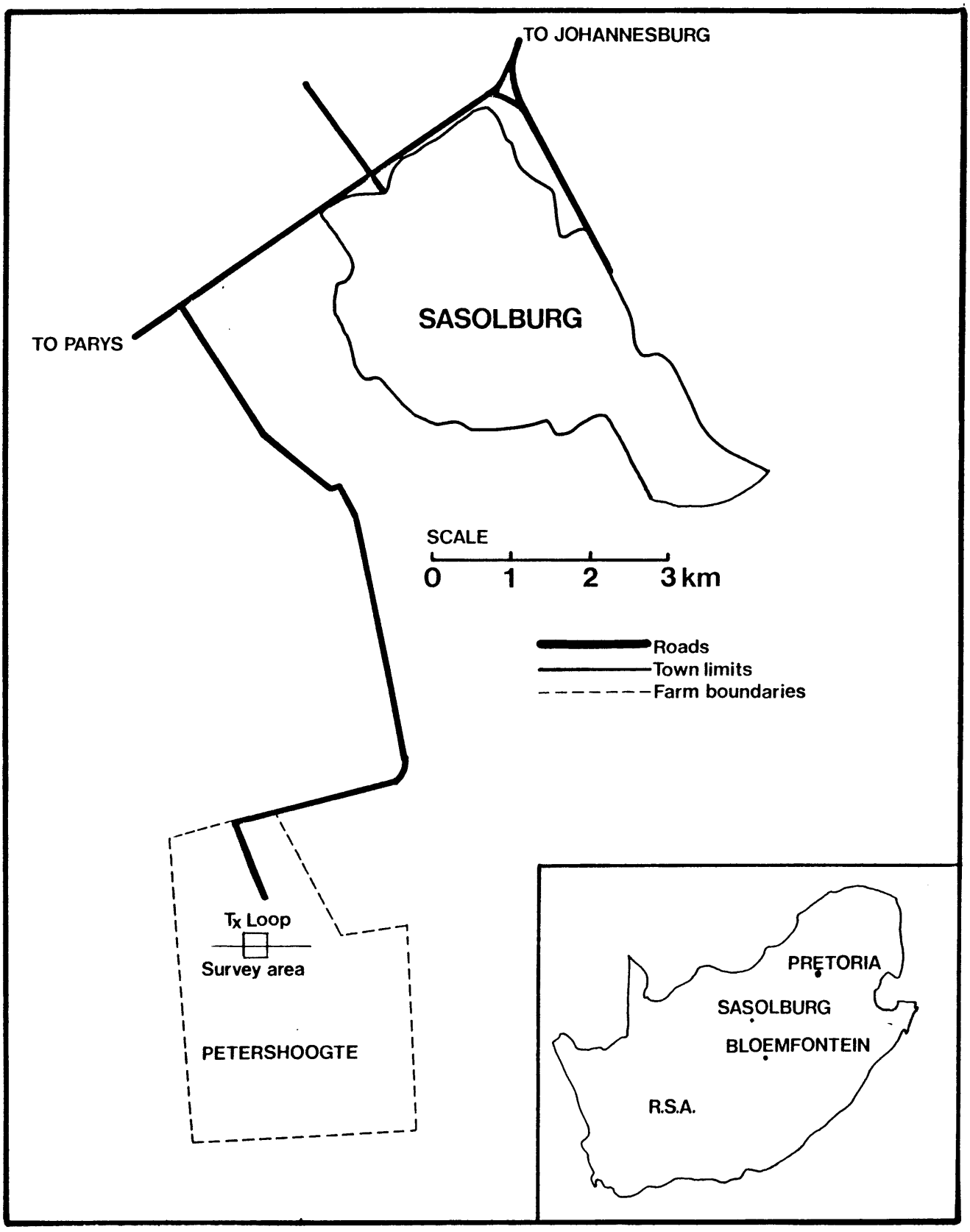

Figure 6.38 Locality map of Sasolburg case history.

sandstones, grit and (or) conglomerate occurs. The remaining portion of this zone, apart from the coal seams, consists of shale and sandstone in roughly equal proportions. A dolerite sill with an average thickness of 41m intruded into the sandstone above the top coal seam.

On the farm Petershoogte a fault that dips with an angle of 70 degrees to the east was intersected by mine tunnelling at a depth of 150m below the surface. The position of the intersection of the fault is approximately 260m to the east of the centre of the transmitter loop. A dolerite dyke occurs 300m east of the centre of the transmitter loop. Figure 6.39 depicts the loop position in reference to the known geology.

6.3.3 Interpretation

Figures 6.40 and 6.41 depicts the $\dot{B}z$ and $\dot{B}x$ component field data together with the best fitting calculated host rock responses. The anomalies after subtraction of the theoretical responses are depicted in Figures 6.42 and 6.43. The comparison of this anomaly with theoretical confined conductor anomalies (Gallagher *et al.*, 1985) clearly indicates it to be of a combined nature. The superpositioning of the anomalies make it impossible to give a clear indication as to the type of conductor that causes the anomalies. Decay constant calculations indicate that the anomalies are not due to rining.

Figures 6.44 and 6.45 depict the anomalies obtained from the removal of the host rock response by means of frequency domain filtering. It should be noted that the data were subjected to the same low pass filter as discussed for the Lake Ngami case history.

On these profiles three anomalies are recognisable:

i. The shape of the anomaly situated between stations -80 and -180 indicates a steep west dipping confined conductor with the top of the conductor at station -160. The decay plots for this anomaly are depicted in Figure 6.46. Decay constants of 0,98ms for the $\dot{B}z$ component and 1,1ms for the $\dot{B}x$ component were calculated. This indicates a fairly strong conductor.

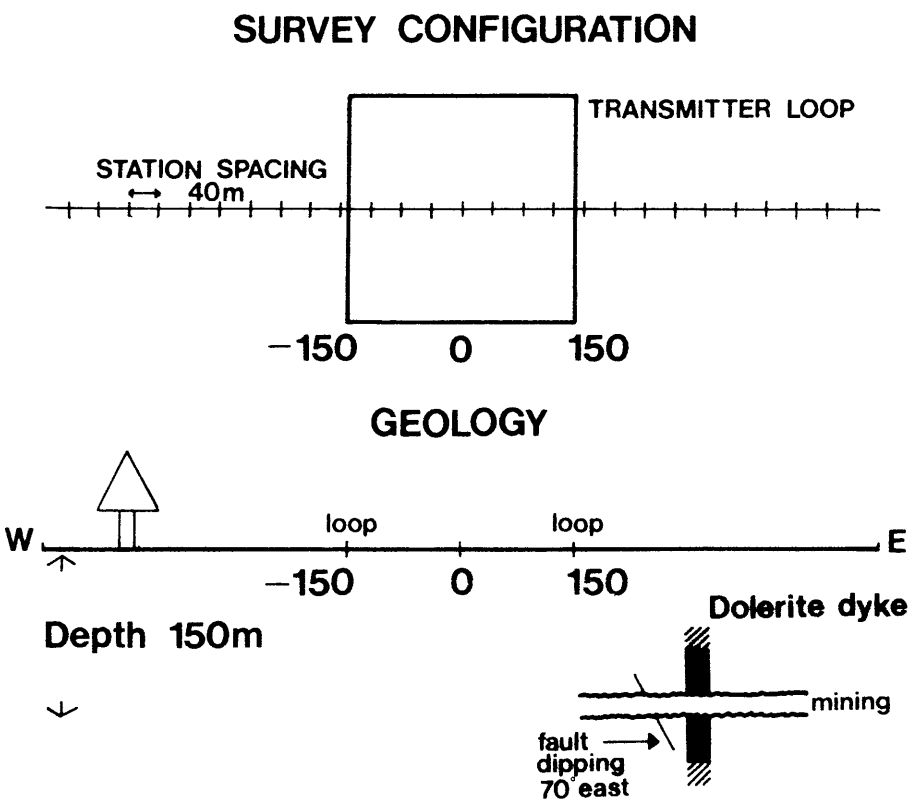

Figure 6.39 Field lay-out and geology.

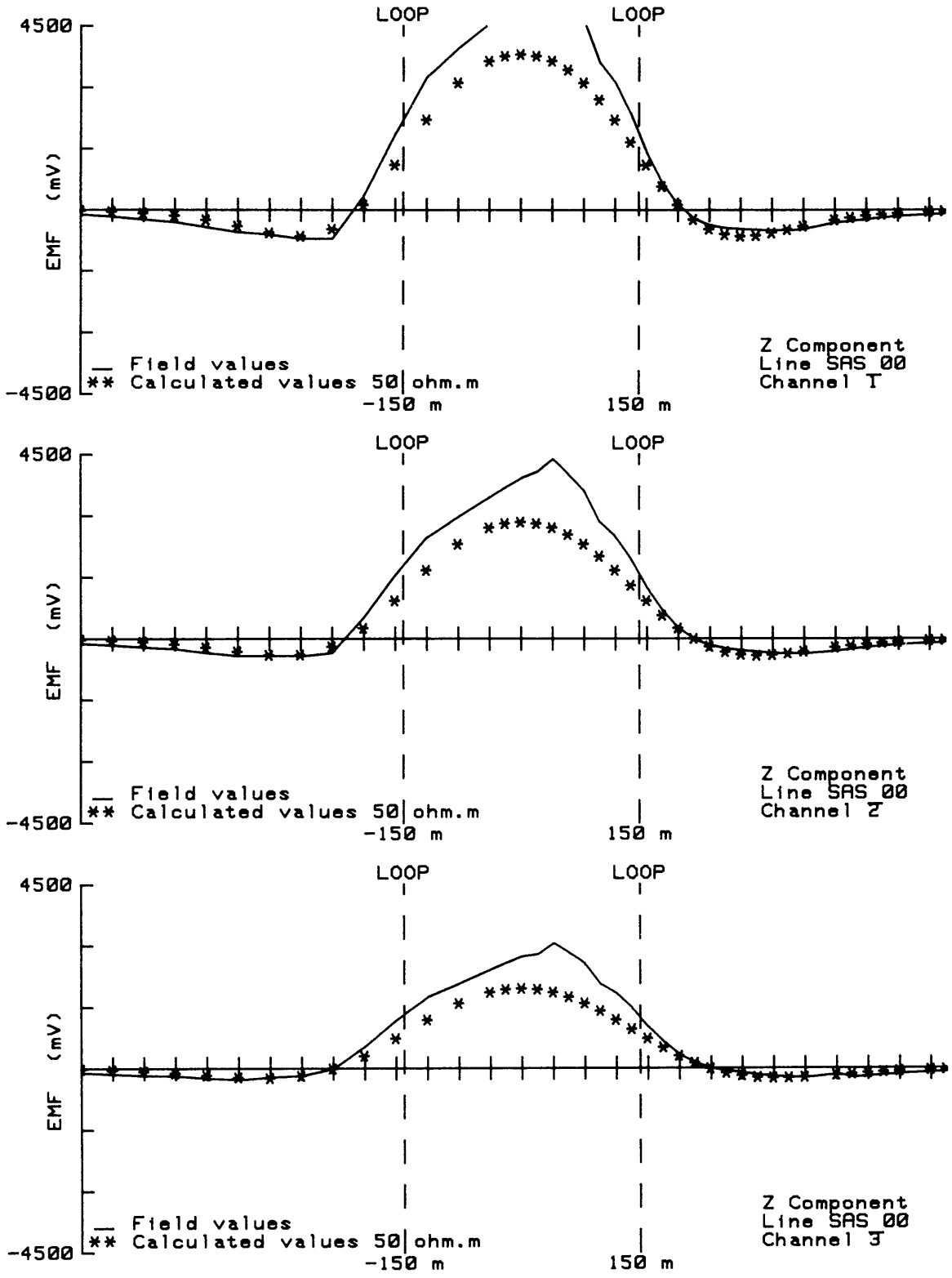

Figure 6.40 Line SAS-00 field data for channels 1, 2 and 3 together with the best fitting host rock responses. $\dot{B}z$ component.

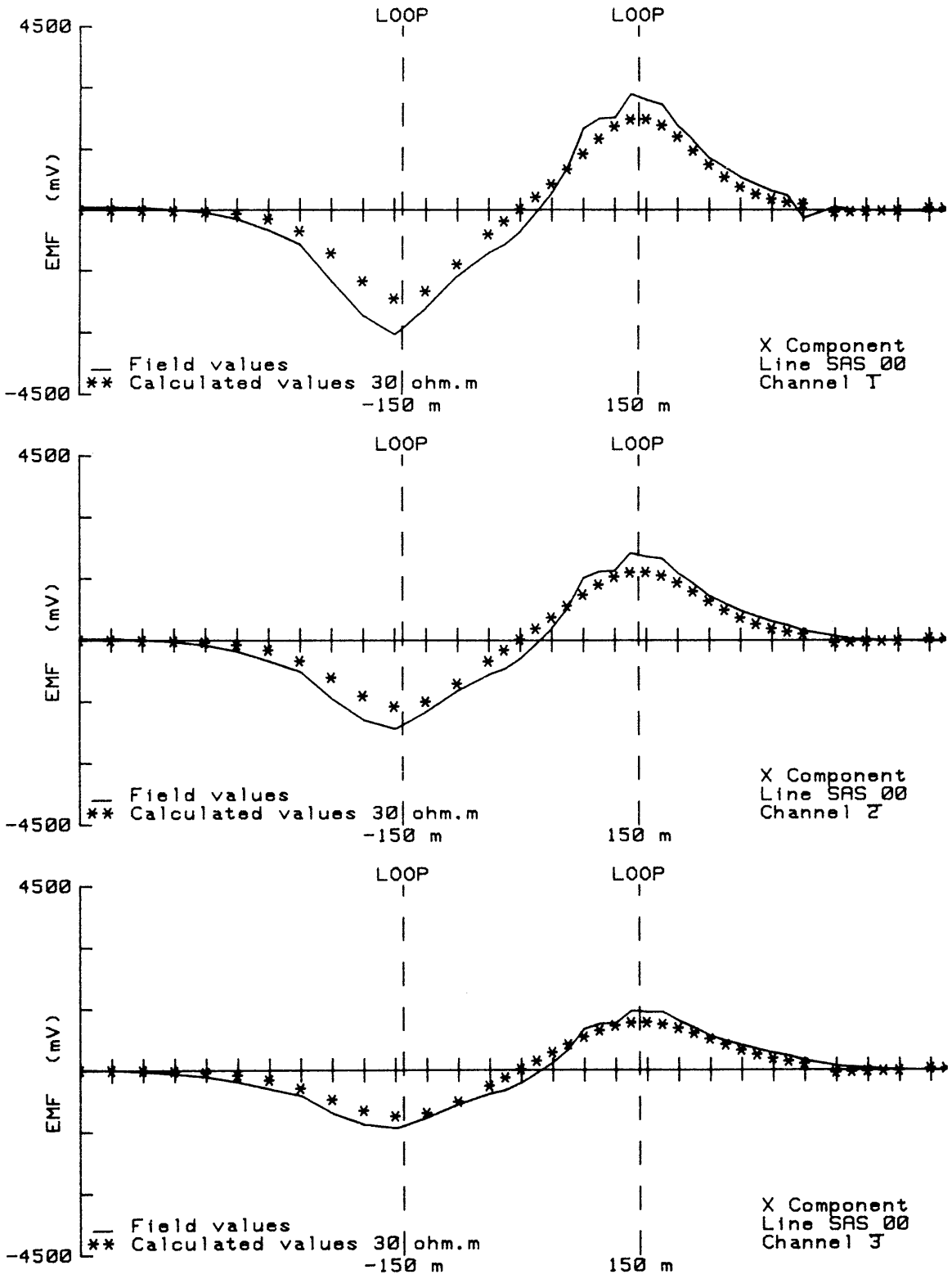

Figure 6.41 Line SAS-00 field data for channels 1, 2 and 3 together with the best fitting host rock responses. Bx component.

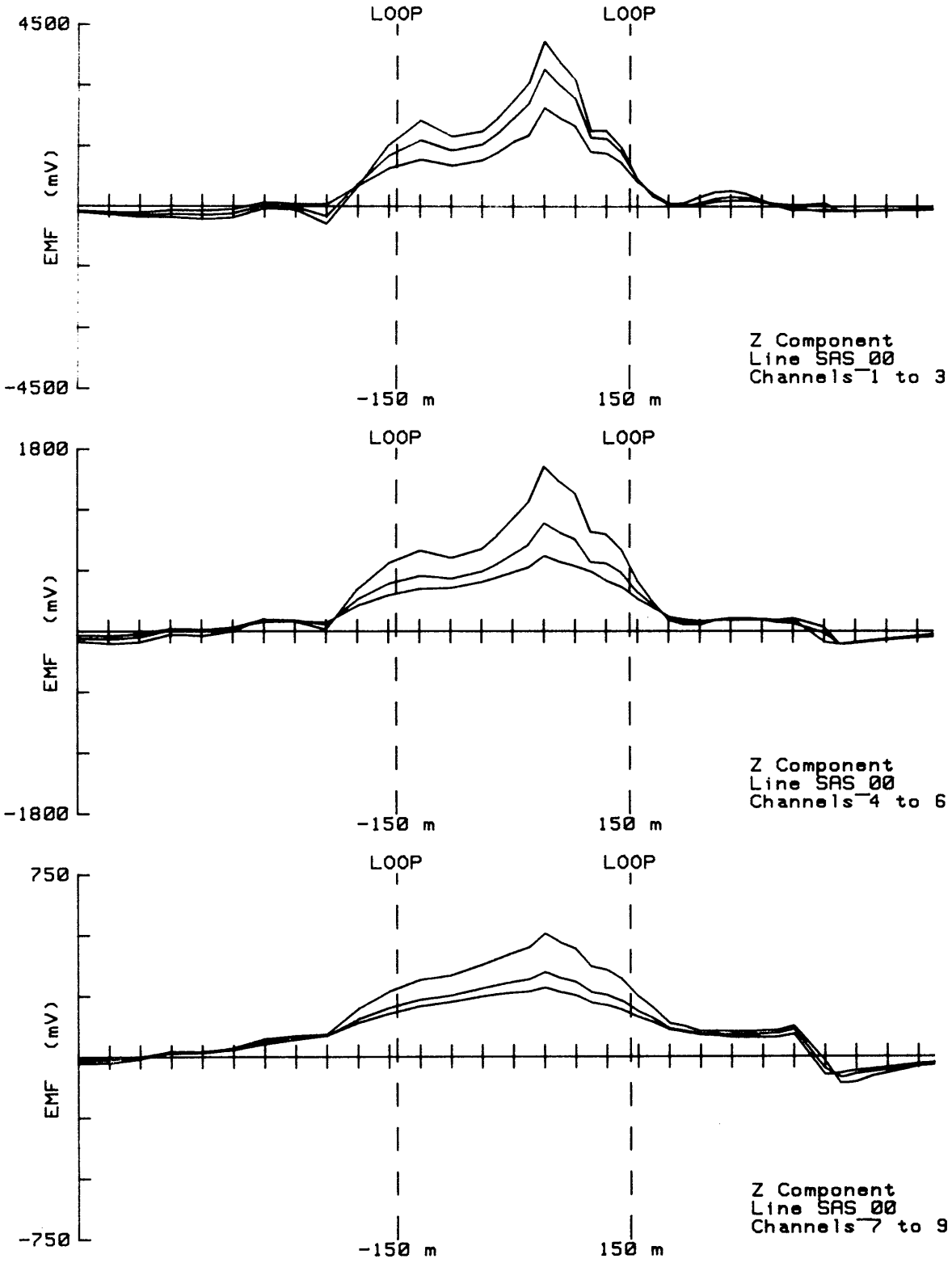

Figure 6.42 Isolated anomalies for channels 1 to 9 of line SAS-00 obtained by the traditional host rock removal method. $\dot{B}z$ component.

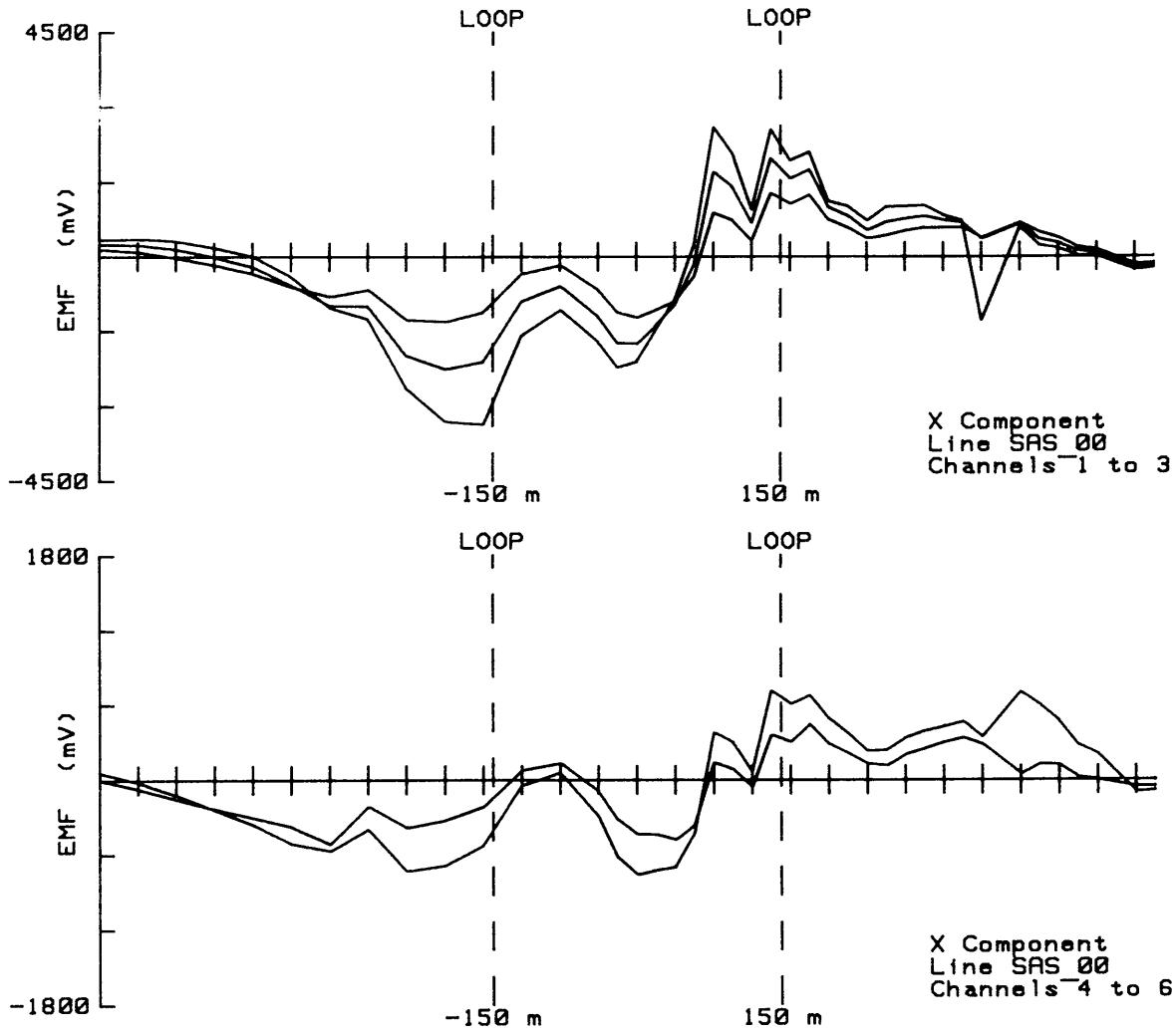

Figure 6.43 Isolated anomalies for channels 1 to 6 of line SAS-00 obtained by the traditional host rock removal method. $\dot{B}x$ component.

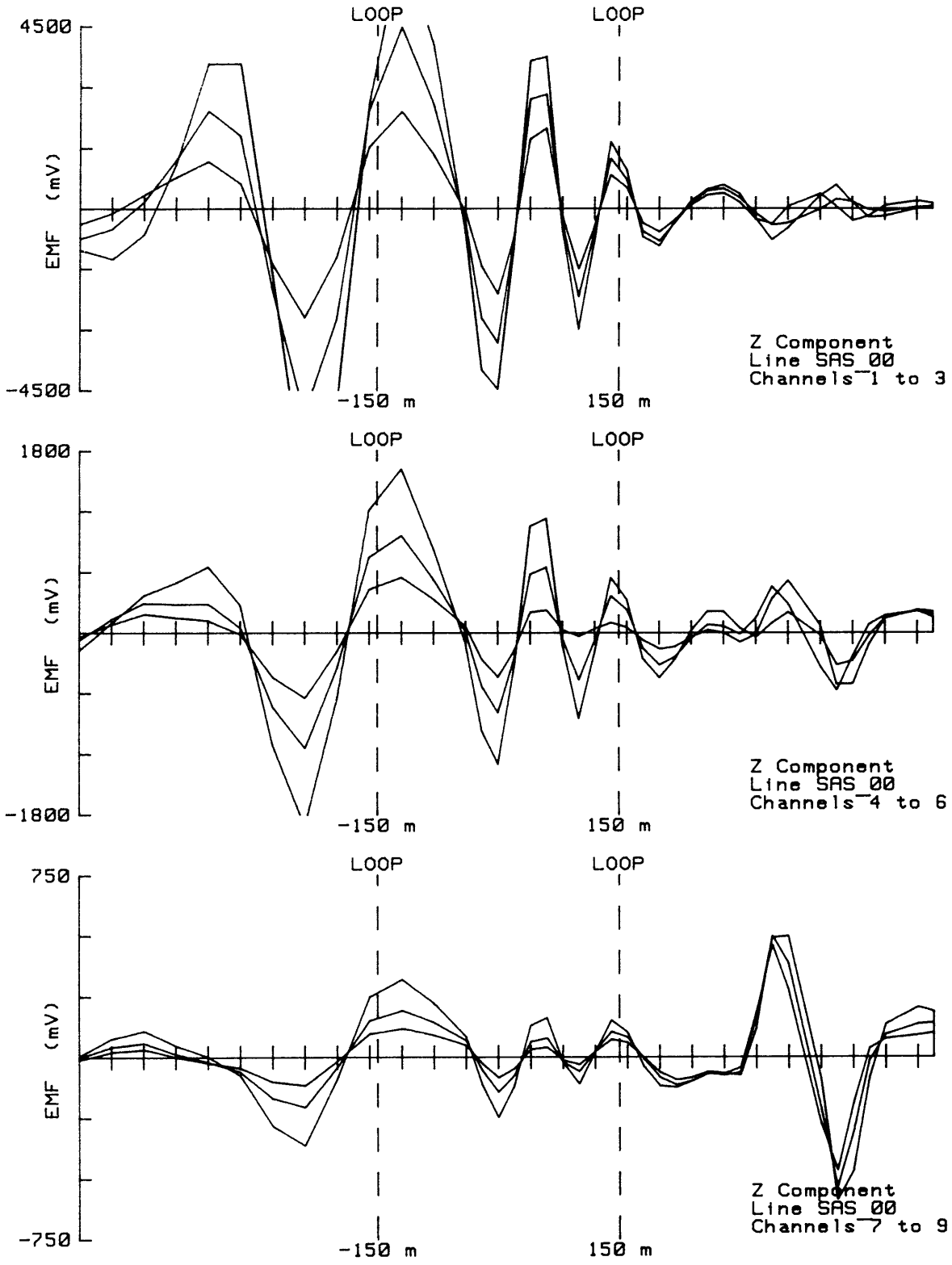

Figure 6.44 Isolated anomalies for channels 1 to 9 of line SAS-00 obtained by filtering method. $\dot{B}z$ component.

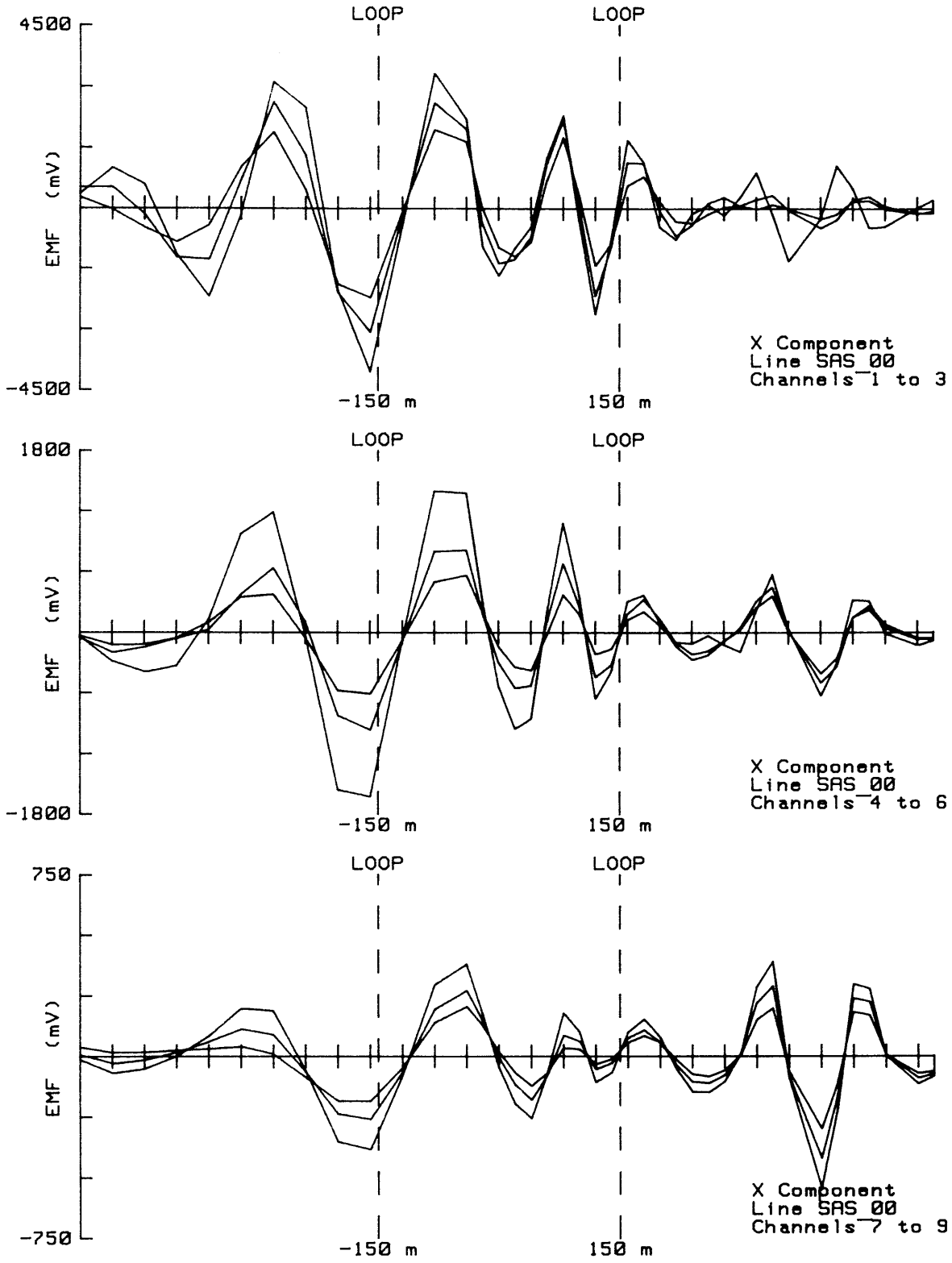

Figure 6.45 Isolated anomalies for channels 1 to 9 of line SAS-00 obtained by filtering method. $\dot{B}x$ component.

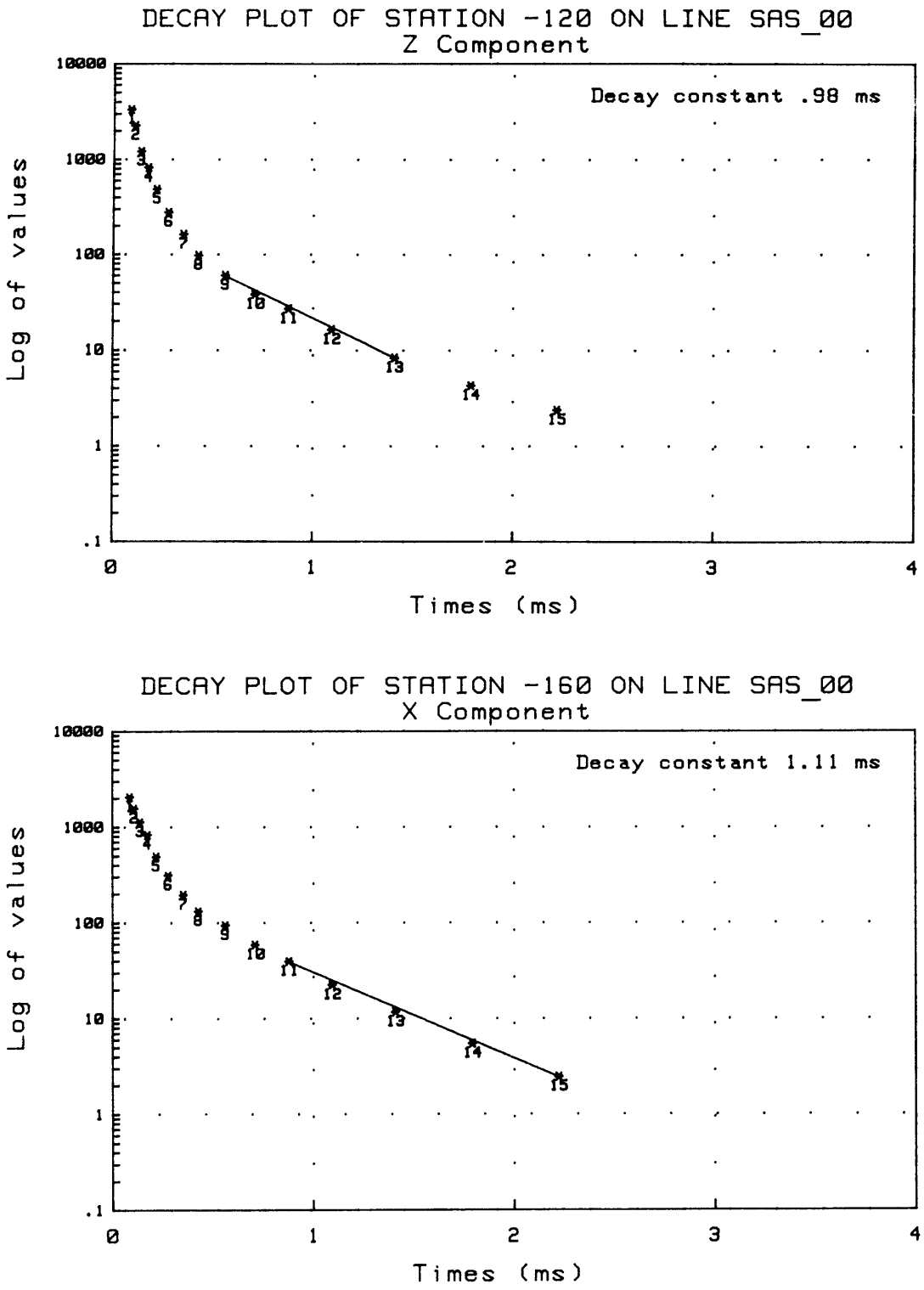

Figure 6.46 Stations -120 and -160 decay plots for anomalies obtained by the filtering method for both $\dot{B}z$ and $\dot{B}x$ components.

ii. The anomaly situated between station 0 and station 150 indicates a near vertical confined conductor with decay constants of 0,19ms and 0,24ms for $\dot{B}z$ and $\dot{B}x$ respectively (Figure 6.47). This anomaly might be the result of the vertical extension of the fault that was intersected by mining. From Figure 6.41 it can be seen that the position of the anomaly corresponds with the position of the fault if it is extended to the surface. The fact that the shape of the anomaly does not indicate an east dipping body might be explained by the distortion that the superpositioning of the anomalies causes.

iii. The known dolerite dyke supposedly situated at 300m east of the centre of the transmitter loop causes an anomaly situated between stations 320 and 480. The shape of the anomaly indicates a vertical conductor. The position as derived from the cross-over and peak positions of $\dot{B}z$ and $\dot{B}x$ respectively indicates the dyke to be at station 400.

6.3.4 Summary

Figure 6.48 depicts a summary of the interpretation. Comparing the results obtained from the filtering technique to that of traditional results it can be seen that on the filtered profiles the anomalies tend to separate and the distortion due to superpositioning has decreased to an extent that the anomalies can, with the necessary caution, be viewed as separate entities. It is however, important to do a decay constant analyses on all the suspected anomalies to determine whether the decay in late time becomes random as is the case with an "anomaly" generated by the filter or tends to decay in the manner as expected from an conductor.

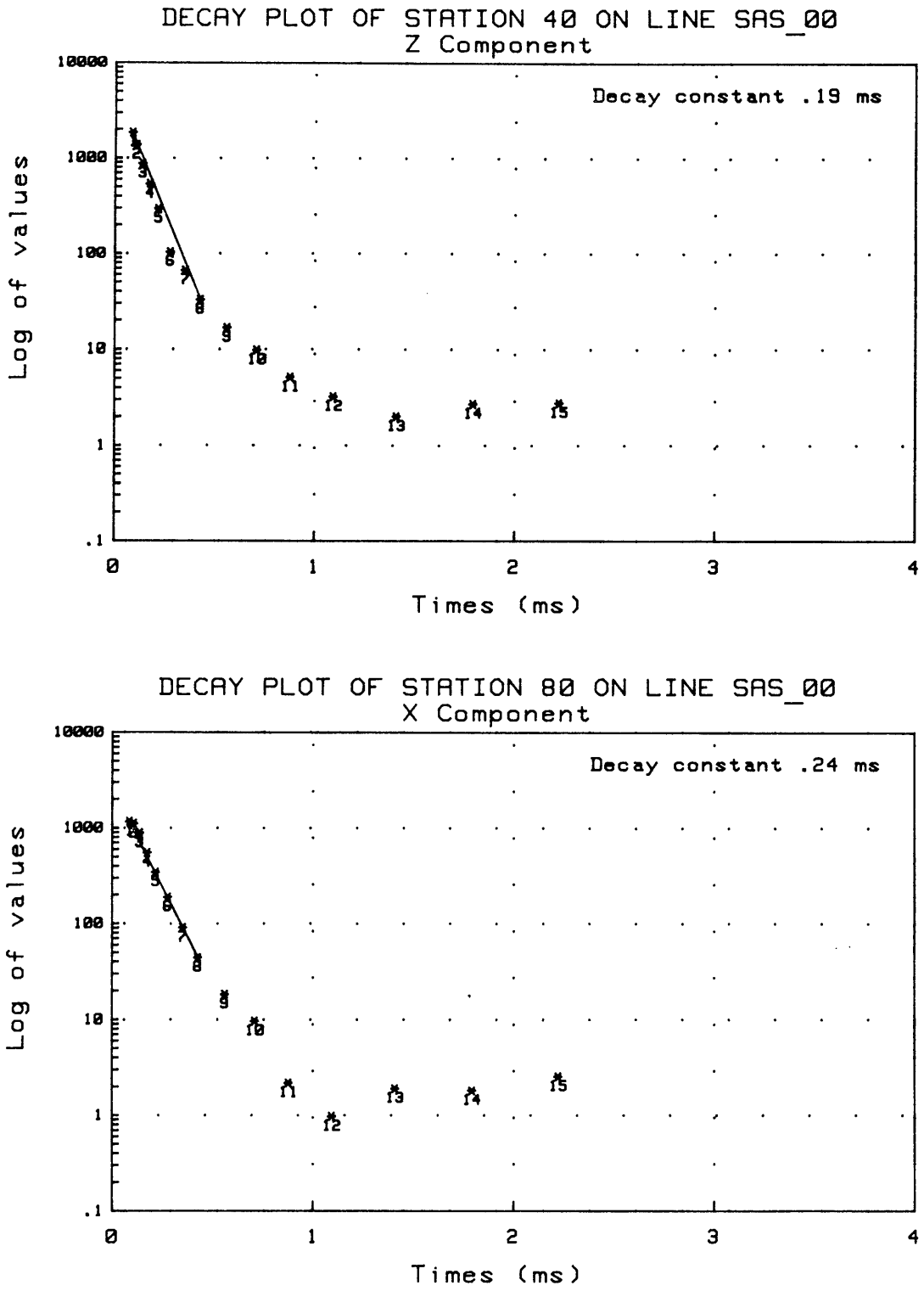

Figure 6.47 Stations 40 and 80 decay plots for anomalies obtained by the filtering method for both $\dot{B}z$ and $\dot{B}x$ components.

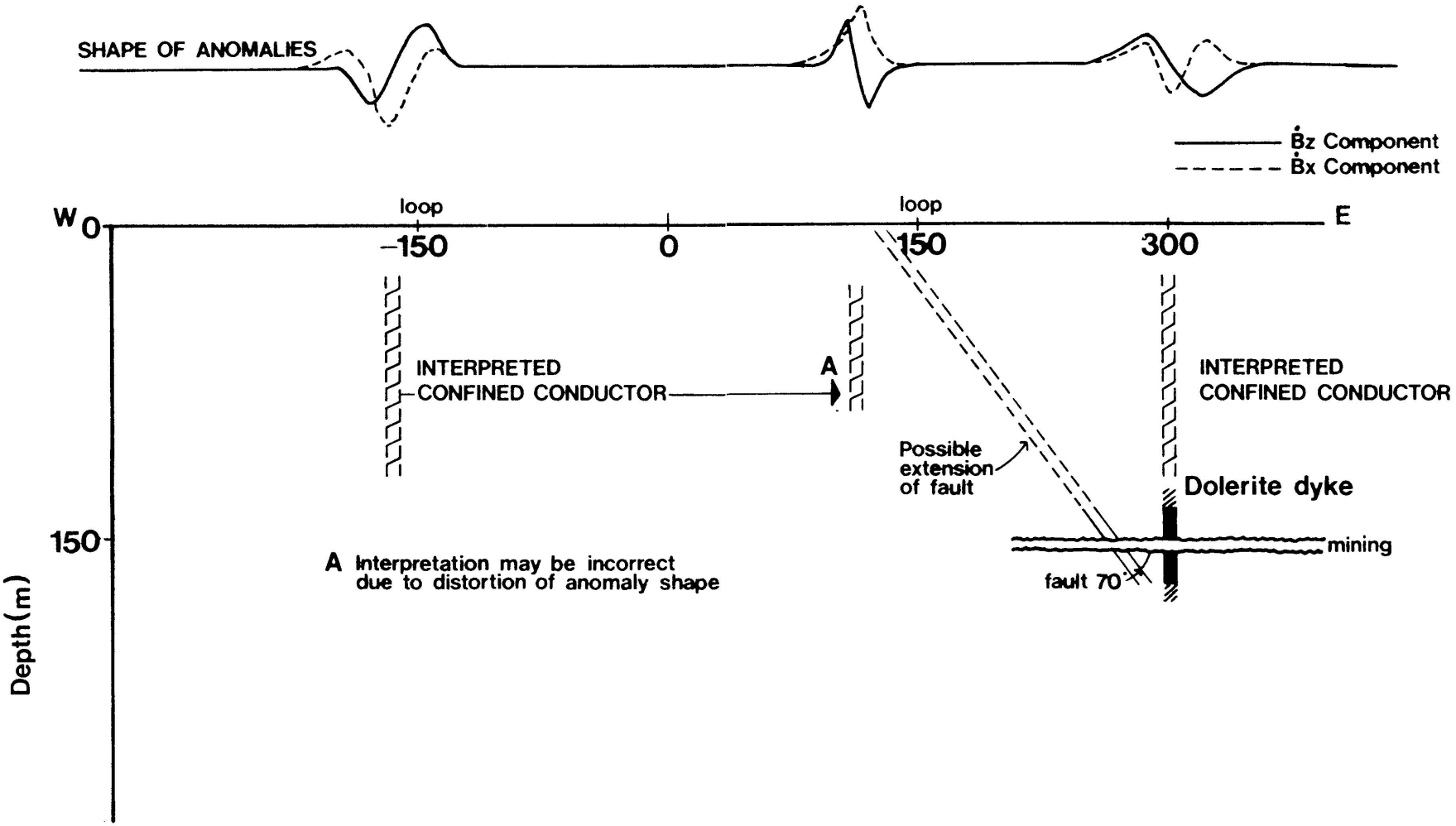

Figure 6.48 Summary of interpretation including qualitative interpretation and known geology.

CHAPTER 7

CONCLUSIONS

i. An alternative approach of isolating anomalies in the frequency domain from time domain electromagnetic profiling data has been established.

ii. By employing the filtering method the speed at which field data can be processed is greatly increased especially when a microcomputer is used.

iii. Equal computational time is needed to remove the host rock response from either the $\dot{B}z$ or $\dot{B}x$ component if one uses the filtering method. The time needed to calculate a $\dot{B}x$ component host rock response for the traditional host rock removal method is 8 times slower than to calculate the corresponding $\dot{B}z$ component response.

iv. The knowledge of the geoelectrical parameters of the host rock medium is of lesser importance if one uses the filtering method.

v. The filter technique tends to sharpen the anomaly. It does not however, change the spatial position or the ratio of the side lobe amplitudes on the $\dot{B}z$ component, and would thus not influence the locality and dip interpretation.

vi. The Lake Ngami Copper prospect case history implies that the filtering technique can be applied for survey parameters outside those specified for the theoretical investigation.

vii. The decay constants calculated from anomalies obtained by the filtering method correlate well with those calculated for the same anomalies obtained from the traditional host rock removal method.

viii. The filtering technique should not be seen as a replacement of the existing host rock response removal algorithms but rather as an additional method.

ix. Due to the higher frequency of the resulting anomalies obtained it is important to note that both the $\dot{B}z$ and $\dot{B}x$ component anomalies should be investigated simultaneously in order to interpret the data.

In summation, the filtering technique allows one to recognize the presence of a conductor and to determine the surface position above the top of the conductor, the dip of the conductor and the decay constant of the conductor. It will not allow a conventional depth interpretation.

The relative speed of execution compared to conventional interpretation techniques, makes it an important interpretation tool, allowing a daily, field-based micro-computer evaluation of the data.

REFERENCES

Båth, M. (1974). Spectral analysis in Geophysics. Seismological Institute, University of Uppsola, Sweden, 563pp.

Clearbout, J.F. (1976). Fundamentals of Geophysical Data Processing. McGraw-Hill, New York, 274pp.

Cooley, J.W. and Tukey, S.W. (1965). An algorithm for the machine calculation of complex Fourier series. Maths Comp., **19**, 297-301.

Davis, S.N. and De Wiest, R.J.M. (1966). Hydrogeology. John Wiley and Sons Inc., New York, 318-417.

Dyck, A.V., Bloore, M. and Vallee, M.A. (1980). User manual for programs PLATE and SPHERE. Res. In Appl. Geophys., **14**, Univ. of Toronto.

Eaton, P.A. and Hohmann, G.W. (1984). The influence of a conductive host on two-dimensional borehole transient electromagnetic responses. Geophysics, **49**, 861-869.

Gallagher, P.R., Ward, S.H. and Hohmann, G.W. (1985). A model study of a thin plate in free space for the EM37 transient electromagnetic system. Geophysics, **50**, 1002-1019.

Higgins, R.J. (1976). Fast Fourier Transform: An introduction with some minicomputer experiments. American Journal of Physics, **44**, 766-773.

Hoekstra, P. and Pesowski, M. (1982). Exploration for conductive targets with transient electromagnetic systems. Technical program abstracts and biographies. Society of Exploration Geophysicists. 52nd Annual international meeting and exposition, 374-376.

Kaufman, A.A. (1981). The influence of currents induced in the host rock on electromagnetic response of a spheriod directly beneath a loop. Geophysics, **46**, 1002-1019.

Kaufman, A.A. and Keller, G.V. (1981). The magnetotelluric sounding method. Elsevier, New York, 583pp.

McCracken, K.G. (1983). The optimisation of EM exploration procedures. CSIRO Institute of Earth Resources.

McNeill, J.D. (1980). Applications of transient electromagnetic Techniques. Technical Note TN-7. Geonics Limited.

McNeill, J.D. (1982). Interpretation of large-loop transmitter transient electromagnetic surveys. Technical program abstracts and biographies, Society of Exploration Geophysicists, 52nd Annual international eeeting and exposition, 373-374.

McNeill, J.D., Edwards, R.N. and Levy, G.M. (1984). Approximate calculations of the transient electromagnetic response from buried conductors in a conductive half-space. Geophysics, **49**, 918-924.

Nabighian, M.N. (1979). Quasi-static transient response, of a conducting half-space. An approximate representation. Geophysics, **44**, 1700-1705.

Nabighian, M.N. (1982). A review of time domain electromagnetic exploration. Proc. of the Internat. Symp. on Appl. Geophys. in Tropical Regions. Belem, Brazil, 1983, Lourenzo, J.S. and Rijo, L. Eds., 385-429.

Rozenberg, G., Tykajlo, R., Pesowski, M. and Eaton, D. (1985). Combined mode transient electromagnetic survey for mineral exploration: A case history. Expanded abstracts of the technical program with authors' biographies, Society of Exploration Geophysicists, 55th Annual meeting and exposition, 257-258.

San Filipo, W.A., Eaton, P.A. and Hohmann, G.W. (1985). The effect of a conductive half-space on the transient response of a three-dimensional body. Geophysics, 50, 1144-1162.

Savarenski, E. (1975). Seismic waves. Mir, Moscow. English translation A Petrosyan, 349pp.

Silic, J., Eadie, E.T. and Jack, D.J. (1985). Application of time-domain electromagnetic methods in the discovery of the Hellyer ore deposit, Tasmania, Australia. Expanded abstracts of the technical program with authors' biographies, Society of Exploration Geophysicists, 55th Annual meeting and exposition, 241-243.

Spies, B.R. (1980). The application of the transient electromagnetic method in Australian conditions. Ph.D. thesis, Macquire University.

APPENDIX A

FOURIER THEORY

APPENDIX A

FOURIER THEORY

A.1 FOURIER TRANSFORMATIONS

Any periodic function can be approximated by a series of sine and cosine functions. According to the Fourier theorem any function f(t) that satisfies certain conditions can be expressed as a sum of an infinite number of sinusoidal terms.

The conditions to which the function f(t) must adhere, are called the Dirichlet conditions and are expressed as follows (Savarenski, 1975).

i. Function should be periodic, i.e. $f(t)=f(t+2\pi)$. If the function is not periodic, but is continuous and defined over a finite range, then the sum of the sinusoidal terms will still converge to f(t) over the defined range. Outside the range the sum will represent a repetition of f(t).

ii. In general we cannot measure from minus infinity to plus infinity so we assume a periodic function.

iii. f(t) should be at least sectionally continuous with a finite number of discontinuities.

iv. f(t) should possess a finite number of maxima and minima.

v. The integral $\int_{-\pi}^{\pi} f(t)dt$ should be convergent, i.e. $\int_{-\infty}^{\infty} |f(t)|\,dt$ should be finite.

A.2 THE FOURIER THEOREM

A function f(t) having a fundamental period of 2π and satisfying the Dirichlet conditions can be expressed by the following infinite Fourier series, with constants a_o, a_n and b_n, n=1,2,3,-,-,-

$$f(t) = a_o + \sum_{n=1}^{\infty} (a \cos nt + b_n \sin nt) \qquad (A.2.1)$$

Using the orthogonality properties of sine and cosine functions

$$\int_{-\pi}^{\pi} \sin(nt)\sin(mt)dt = \begin{cases} 0 & m \neq n \\ \pi & m=n\neq 0 \\ 0 & m=n=0 \end{cases} \qquad (A.2.2)$$

$$\int_{-\pi}^{\pi} \cos(nt)\cos(mt) = \begin{cases} 0 & m \neq n \\ \pi & m=n=0 \\ 2\pi & m=n=0 \end{cases}$$

$$\int_{-\pi}^{\pi} \sin(mt)\cos(nt)dt = 0 \quad \text{for all } m,n. \qquad (A.2.3)$$

The series is then multiplied by

i. cos(0)t
ii. cos(n)t
iii. sin(n)t

and integrated over the period 2π.

This yields

$$a_o = \frac{1}{2\pi} \int_{-\pi}^{\pi} f(t)dt \qquad (A.2.4)$$

$$a_n = \frac{1}{\pi} \int_{-\pi}^{\pi} f(t)\cos nt\, dt \qquad (A.2.5)$$

$$b_n = \frac{1}{\pi} \int_{-\pi}^{\pi} f(t)\sin nt\, dt \qquad (A.2.6)$$

In general we would use some fundamental period T, hence

$$f(t) = a_o + \sum_{n=1}^{\infty} \{a_n \cos \frac{2\pi nt}{T} + b_n \sin \frac{2\pi nt}{T}\} \qquad (A.2.7)$$

$$a_o = \frac{1}{T} \int_{-T/2}^{T/2} f(t)dt \qquad (A.2.8)$$

$$a_n = \frac{2}{T}\int_{-T/2}^{T/2} f(t)\cos\frac{2\pi nt}{T}\,dt \qquad (A.2.9)$$

$$b_n = \frac{2}{T}\int_{-T/2}^{T/2} f(t)\sin\frac{2\pi nt}{T}\,dt \qquad (A.2.10)$$

A.3 THE FOURIER TRANSFORM

By replacing t, in equation (A.2.6), with a dummy integration variable λ and then substitute for a_o, a_n and b_n into the Fourier series the following is obtained:

$$f(t) = \frac{1}{T}\int_{-T/2}^{T/2} f(\lambda)d\lambda + \sum_{n=1}^{\infty}\left(\left\{\frac{2}{T}\int_{-T/2}^{T/2} f(\lambda)\cos\frac{2\pi n\lambda}{T}\,d\lambda\right\}\cos\frac{2\pi nt}{T} + \left\{\frac{2}{T}\int_{-T/2}^{T/2} f(\lambda)\sin\frac{2\pi n\lambda}{T}\,d\lambda\right\}\sin\frac{2\pi nt}{T}\right)$$

$$= \frac{1}{T}\int_{-T/2}^{T/2} f(\lambda)d\lambda + \sum_{n=1}^{\infty}\frac{2}{T}\int_{-T/2}^{T/2} f(\lambda)\cos\frac{2n\pi}{T}(t-\lambda)d\lambda \qquad (A.3.1)$$

Because $\cos(A\pm B)=\cos A\pm\cos B\mp\sin A\cdot\sin B$ (A.3.2)

Let

$$\omega_n = \frac{2\pi n}{T}$$

$$\omega_{n-1} = \frac{2\pi(n-1)}{T}$$

$$\Delta\omega = \frac{2\pi}{T} \qquad (A.3.3)$$

$$\therefore\ f(t) = \frac{\Delta\omega}{2\pi}\int_{-T/2}^{T/2} f(\lambda)d\lambda + \sum_{n=1}^{\infty}\frac{\Delta\omega}{\pi}\int_{-T/2}^{T/2} f(\lambda)\cos\left(\omega_n(t-\lambda)\right)d\lambda \qquad (A.3.4)$$

Now if the period tends to infinity then

i. $\frac{1}{T}\int_{-T/2}^{T/2} f(\lambda)d\lambda \to 0$

since $f(\lambda)$ satisfies the Dirichlet conditions.

ii. When the increment $\Delta\omega = \frac{2\pi}{T} \to d\omega$ in the limit the discretely increasing ω_n becomes a continuous variable ω.

iii. The summation $\sum_{n=1}^{\infty}$ is converted to an integral with lower and upper limits 0 and ∞ respectively and

$$f(t) = \frac{1}{\pi}\int_0^{\infty} d\omega \int_{-\infty}^{\infty} f(\lambda)\cos\{\omega(t-\lambda)\}d\lambda \qquad (A.3.5)$$

Which is the expression of the Fourier integral.

Introducing the sine and cosine transforms

$$a(\omega) = \int_{-\infty}^{\infty} f(\lambda)\cos(\omega\lambda)d\lambda \qquad (A.3.6)$$

and

$$b(\omega) = \int_{-\infty}^{\infty} f(\lambda)\sin(\omega\lambda)d\lambda \qquad (A.3.7)$$

and defining the function $\phi(\omega)$ by

$$\sin\phi(\omega) = \frac{-b(\omega)}{(a^2(\omega)+b^2(\omega))^{\frac{1}{2}}} \qquad (A.3.8)$$

$$\cos\phi(\omega) = \frac{a(\omega)}{(a^2(\omega)+b^2(\omega))^{\frac{1}{2}}} \qquad (A.3.9)$$

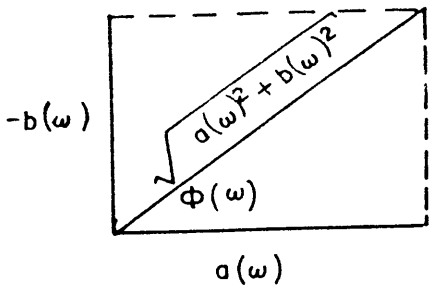

$$\tan\phi(\omega) = \frac{-b(\omega)}{a(\omega)} \qquad \text{(A.3.10)}$$

substituting equation (A.3.10) back into the Fourier integral equation (A.3.5) the following is obtained

$$f(t) = \frac{1}{2\pi} \int_{-\infty}^{\infty} F(\omega) e^{i\omega t} d\omega \qquad \text{(A.3.11)}$$

where $F(\omega) = (a^2 + b^2)^{\frac{1}{2}} e^{-i\phi(\omega)}$

$$= (a^2 + b^2)^{\frac{1}{2}} (\cos\phi(\omega) + i \sin\phi(\omega)) \qquad \text{(A.3.12)}$$

Furthermore we can write

$$F(\omega) = \int_{-\infty}^{\infty} f(t) e^{-i\omega t} dt \qquad \text{(A.3.13)}$$

$F(\omega)$ is called the Fourier Transform of $f(t)$. The absolute value of $|F(\omega)| = (a^2+b^2)^{\frac{1}{2}}$ is called the amplitude spectrum of $f(t)$.

The above transform is only valid for a continuous function. Due to the fact that the profiles under investigation are of a finite range and sampled at discreet intervals the theory needs to be adapted to cater for a digital transform that handles a finite sampled data set.

A.4 THE DISCREET FOURIER TRANSFORM

Examine the following:

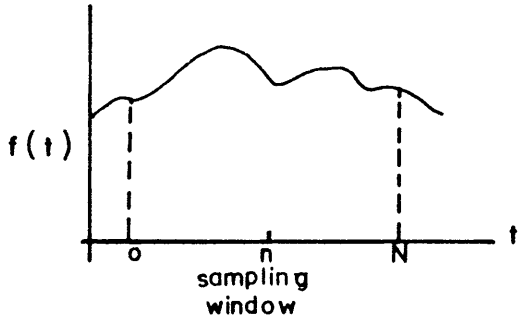

with a finite interval (N-1) t with N the total number of sampling points and n any sampling point so that $0 \leqq n \leqq N-1$. Assume that this interval is the period of the function.

From the assumption that any finite series is one period of an infinite periodic series, equation (A.3.11) becomes

$$f_n = \sum_{n=-\infty}^{\infty} F_n e^{i\omega_0 nt} \qquad \text{with} \quad \omega_0 = \frac{2\pi}{N} \tag{A.4.1}$$

and f_t now denotes the discreet values of the continuous function f(t). F_n is the Fourier coefficients.

From $e^{i\omega_0 nt} = e^{(i\omega_0 n)t}$ it is seen that $e^{i\omega_0 n}$ is a periodic function in n terms. There are only N unique values of $e^{i\omega_0 n}$. The infinite series can then be written as follows:

$$f_t = \sum_{n=0}^{N-1} F_n e^{i\omega_0 nt} = \sum_{n=0}^{N-1} F_n e^{\left(\frac{i2\pi nt}{N}\right)} \tag{A.4.2}$$

and $$F_n = \sum_{t=0}^{N-1} f_t e^{\left(\frac{-it2\pi}{N} n\right)} \tag{A.4.3}$$

Equation (A.4.2) is called the Digital Fourier Transform of the discreet periodic function f_t (Savarenski, 1975).

To illustrate the use of the above equation in the calculation of a Fast Fourier Transform we derive the Cooley Tukey algorithm for 2^2 sampling points (Cooley and Tukey, 1965).

From equation (A.4.3) it follows that

$$F_n = \sum_{t=0}^{N-1} f_t e^{\left(\frac{-it2\pi n}{N}\right)} \qquad n = 0,1,..,N-1$$

or $$F_n = \sum_{t=0}^{N-1} f_t W^{nt} \qquad \text{(A.4.4)}$$

with $W = e^{\left(\frac{-2\pi i}{N}\right)}$

For 2^2 sampling points n=4, and γ=2.

From the summation of equation (A.4.4) it follows that

t=0,1,2,3
and n=0,1,2,3

In binary form we have 0=00, 1=01, 2=10 and 3=11 and t,n in binary form is

t=00,01,10,11 = (t_0t_1)
and n=00,01,10,11 = (n_0n_1) (A.4.5)

where t_0t_1 and n_0n_1 each form a binary pair and by assigning a zero or one to t_0, t_1 or n_0, n_1 all 4 values of t and n can be obtained.

Equation (A.4.5) can also be written as

$t=t_1 2^1 + t_0 2^0$
and $n=n_1 2^1 + n_0 2^0$

Substituting the binary forms of t and n into equation (A.4.4) we get

$$F(n_1n_0) = \sum_{t_0=0}^{1} \sum_{n_0=0}^{1} f_0(t_1t_0) W^{(2n_1+n_0)(2t_1+t_0)} \qquad \text{(A.4.6.)}$$

and $W^{(2n_1+n_0)(2t_1+t_0)}$

$$= W^{(2n_1+n_0)2t_1} W^{(2n_1+n_0)t_0}$$

$$= W^{4n_1t_1} W^{2t_1n_0} W^{(2n_1+n_0)t_0}$$

$$= 1.W^{2n_0t_1} W^{(2n_1+n_0)t_0} \qquad \text{(A.4.7)}$$

Because $W^{4n_1t_1} = (e^{-\frac{i2\pi}{N}})^{4n_1t_1} = 1$

it follows that

$$F(n_1n_0) = \sum_{t_0=0}^{1} \left(\sum_{t_1=0}^{1} f_0(t_1t_0) W^{(2n_0t_1)} W^{(2n_1+n_0)t_0} \right) \qquad \text{(A.4.8)}$$

For calculation purposes the inside summation of equation (A.4.8) is defined as follows

$$f_1(n_0t_0) = \sum_{t_1=0}^{1} f_0(t_1t_0) W^{2n_0t_1} \qquad \text{(A.4.9)}$$

and the outside summation of equation (A.4.8) as

$$f_2(n_0n_1) = \sum_{t_0=0}^{1} f_1(n_0t_0) W^{(2n_1+n_0)t_0} \qquad \text{(A.4.10)}$$

Equation (A.4.6) then becomes

$$F(n_1n_0) = f_2(n_0n_1) \qquad \text{(A.4.11)}$$

Equation (A.4.8) to (A.4.10) are known as the Cooley Tuckey FFT algorithm (base 2) for N=4. The above can also be computed for 2^γ,3^γ and 5^γ depending on the application. The above algorithm is programmable and is valid for a finite sampled data set (Higgins, 1976).

APPENDIX B

PROGRAM COMBFIL FOR THE TRANSFORMATION AND FILTERING OF THE DOMAIN ELECTROMAGNETIC PROFILE DATA

APPENDIX B

PROGRAM DESCRIPTION

The program COMBFIL was written to transform data to the frequency domain and to filter the data.

The Fast Fourier Transform (FFT) routine was obtained from Higgins (1976).

The program was adapted for specific needs of the writer The essential parts are contained in lines 2660 to 3230, 5230 to 5340 and 1270 to 2230 being the FFT routine, the amplitude spectrum calculation routine and the filter routines.

Some important notes to take into consideration when using or adapting the program.

i. Variable I and N must be specified INTEGER.

ii. Program works in RADIANS.

iii. The length of the data set will automatically set to 2^N.

iv. Lines 5580 to 5780 adds the first and last values of the orignal data set to the ends of the data set.

v. The original data are contained in array SMOOTH(*).

vi. The array STA(*) and STA2(*) contains station numbers, this can be omitted as this is not used in the FFT but only in the plotting routines.

vii. The data read subroutines can be changed to suit the users' needs.

viii. Lines 4770 to 720 sets up arrays VALU(*) and N1(*). Each second value is set to zero as required by the FFT routine.

ix. Lines 720 to 880 performs the Hamming windowing on the data.

x. The program runs on either a Hewlett Packard 9816 or a Hewlett Packard 9000 series 300 computer. Errors might occur with the OUTPUT KBD statements depending on the configurations of the machines. These statements are of cosmetic importance only and can be omitted.

```
10    !*************************************************************************
20    ! TWO DIMENSIONAL FILTERING PROGRAMME
30    !*************************************************************************
40    ! FFT routine obtained from: HIGGINS R.J. "Fast Fourier Transform: An in-
50    ! troduction with some minicomputer experiments"; Amer Jour of Phys.
60    !*************************************************************************
70    ! Program filters 2 dimensional data. Data read subroutines for PLATE
80    ! HOST ROCK and COMBINATIONS, Program will also read EM37 field data.
90    !
100   ! Program name : "COMBFIL"
110   ! Written by   : J.C.SLEE
120   ! LAST CHANGES : 8.9.87
130   !*************************************************************************
140   OPTION BASE 1
150   INTEGER I,N
160   Loopdim=400           ! Tx-loop dim. Used in DATAPLOT routine
170   !-------------------------------------------------------------------------
180   ! Softkey on/off check
190   !-------------------------------------------------------------------------
200   STATUS 1,12;Keyson
210   IF Keyson=2 THEN
220     OUTPUT KBD;" |";
230   END IF
240   !-------------------------------------------------------------------------
250   DIM Valu(364),N1(364),P1(364),Ans$[1],H(364),Frek(364),Label$[12],Nn1(364
260   DIM Field(52,20,3,3),Comp$(3)[1],Times(20),Plt(52),Primary(52,3,3)
270   DIM Gain(52,3),Nrchan(52,3),Frequ(52,3),Nr_freq(52)
280   DIM Phase(364),Datta(20,164),Sta(164),Filres(364),Filplot(364),Smooth(364
290   DIM Dummy(3,100),Sta2(164)
300   !-------------------------------------------------------------------------
310   ! Selection for HP9816 or BOBCAT. Set mass storage default
320   !-------------------------------------------------------------------------
330   GCLEAR
340   OUTPUT KBD;" K";
350   INPUT "Type 'A' for HP9816 or 'B' for BOBCAT",Compsel$
360   SELECT Compsel$
370   CASE "A","a"
380     Mass$=":,700"
390   CASE "B","b"
400     Mass$=":,700,1"
410   CASE ELSE
420     GOTO 360
430   END SELECT
440   !-------------------------------------------------------------------------
450   GOSUB Dataread
460   !-------------------------------------------------------------------------
470   ! Check dataset length, pad to length
480   !-------------------------------------------------------------------------
490   N=Amt
500   FOR I=1 TO 7
510     IF N<2^I THEN
520       FOR K=N+1 TO 2^I
530         Smooth(K)=0
540         Sta2(K)=(Sta2(K-1)+Stsp)
550       NEXT K
560       N=2^I
570       GOTO 600
580     END IF
590   NEXT I
```

```
600   !-------------------------------------------------------------------------
610   Ii=1
620   FOR I=1 TO 2*N STEP 2
630     Valu(I)=Smooth(Ii)
640     N1(I)=Valu(I)                !
650     Valu(I+1)=0.                 ! SET EVERY SECOND VALUE A ZERO
660     N1(I+1)=Valu(I+1)            !
670     Ii=Ii+1
680   NEXT I
690   Isign=0
700   GOSUB Dataplot
710   !-------------------------------------------------------------------------
720   ! Hamming window routine
730   !-------------------------------------------------------------------------
740   C5=0.
750   FOR I=1 TO N
760     H(I)=1
770     C5=-((N-1)/2)-1+I
780     IF C5<-(.4*(N-1)) THEN H(I)=.5*(1+COS(PI*5*C5/(N-1)))
790     IF C5>.4*(N-1) THEN H(I)=.5*(1+COS(PI*5*C5/(N-1)))
800   NEXT I
810   C5=0.
820   FOR I=1 TO 2*N STEP 2
830     C5=C5+1
840     N1(I)=H(C5)*N1(I)
850   NEXT I
860   S=-1
870   !-------------------------------------------------------------------------
880   GOSUB Fft                    ! GOTO FFT SUBROUTINE
890   !-------------------------------------------------------------------------
900   Ii=0.
910   FOR I=1 TO N*2 STEP 2
920     Ii=Ii+1
930     P1(Ii)=SQR(N1(I)^2+N1(I+1)^2)
940   NEXT I
950   Scaleflag=0
960   GOSUB Spectrumplot
970   !-------------------------------------------------------------------------
980   ! Select filter to use from softkeys
990   !-------------------------------------------------------------------------
1000 Filter:      !
1010  PRINT TABXY(1,1);CHR$(131);" USE SOFTKEY TO INDICATE CHOICE ";CHR$(128)
1020  OUTPUT KBD;" |";
1030  SELECT Compsel$
1040  CASE "A","a"
1050    ON KEY 0 LABEL "LOW PASS" GOTO Lowpassfilter
1060    ON KEY 5 LABEL "FILTER" GOTO Lowpassfilter
1070    ON KEY 2 LABEL "HIGH PASS" GOTO Highpassfilter
1080    ON KEY 7 LABEL "FILTER" GOTO Highpassfilter
1090    ON KEY 4 LABEL "INVERSE" GOTO Ifft
1100    ON KEY 9 LABEL "FOURIER TR" GOTO Ifft
1110  CASE "B","b"
1120    OUTPUT KBD;" {";
1130    ON KEY 1 LABEL "LOW PASS FILTER" GOTO Lowpassfilter
1140    ON KEY 2 LABEL "" GOTO 1030
1150    ON KEY 3 LABEL "" GOTO 1030
1160    ON KEY 4 LABEL "INVERSE FFT" GOTO Ifft
1170    ON KEY 5 LABEL "" GOTO 1030
1180    ON KEY 6 LABEL "" GOTO 1030
1190    ON KEY 7 LABEL "" GOTO 1030
```

```
1200    ON KEY 8 LABEL "HIGH PASS FILTER" GOTO Highpassfilter
1210  CASE ELSE
1220    GOTO 1030
1230  END SELECT
1240 Spin:GOTO Spin
1250  RETURN
1260  !-------------------------------------------------------------------------
1270  ! Low pass filter
1280  !-------------------------------------------------------------------------
1290 Lowpassfilter:           !
1300  PRINT TABXY(1,1);"                                          "
1310  OUTPUT KBD;" |";
1320  INPUT "Cutoff frequency for LOW PASS filter",Freq
1330  INPUT "Sharpness of LOW PASS filter (0 to 100)",A
1340  Ii=0
1350  FOR I=1 TO 2*N STEP 2
1360    Ii=Ii+1
1370    IF I/(N*2)<Freq OR I/(N*2)>(1-Freq) THEN
1380      Filplot(Ii)=1
1390      Filres(I)=1
1400      GOTO 1610
1410    END IF
1420    Pfac=(I-1)/(N*2-1)
1430    Filfac=Pfac-Freq
1440    IF I/(N*2)>.5 THEN
1450      Nqfreq=1-Freq
1460      Filfac=Pfac-Nqfreq
1470    END IF
1480    Filres(I)=(EXP(-A*2.*PI*(Filfac)^2))
1490    Filres(I+1)=0.
1500    ON ERROR GOTO 1520
1510    Filplot(Ii)=SQR(Filres(I)^2+Filres(I+1)^2)
1520    IF ERRN=136 THEN
1530      Filres(I)=0
1540      ON ERROR GOTO 1560          !  This is done to ghange
1550      Fault=SQR(-1)               !  the ERRN.
1560      OFF ERROR                   !
1570      GOTO 1500
1580    END IF
1590    N1(I)=N1(I)*(Filres(I))
1600    N1(I+1)=N1(I+1)*(Filres(I))
1610  NEXT I
1620  Ii=0
1630  GOTO Escape
1640  RETURN
1650  !-------------------------------------------------------------------------
1660  ! High pass filter
1670  !-------------------------------------------------------------------------
1680 Highpassfilter:          !
1690  PRINT TABXY(1,1);"                                          "
1700  OUTPUT KBD;" |";
1710  INPUT "Cutoff frequency for HIGH PASS filter",Freq
1720  INPUT "Sharpness of HIGH PASS filter (0 to 100)",A
1730  Ii=0
1740  FOR I=1 TO 2*N STEP 2
1750    Ii=Ii+1
1760    IF I/(N*2)>Freq AND I/(N*2)<(1-Freq) THEN
1770      Filplot(Ii)=1
1780      Filres(I)=1
1790      GOTO 2000
```

```
1800    END IF
1810    Pfac=(I-1)/(N*2-1)
1820    Filfac=Pfac-Freq
1830    IF I/(N*2)>.5 THEN
1840      Nqfreq=1-Freq
1850      Filfac=Pfac-Nqfreq
1860    END IF
1870    Filres(I)=(EXP(-A*2.*PI*(Filfac)^2))
1880    Filres(I+1)=0.
1890    ON ERROR GOTO 1910
1900    Filplot(Ii)=SQR(Filres(I)^2+Filres(I+1)^2)
1910    IF ERRN=136 THEN
1920      Filres(I)=0
1930      ON ERROR GOTO 1950
1940      Fault=SQR(-1)
1950      OFF ERROR
1960      GOTO 1890
1970    END IF
1980    N1(I)=N1(I)*(Filres(I))
1990    N1(I+1)=N1(I+1)*(Filres(I))
2000  NEXT I
2010  Ii=0
2020  GOTO Escape
2030  RETURN
2040  !-------------------------------------------------------------------------
2050  !  Escape from filter to amplitude spectrum calculation and plotting
2060  !-------------------------------------------------------------------------
2070 Escape:        !
2080  GOSUB Amplitude
2090  GOSUB Spectrumplot
2100  FOR I=1 TO N*2
2110    Filplot(I)=0
2120    Filres(I)=0
2130  NEXT I
2140  GOSUB Filter
2150  RETURN
2160  !-------------------------------------------------------------------------
2170  ! Inverse Fourier Transform routine  !
2180  !-------------------------------------------------------------------------
2190 Ifft:          !
2200  OUTPUT KBD;" |";
2210  S=1
2220  Isign=1
2230  GOSUB Fft
2240  GOSUB Dataplot
2250  !-------------------------------------------------------------------------
2260  ! Disc storage of filtered EM37 field values
2270  !-------------------------------------------------------------------------
2280  IF Ans1$="E" THEN
2290    INPUT "Store filtered data (Y/N)",Qes$
2300    IF Qes$="Y" OR Qes$="y" THEN
2310      MASS STORAGE IS Mass$
2320      Filename$=VAL$(Ch)&Job$&Line$&Com$
2330      CREATE BDAT Filename$,1,364*8*2+20
2340      ASSIGN @Path TO Filename$
2360      OUTPUT @Path;Gnor,Com$,Ch,Ch
2361      Ii=11
2363      FOR I=23 TO 2*Amt-21 STEP 2
2364      Ii=Ii+1
2365      OUTPUT @Path;N1(I),Sta2(Ii)
```

```
2371      NEXT I
2380      ASSIGN @Path TO *
2390  !-------------------------------------------------------------------------
2400    END IF
2410    INPUT "Filter another channel (Y/N)",Qs$
2420    IF Qs$="Y" OR Qs$="y" THEN
2430      FOR I=1 TO N
2440        Filplot(I)=0
2450      NEXT I
2460      Amt=Amt-20
2470      INPUT "Channel to filter",Ch
2480      GOSUB Smoothing
2490      GOTO 470
2500    ELSE
2510      STOP
2520    END IF
2530  ELSE
2540    INPUT "Refilter of filtered values (Y/N)",Qs1$
2550    IF Qs1$="Y" OR Qs1$="y" THEN
2560      FOR I=1 TO N
2570        Filplot(I)=0
2580      NEXT I
2590      GOTO 860
2600    ELSE
2610      STOP
2620    END IF
2630  END IF
2640  RETURN
2650  !-------------------------------------------------------------------------
2660  !Fast Fourier Routine
2670  !-------------------------------------------------------------------------
2680 Fft:            !
2690  DISP "FFT CALCULATING"
2700  N3=2*N
2710  J=1
2720  FOR I=1 TO N3 STEP 2
2730    IF I-J<0 THEN GOTO 2750
2740    IF I-J>=0 THEN GOTO 2810
2750    T=N1(J)
2760    T1=N1(J+1)
2770    N1(J)=N1(I)
2780    N1(J+1)=N1(I+1)
2790    N1(I)=T
2800    N1(I+1)=T1
2810    M=N3/2
2820    IF J-M<=0 THEN GOTO 2880
2830    IF J-M>0 THEN GOTO 2840
2840    J=J-M
2850    M=M/2
2860    IF M-2<0 THEN GOTO 2880
2870    IF M-2>=0 THEN GOTO 2820
2880    J=J+M
2890  NEXT I
2900  M1=2
2910  IF M1-N3<0 THEN GOTO 2930
2920  IF M1-N3>=0 THEN GOTO 3160
2930  I1=2*M1
2940  T2=2*PI/(S*M1)
2950  S1=SIN(T2/2)
2960  W1=-(2.*S1*S1)
```

```
2970  W2=SIN(T2)
2980  W3=1
2990  W4=0
3000  FOR M=1 TO M1 STEP 2
3010    FOR I=M TO N3 STEP I1
3020      J=I+M1
3030      T=W3*N1(J)-W4*N1(J+1)
3040      T1=W3*N1(J+1)+W4*N1(J)
3050      N1(J)=N1(I)-T
3060      N1(J+1)=N1(I+1)-T1
3070      N1(I)=N1(I)+T
3080      N1(I+1)=N1(I+1)+T1
3090    NEXT I
3100    T=W3
3110    W3=W3*W1-W4*W2+W3
3120    W4=W4*W1+T*W2+W4
3130  NEXT M
3140  M1=I1
3150  GOTO 2910
3160  FOR I=1 TO N3 STEP 2
3170    IF S=-1 THEN N1(I)=N1(I)/N
3180    IF S=-1 THEN N1(I+1)=N1(I+1)/N
3190  !PRINT USING " 3D,3D.3D,3D.3D";I,N1(I),N1(I+1)
3200  NEXT I
3210  RETURN
3220  !-------------------------------------------------------------------------
3230  !Plot of amplitude spectrum
3240  !-------------------------------------------------------------------------
3250 Spectrumplot:        !
3260  OUTPUT KBD;" K";
3270  GINIT
3280  GCLEAR
3290  GRAPHICS ON
3300  IF Scaleflag=0 THEN
3310    Amax=MAX(P1(*))
3320    Amin=MIN(P1(*))
3330    Scaleflag=1
3340  END IF
3350  FOR I=1 TO N
3360    P1(I)=P1(I)/Amax
3370  NEXT I
3380  VIEWPORT 0,100*RATIO,10,90
3390  WINDOW 0,133,10,90
3400  CSIZE 3
3410  CLIP OFF
3420  LORG 6
3430  MOVE 133/2,25
3440  LABEL "FREQ IN CYCLES/DATA LENGTH"
3450  MOVE 133/2,15
3460  LABEL "MAX VALUE "&VAL$(INT(100*Amax)/100)
3470  MOVE 5,50
3480  DEG
3490  LDIR 90
3500  LABEL "    AMPLITUDE SPECTRUM"
3510  RAD
3520  LDIR 0
3530  MOVE 133/2,90
3540  SELECT Ans1$
3550  CASE "P"
3560    LABEL "AMPLITUDE SPECTRUM PLATE DEPTH="&VAL$(Depth)&" m Ch="&VAL$(Ch)
```

```
3570  CASE "C"
3580    LABEL "PLATE + HS "&VAL$(Depth)&" m AND "&VAL$(Rho)&" ohmm"
3590  CASE "H"
3600    LABEL "AMPLITUDE SPECTRUM   "&Com$&" COMP  "&VAL$(Rho)&" Ohmm"&"Ch "&VA
$(Ch)
3610  CASE "E"
3620    LABEL "AMPLITUDE SPECTRUM LINE "&Fil$&" COM="&Com$
3630  END SELECT
3640  VIEWPORT 20,RATIO*100,30,85
3650  FRAME
3660  WINDOW 0,N/2+1,0,1
3670  AXES 0,.2,0,0
3680  CLIP OFF
3690  LORG 8
3700  CSIZE 3
3710  FOR I=1 TO 5
3720    MOVE -.1,I*.2
3730    LABEL USING "#,DDD.DD";I*.2
3740  NEXT I
3750  LORG 6
3760  CSIZE 3,1
3770  Ii=0
3780  FOR I=0 TO N/2 STEP N/8
3790    MOVE I,-.05
3800    LABEL USING "#,D.DDD";Ii
3810    Ii=Ii+.125
3820  NEXT I
3830  FOR I=0 TO N/2 STEP N/8
3840    MOVE I,0
3850    DRAW I,-.02
3860  NEXT I
3870  LORG 5
3880  FOR I=1 TO N/2
3890    MOVE I,0
3900    Frek(I)=I/N
3910    DRAW I,P1(I)
3920  NEXT I
3930  MOVE 1,Filplot(1)
3940  FOR I=2 TO N/2
3950    DRAW I,Filplot(I)
3960  NEXT I
3970  FOR I=1 TO N/2
3980    P1(I)=P1(I)*Amax
3990  NEXT I
4000  RETURN
4010  !-------------------------------------------------------------------------
4020  ! Plot of origional and filtered data
4030  !-------------------------------------------------------------------------
4040 Dataplot:       !
4050  OFF ERROR
4060  OUTPUT KBD;" K";
4070  DEG
4080  GRAPHICS ON
4090  GCLEAR
4100  VIEWPORT 0,100*RATIO,0,100
4110  WINDOW 0,133,0,100
4120  IF Isign=0 THEN
4130    Amax=MAX(N1(*))
4140    Amin=MIN(N1(*))
4150    Amaxorg=Amax
```

```
4160    Aminorg=Amin
4170  ELSE
4180    INPUT "Scale of origional data (Y/N)",Qes$
4190    IF Qes$="Y" OR Qes$="y" THEN
4200      Amin=Aminorg
4210      Amax=Amaxorg
4220      GOTO 4450
4230    END IF
4240    Amax=0
4250    Amin=10000
4260    FOR I=23 TO 2*Amt-1 STEP 2
4270      Amax=MAX(Amax,N1(I))
4280      Amin=MIN(Amin,N1(I))
4290    NEXT I
4300  END IF
4310  IF ABS(Amax)>10 OR ABS(Amin)>10 THEN
4320    IF ABS(Amax)>ABS(Amin) THEN
4330      Amax=ABS(10*INT(Amax/10))
4340    ELSE
4350      Amax=ABS(10*INT(Amin/10))
4360    END IF
4370  ELSE
4380    IF ABS(Amax)>ABS(Amin) THEN
4390      Amax=ABS(Amax)
4400    ELSE
4410      Amax=ABS(Amin)
4420    END IF
4430  END IF
4440  Amount=Amax-Amin
4450  LORG 3
4460  CSIZE 3.5
4470  MOVE 5,15
4480  IF Isign=0 THEN
4490    SELECT Ans1$
4500    CASE "P"
4510      LABEL "PLATE    SIGMA*T="&VAL$(St)&" DEPTH "&VAL$(Depth)
4520    CASE "C"
4530      LABEL "PLATE AND HOST ROCK "&VAL$(Depth)&" m AND "&VAL$(Rho)&" ohmm"
4540    CASE "H"
4550      LABEL "HALFSPACE VALUES "&VAL$(Rho)&" Ohmm"
4560    CASE "E"
4570      LABEL "FIELD VALUES LINE "&Fil$
4580    END SELECT
4590  ELSE
4600    LABEL "FILTERED VALUES"
4610  END IF
4620  MOVE 5,10
4630  LABEL "CHANNEL "&VAL$(Ch)
4640  MOVE 5,5
4650  LABEL Com$&" COMPONENT"
4660  VIEWPORT 15,120,25,85
4670  CSIZE 3
4680  LORG 8
4690  CLIP ON
4700  WINDOW Sta2(11),Sta2(Amt-10),-Amax,Amax
4710  AXES Stsp,Amax/3,Sta2(11)
4720  MOVE Loop1,Amax
4730  DRAW Loop1,-Amax
4740  MOVE Loop2,Amax
4750  DRAW Loop2,-Amax
```

```
4760  CLIP OFF
4770  MOVE Sta2(11)-.3*Stsp,Amax
4780  LABEL DROUND(Amax,1)
4790  MOVE Sta2(11)-.3*Stsp,-Amax
4800  LABEL -DROUND(Amax,1)
4810  MOVE Sta2(11)-.3*Stsp,0
4820  LORG 4
4830  LDIR 90
4840  LABEL "EMF (mv)"
4850  LDIR 0
4860  RAD
4870  LORG 6
4880  FOR I=12 TO Amt-10 STEP 3
4890    MOVE Sta2(I),0
4900    LABEL Sta2(I)
4910  NEXT I
4920  LORG 5
4930  CLIP OFF
4940  IF Isign<>0 THEN 5010
4950  Ii=11
4960  MOVE Sta2(11),Valu(21)
4970  FOR I=23 TO 2*Amt-21 STEP 2
4980    Ii=Ii+1
4990    DRAW Sta2(Ii),Valu(I)
5000  NEXT I
5010  IF Isign=0 THEN GOTO 5100
5020  PENUP
5030  Ii=11
5040  MOVE Sta2(11),N1(21)
5050  FOR I=23 TO 2*Amt-21 STEP 2
5060    Ii=Ii+1
5070    DRAW Sta2(Ii),N1(I)
5080  NEXT I
5090  Ii=11
5100  DISP "Hit 'RETURN' to CONTINUE"
5110  ON KBD GOTO 5130
5120 Sit:GOTO Sit
5130  Key$=KBD$
5140  OFF KBD
5150  IF Key$=" E" THEN
5160    GOTO 5200
5170  ELSE
5180    GOTO 5110
5190  END IF
5200  GCLEAR
5210  RETURN
5220  !-------------------------------------------------------------------------
5230  !Amplitude spectrum calculation
5240  !-------------------------------------------------------------------------
5250 Amplitude:          !
5260  Ii=0.
5270  FOR I=1 TO N*2 STEP 2
5280    Ii=Ii+1
5290 !  Phase(Ii)=ATN(-N1(I+1)/N1(I))
5300    P1(Ii)=SQR(N1(I)^2+N1(I+1)^2)
5310  NEXT I
5320  RETURN
5330  !-------------------------------------------------------------------------
5340  !  Selection for dataread subroutines
5350  !-------------------------------------------------------------------------
```

```
5360 Dataread:          !
5370                    !
5380  INPUT "File to read : COMBINATION <C>, PLATE <P>, HOST ROCK <H>, EM37 FIE
D DATA <E>",Ans1$
5390  SELECT Ans1$
5400  CASE "C","c"
5410    GOSUB Combread
5420  CASE "P","p"
5430    GOSUB Plateread
5440  CASE "H","h"
5450    GOSUB Halfread
5460  CASE "E","e"
5470    GOSUB Em37read
5480  CASE ELSE
5490    GOTO 5380
5500  END SELECT
5510  Stsp=ABS(Sta(1)-Sta(2))
5520  FOR I=1 TO Amt
5530    IF Datta(Ch,I)=0 THEN Datta(Ch,I)=(Datta(Ch,I-1)+Datta(Ch,I+1))/2
5540  NEXT I
5550  GOSUB Smoothing
5560  RETURN
5570  !-------------------------------------------------------------------------
5580  ! Smoothing of data on ends by adding first and last value
5590  !-------------------------------------------------------------------------
5600 Smoothing:    !
5610  FOR I=1 TO 10
5620    Smooth(I)=Datta(Ch,1)
5630    Sta2(I)=Sta(1)-(11-I)*Stsp
5640  NEXT I
5650  FOR I=11 TO Amt+10
5660    Smooth(I)=Datta(Ch,I-10)
5670    Sta2(I)=Sta(I-10)
5680  NEXT I
5690  Tel=9
5700  FOR I=Amt+11 TO Amt+20
5710    Smooth(I)=Datta(Ch,Amt)
5720    Sta2(I)=Sta(Amt)+(I-(Amt+10))*Stsp
5730    Tel=Tel-1
5740  NEXT I
5750  Amt=Amt+20
5760  RETURN
5770  !-------------------------------------------------------------------------
5780  !  Subroutine to read host rock and plate response combinations
5790  !-------------------------------------------------------------------------
5800 Combread:          !
5810  MASS STORAGE IS Mass$
5820  INPUT "Resistivity of host rock respose",Rho
5830  INPUT "SIGMA T of plate response",St
5840  INPUT "Channel ",Ch
5850  INPUT "Component ",Com$
5860  INPUT "Depth to top of plate (20 to 140 step 20)",Depth
5870  SELECT Depth
5880  CASE 20
5890    Depth$="A"
5900  CASE 40
5910    Depth$="B"
5920  CASE 60
5930    Depth$="C"
5940  CASE 80
```

```
5950    Depth$="D"
5960  CASE 100
5970    Depth$="E"
5980  CASE 120
5990    Depth$="F"
6000  CASE 140
6010    Depth$="G"
6020  END SELECT
6030  Fil$=Com$&Depth$&VAL$(Rho)&"_"&VAL$(St)
6040  ON ERROR GOSUB Massstore
6050  ASSIGN @Old TO Fil$
6060  ENTER @Old;Amt,Z1,Z2,Z3,Z4,Z5,Z6,Z7,Z8,Z9,Z10
6070  FOR I=1 TO Amt
6080    ENTER @Old;Sta(I),Datta(Ch,I)
6090  NEXT I
6100  ASSIGN @Old TO *
6110  MASS STORAGE IS Mass$
6120  RETURN
6130 Massstore:     !
6140  IF ERRN=56 THEN
6150    DISP "FILE NOT ON DISC, REPLACE AND PRESS CONTINUE"
6160    PAUSE
6170  ELSE
6180  END IF
6190  OFF ERROR
6200  Loop1=-Lx/2
6210  Loop2=Lx/2
6220  RETURN
6230  !-------------------------------------------------------------------------
6240  ! Subroutine to read host rock response
6250  !-------------------------------------------------------------------------
6260 Halfread:   !
6270  MASS STORAGE IS Mass$
6280  INPUT "Component of host rock response (Z or X)",Com$
6290  INPUT "Resistivity of host rock response",Rho
6300  INPUT "Channel",Ch
6310  Fil$="0"&Com$&VAL$(Ch)&"_"&VAL$(Rho)
6320  ASSIGN @Old TO Fil$
6330  ENTER @Old;Gnor,Com$,Amt
6340  FOR I=1 TO Amt
6350    ENTER @Old;Datta(Ch,I),Sta(I)
6360  NEXT I
6370  Loop1=-Loopdim/2
6380  Loop2=Loopdim/2
6390  ASSIGN @Old TO *
6400  RETURN
6410  !-------------------------------------------------------------------------
6420  ! Subroutine to read plate response
6430  !-------------------------------------------------------------------------
6440 Plateread:        !
6450                   ! DUMMY(J,I) 1=X-COMP,2=Y-COMP,3=Z-COMP
6460  MASS STORAGE IS Mass$
6470  INPUT "Depth to top of plate (20 to 140 step 20)",Depth
6480  INPUT "SIGMA T of plate response",St
6490  INPUT "Channel",Ch
6500  INPUT "Component (X,Y,Z)",Com$
6510  SELECT Com$
6520  CASE "X","x"
6530    Comnr=1
6540  CASE "Y","y"
```

```
6550    Comnr=2
6560  CASE "Z","z"
6570    Comnr=3
6580  CASE ELSE
6590    GOTO 6500
6600  END SELECT
6610  Fil$=VAL$(Depth)&"_"&VAL$(St)&"_"&VAL$(Ch)
6620  ON ERROR GOTO 6640
6630  ASSIGN @Old TO Fil$
6640  IF ERRN=56 THEN
6650    OFF ERROR
6660    DISP "File not on disc, insert correct disc and hit 'RETURN'"
6670    ON KBD GOTO 6690
6680 Relax:GOTO Relax
6690    Key$=KBD$
6700    OFF KBD
6710    IF Key$=" E" THEN
6720      ON ERROR GOTO 6740
6730      Fault=SQR(-1)
6740      OFF ERROR
6750      GOTO 6630
6760    ELSE
6770      GOTO 6660
6780    END IF
6790  END IF
6800  ENTER @Old;Z1,Z2,Z3,Z4,Z5,Z6,Z7,Z8,Z9,Z10
6810  ON END @Old GOTO 6870
6820  FOR I=1 TO 100
6830    FOR J=1 TO 3
6840      ENTER @Old;Dummy(J,I)
6850    NEXT J
6860  NEXT I
6870  ASSIGN @Old TO *
6880  MASS STORAGE IS Mass$
6890  Amt=I-1
6900  Sta(1)=-1000
6910  FOR I=1 TO Amt
6920    Datta(Ch,I)=Dummy(Comnr,I)
6930    Sta(I+1)=Sta(I)+50
6940  NEXT I
6950  Loop1=-Loopdim
6960  Loop2=Loopdim
6970  RETURN
6980  !-------------------------------------------------------------------------
6990  !  Subroutine to read EM37 field data (Old or New format)
7000  !-------------------------------------------------------------------------
7010  !
7020 Em37read:    !
7030  OUTPUT KBD;" K";
7040  INPUT "Job identifier -- Max 3 alphanumericals",Job$
7050  INPUT "Line identifier ",Line$
7060  INPUT "Component to work with (Z or X)",Com$
7070  INPUT "Data stored in OLD <O> or NEW <N> format",Format$
7080  IF Com$="Z" THEN Ii=1
7090  IF Com$="X" THEN Ii=3
7100  PRINT CHR$(12)
7110  Fil$=Job$&"_"&Line$
7120!
7130  OUTPUT KBD;" K";
7140  PRINT TABXY(25,10),"READING DATA FROM FILE ";Fil$
```

```
7150  PRINT TABXY(25,12),"READING HEADER"
7160  MASS STORAGE IS Mass$
7170  ASSIGN @Old TO Fil$
7180  SELECT Format$
7190  CASE "N"
7200  !-------------------------------------------------------------------
7210    ENTER @Old;Pr$,Da$,Lx,Ly,Cur,Tot,Dir1$,Dir2$,Lc$,Loop1,Loop2
7220    ENTER @Old;Nrcomp,Comp$(1),Comp$(2),Comp$(3),Amt
7230    FOR I=1 TO Amt
7240      ENTER @Old;Sta(I),Nr_freq(I)
7250      PRINT TABXY(25,12),"READING STATION ";Sta(I)
7260      FOR F_comp=1 TO Nr_freq(I)
7270        ENTER @Old;Primary(I,1,F_comp),Primary(I,2,F_comp),Primary(I,3,F_co
p)
7280        ENTER @Old;Frequ(I,F_comp)
7290        IF Frequ(I,F_comp)=0 THEN 7360
7300        ENTER @Old;Gain(I,F_comp),Nrchan(I,F_comp)
7310        FOR Ch=1 TO Nrchan(I,F_comp)
7320          ENTER @Old;Field(I,Ch,1,F_comp),Field(I,Ch,2,F_comp),Field(I,Ch,3
F_comp)
7330          IF Ch>5 AND Ch<11 THEN Field(I,Ch,Ii,F_comp)=Field(I,Ch,Ii,F_comp
/4
7340          IF Ch>15 AND Ch<21 THEN Field(I,Ch,Ii,F_comp)=Field(I,Ch,Ii,F_con
)/4
7350        NEXT Ch
7360      NEXT F_comp
7370    NEXT I
7380  !-------------------------------------------------------------------
7390  CASE "O"
7400    ENTER @Old;Pr$,Da$,Lx,Ly,Cur,Tot,Lc$,Loop1,Loop2
7410    ENTER @Old;Nrcomp,Comp$(1),Comp$(2),Comp$(3),Amt
7420    FOR I=1 TO Amt
7430      ENTER @Old;Primary(I,1,1),Primary(I,2,1),Primary(I,3,1)
7440      ENTER @Old;Sta(I),Nr_freq(I)
7450      PRINT TABXY(25,12),"READING STATION ";Sta(I)
7460      FOR F_comp=1 TO 3
7470        ENTER @Old;Frequ(I,F_comp)
7480        IF Frequ(I,F_comp)=0 THEN 7530
7490        ENTER @Old;Gain(I,F_comp),Nrchan(I,F_comp)
7500        FOR Ch=1 TO Nrchan(I,F_comp)
7510          ENTER @Old;Field(I,Ch,1,F_comp),Field(I,Ch,2,F_comp),Field(I,Ch,3
F_comp)
7520        NEXT Ch
7530      NEXT F_comp
7540      F_comp=3
7550    NEXT I
7560    ASSIGN @Old TO *
7570    MASS STORAGE IS Mass$
7580  CASE ELSE
7590    GOTO 7070
7600  END SELECT
7610  PRINT TABXY(25,10),"                                                  "
7620  PRINT TABXY(25,12),"                          "
7630  !-------------------------------------------------------------------
7640  ! Normalization of data
7650  !-------------------------------------------------------------------
7660  Stsp=ABS(Sta(1)-Sta(2))
7670  Gnor=6
7680  FOR I=1 TO Amt
7690    FOR Ch=1 TO 20
```

```
7700      Datta(Ch,I)=Field(I,Ch,Ii,1)/(2^Gain(I,1))*2^Gnor
7710      IF Format$="O" THEN
7720        IF Ch>5 AND Ch<11 THEN Datta(Ch,I)=Datta(Ch,I)/4
7730        IF Ch>15 THEN Datta(Ch,I)=Datta(Ch,I)/4
7740      END IF
7750    NEXT Ch
7760    PRINT TABXY(30,10),"NORMALIZING STATION ";Sta(I)
7770  NEXT I
7780  PRINT TABXY(30,10),"                                        "
7790  BEEP
7800  INPUT "Channel to filter",Ch
7810  RETURN
7820  END
7830  !*************************************************************************
```